CYCLOTRON LABORATORY

EAST LANSING, MICHIGAN

# Proposal for Operating Support
for a
# National Facility for
# Research with Heavy Ions
using a
# 500 MeV Superconducting Cyclotron

MARCH 1980

MSUCL-321

PROPOSAL

to the

NATIONAL SCIENCE FOUNDATION

for

OPERATING SUPPORT

for a

NATIONAL FACILITY

for

RESEARCH WITH HEAVY IONS

Using a

500 MeV SUPERCONDUCTING CYCLOTRON

Period: Nov. 1. 1980 thru Oct. 31, 1983

Submitted by

Michigan State University
East Lansing, Michigan 48824

Principal Investigators

Prof. S.M. Austin
Prof. W. Benenson
Prof. F.M. Bernthal
Prof. H.G. Blosser
Prof. G.M. Crawley
Prof. A.I. Galonsky
Prof. C.K. Gelbke
Prof. M.M. Gordon
Prof. E. Kashy
Prof. W.C. McHarris
Prof. J.A. Nolen, Jr.
Prof. F. Resmini
Prof. R.G.H. Robertson
Prof. D.K. Scott
Prof. B.H. Wildenthal

## Endorsement

This proposal has the approval and support of Michigan State University.

Henry G. Blosser
Director
Cyclotron Laboratory

R.E. Wilkinson
Vice President for
Business and Finance

## Editoral Note

Figures are labeled with both a Roman and Arabic numeral (e.g. Fig.III.2), the Roman numeral denoting the major section in which the Figure appears. The text of the Roman numeral is omitted when the reference is to a figure within Section III, i.e. "Fig. 3" refers to Fig.III.3. References are placed at the end of major sections and can be quickly located by looking just ahead of the colored pages which are inserted to mark the separation of major sections.

Table of Contents

# I. INTRODUCTION

This proposal requests funding for the operation of a national research facility based on the "K500"* superconducting cyclotron and for support of the research activities of the MSU experimental nuclear science group. The request covers a three-year period corresponding to the years in which the K500 cyclotron will be operating as a stand-alone accelerator with experimental facilities as provided in the "Phase I" NSF grant. (Phase I facilities consist primarily of existing MSU experimental devices connected to the K500 cyclotron by a rearranged and upgraded beam transport system.)

Concurrently with Phase I operations, the Laboratory will be the site of an ongoing four-year construction program supported by the Department of Energy, the "Phase II" program, which will a) approximately double the overall size of the laboratory building, b) add a second superconducting cyclotron, a K800, interconnected to the K500 to form a coupled system, c) provide a new beam-transport system to carry the beam from the second cyclotron to an expanded array of experimental locations and d) add a number of major new experimental devices to the facilities of the laboratory. The DOE-funded program includes support for Research and Development work related

---

*The choice of the name "K500" is based on the conventional symbol for defining cyclotron energy capability, "K"; for an ion of charge $Qe$ and mass $Am_o$, the maximum energy of a cyclotron is $E=KQ^2/A$.

to the Phase II project but does not provide funding for either operation of the K500 cyclotron or for support of the MSU nuclear science program, both of which will continue as NSF-supported activities. (The agreement between the agencies relative to the transfer of Phase II to DOE also provides for the full program to revert to the National Science Foundation for operating support at the end of the four-year Phase II construction period.) The combined support for the Laboratory from NSF and DOE accurately follows the long-range plan given in the 1978 proposal presented to the Nuclear Science Advisory Committee for their fiscal year 1980 facilities review. This review, in turn, was the basis for proceeding with the Phase II project.

Commenting on the status of the Phase I program, we note that the K500 cyclotron is expected to come into operation in August of this year and that the first beams for nuclear science experiments are expected at the end of this year. Section II.A. describes the current status of the cyclotron. We are particularly pleased to see the project coming to completion within the planned budget in spite of recent high inflation rates. (It is perhaps appropriate as well to note that initial major procurements for the Phase II program are within budgeted amounts, although a possible difficulty and need for correction will arise if the current rate of inflation continues or becomes worse - an inflation factor of 0.7%/month was used to convert from 1978 costs to year-of-expenditure

costs in the calculation of the budgets for the Phase II line-item appropriation.)

The increase in project faculty outlined in the 1978 proposal has occurred with the addition of Dr. David Scott as John A. Hannah Professor of Physics and Chemistry. A vacancy in the experimental faculty exists at present as a consequence of the resignation of Professor Kelly; interviewing of candidates is in progress and we expect to fill this vacancy in the near future. An additional faculty position has also been made available in nuclear theory and interviews for this position are likewise in progress.

The shift to national facility status will bring a number of changes in traditional Laboratory procedures including: a) operators on all shifts to handle the accelerator and beam-transport system, b) liaison physicists to provide technical assistance to outside users, and c) a new data processing system which should greatly improve compatibility between the MSU system and systems at users' home institutions. These steps, and others as needed, should make the facility available for efficient use by the national community.

In accord with the plan of the facility proposal, the actual scheduling of experiments on the K500 will be handled with the assistance of a broadly based Program Advisory Committee, following traditional procedures for national facilities. The totality of scientific contributions

which come from the facility will then reflect the creativity and ingenuity of the full user community. The local group, is at the same time, a key element in determining the effectiveness with which the facility is utilized. In particular, this group must bear the main responsibility for developing and bringing on-line advanced instrumentation systems and for investing the effort in debugging and documenting these systems so that they can be used predictably and reliably by users from other laboratories. We believe the staff of our laboratory is an excellent group for this assignment--qualified, experienced and motivated. This, in our view, is the primary factor justifying the operating support herein requested.

The main section of this proposal is the Research Program section which reviews the recent accomplishments and anticipated future directions of the MSU-based research program and provides what we hope is an up-to-date and accurate picture of the status and vitality of the Laboratory. For completeness, the Research Program section is preceded by a major section reviewing the characteristics of the facility as it will exist in the Phase I years. This serves to fix a context for the discussion of major research directions in the following section and also gives a basis for evaluation of the instrumentation research and development component of the program. Another major section of the proposal is devoted to a listing of the publications of the laboratory for the three-year period

January 1977 through December 1979, the length of this period matching the length of the period for which funds are herein requested.

Finally, proposed budgets are reviewed in Section IV, the funding requested being at the levels anticipated in the long-range plan of the 1978 facility proposal. Specifically, the funding levels shown in that plan were $1,600,000 for each of the years 1981 and 1982 and $1,800,000 for 1983, all in 1978 dollars, these amounts covering both operation of the facility and support for MSU Phase I programs. These levels in our opinion continue to be a good compromise between the desire to maximize scientific exploitation of a forefront facility and the reality of severe budget austerity in which the overall scientific community operates. Our funding request is then based on these program levels plus a correction factor to allow for estimated effects of inflation.

## II. THE RESEARCH FACILITY

In this section we review characteristics of the Laboratory's research facilities. As noted in the Introduction, the period covered by this proposal corresponds to the "Phase I" years, with the facility in the configuration provided under NSF Grant PHY76-83254, which was a grant for construction of the K500 cyclotron and a beam transport system to connect it to existing experimental equipment. The research capability will also, in this period, be significantly influenced by the ongoing Phase II program, which is a program to; a) add a second K800 cyclotron, b) provide for operation of the two cyclotrons as a coupled system, c) provide major expansion of building and experimental areas, and d) add a number of specific major experimental devices. Research opportunities in the Phase I period will be significantly augmented as various Phase II devices are installed and brought into operation.

Figure II.1 is a plan view of the experimental floor in its Phase I configuration. The K500 cyclotron is at the left, and beams from the cyclotron are directed to a large switching magnet and then to a series of experimental setups located in two independently shielded rooms ("North" and "South"). The North experimental room contains the Enge split-pole spectrograph, a new low-resolution K320 spectrograph, a precision scattering chamber from the University of Minnesota, a small general purpose scattering

chamber and the collection device for a cryogenic helium jet system. The South experimental room houses the target section of the helium jet apparatus, a recoil product mass separator (a prototype section of a larger device provided in the Phase II program), a 60" scattering chamber, and a gamma ray goniometer. For the first year, the 50 MeV cyclotron will be maintained in a stand-by status for possible use as an accelerator test facility; thereafter it will be removed, and additional experimental setups will be available in this "50 MeV" shielded room, as indicated by dashed lines in Fig. II.1.

For completeness we show in Fig. II.2 a plan view of the experimental floor in its configuration for the Phase II program. The high bay area is extended to both east and west relative to the Phase I building, the west addition housing the K800 cyclotron and the east addition providing an enlarged experimental area. The plan provides for feeding most experimental devices from either the K500 cyclotron or from the combined K500 & K800 system. (The Phase I experimental program will be significantly disrupted in the year 1983 as the experimental halls and transport system are changed into the Phase II configuration; the feature that the transport system can be fed from either cyclotron will however significantly ameliorate the most severe aspects of this disruption, and we expect to be able to provide beams for experimental use from at least one cyclotron to at least one experimental hall through most of the period of the reconfiguration.)

MSUX-80-202

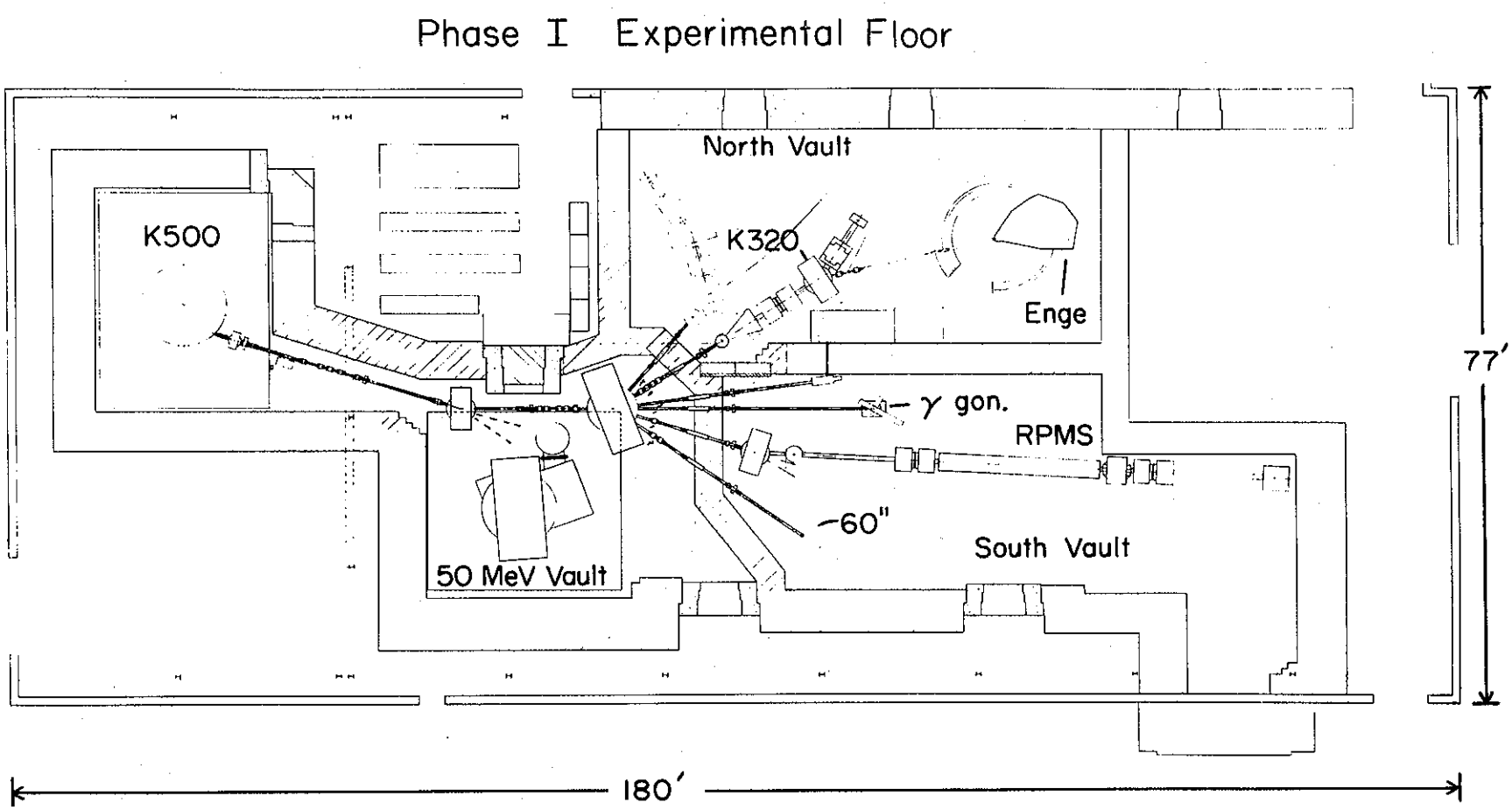


Fig. II. 1. The High Bay part of the Laboratory as it will be arranged for the Phase I program. The K500 cyclotron is at the left housed in a recent 40 foot westward addition to the High Bay. Devices not labelled are a small general purpose scattering chamber on the upper most beam line in the North vault and the cryogenic helium jet system, the target apparatus for which is on the upper most beam line in the South vault with the detection system and pumping apparatus just opposite in the North vault. The area at the upper right corner of the High Bay is used as a heavy machine shop area.

MSUX-80-201

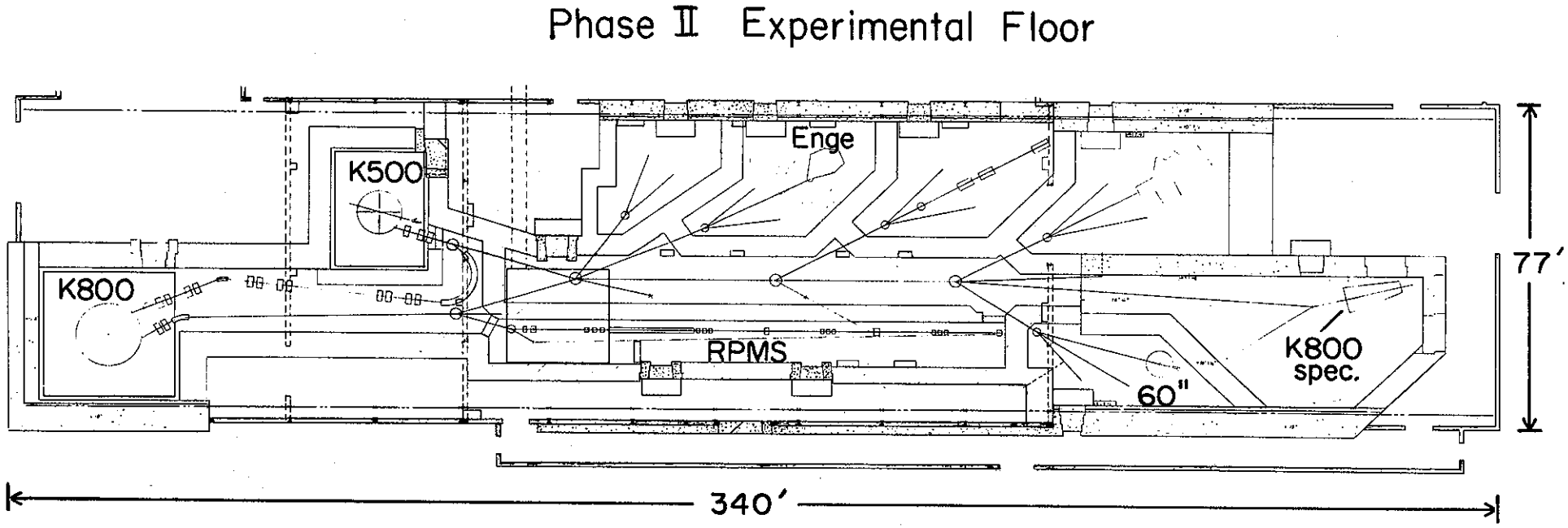


Fig. II. 2. A plan view of the High Bay area as it will be arranged for the Phase II program. A 60 foot extension to the West houses the K800 cyclotron and a 100 foot extension to the East provides space for additional experimental facilities. A new corridor is introduced just outside the South wall of the High Bay (at the bottom of the figure) to provide access to experimental rooms. Steering magnets will be superconducting dipoles similar in construction to the cyclotron magnets.

The following subsections review the status of major devices for the Phase I program. For information purposes one subsection also briefly reviews anticipated characteristics of the large new spectrograph which is part of the Phase II program.

## A. THE K500 CYCLOTRON

The expected performance of the K500 cyclotron is indicated in Fig. II.3, which shows energy per nucleon vs. mass number for various values of the ion charge. The expected energies are particularly interesting and novel for the lighter heavy ions (e.g. carbon, nitrogen, oxygen, and neon)excellent beams of which should be available in the 50 MeV/u range. For the lightest heavy ions, energies up to 80 MeV/u are expected, e.g., 320 MeV alphas, 480 MeV lithium 6, etc. At higher masses in the A=50 to 100 region, the energy is lower and comparable to that available at other accelerators, but with very interesting attributes, nevertheless and possible important advantages associated with overall precision and duty cycle. The upper limit of nuclear physics with the K500 will probably occur at Xenon, where beams in the 2 to 5 MeV/u range offer promise for studies of Coulomb excitation processes.

As noted in the Introduction section, the K500 cyclotron is expected to be ready for first tests with beam in approximately August of this year and to be available for nuclear physics use in either late 1980 or beginning

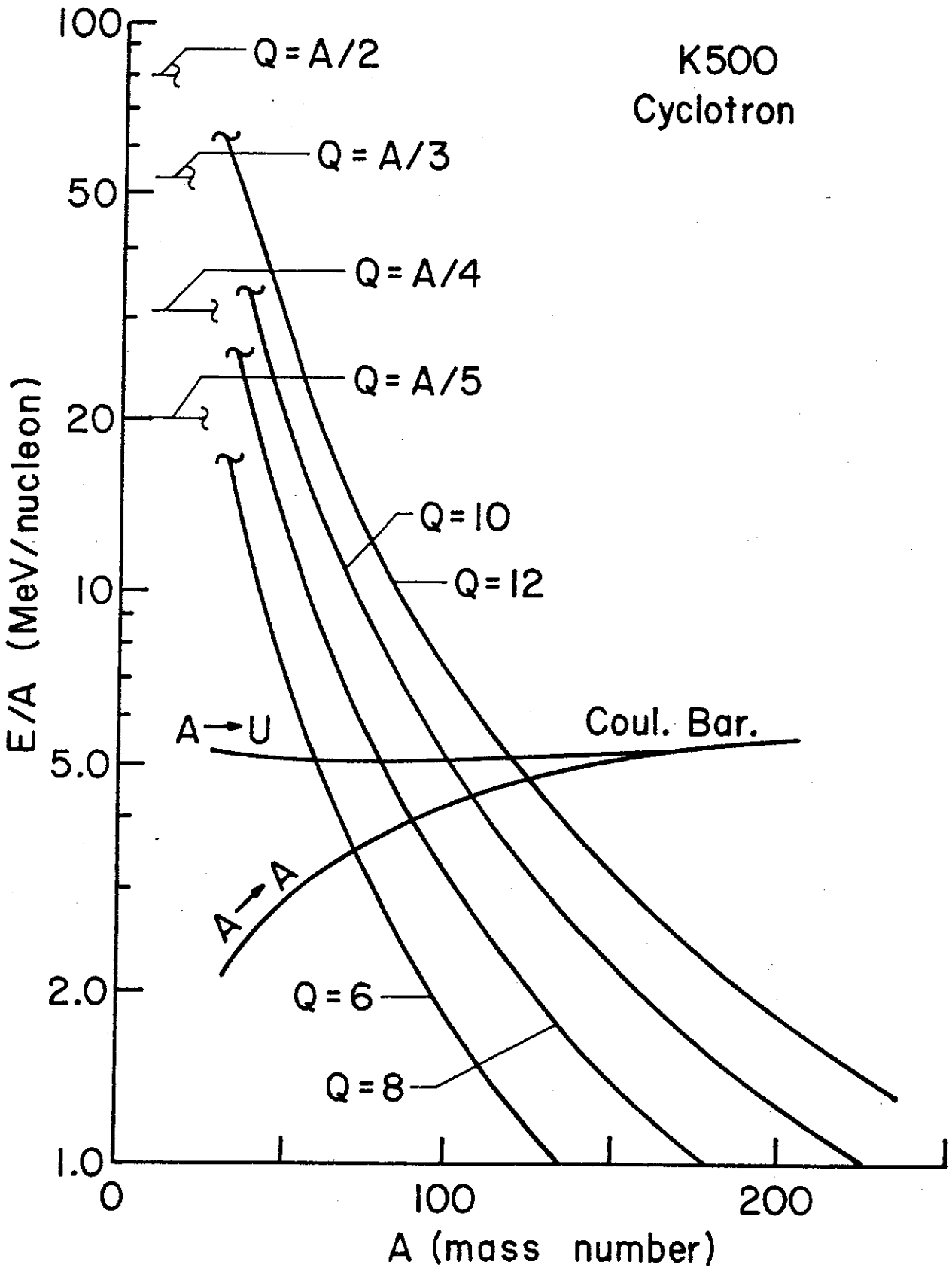


Fig. II. 3. Maximum energy/nucleon versus mass number for Phase I beams. Labels on curves indicate ion charge Qe. Approximate Coulomb barriers for mass A bombarding Uranium and for mass A bombarding mass A are also shown.

1981. Figures II.4 through II.16 are a selection of photographs of components of the cyclotron in various stages of fabrication, the caption of each figure giving a brief explanation of the function of the particular component. The cyclotron design involves significant technical innovations as a consequence of the large reduction in size relative to a normal 15 kilogauss cyclotron. This change in scale leads to novel design requirements in a number of cyclotron sub-systems; we have taken what we believe is a conservative approach to this situation, electing to construct and test prototype assemblies for most major subsystems of the cyclotron. This approach has an advantage in illuminating weak design points at an earlier stage than is the case with the more traditional procedure of deferring operating tests until the complete cyclotron is assembled. The approach also has an advantage in feeding actual subsystem operating experience into the final design, thereby incorporating new features for better operating convenience and easier maintenance. The two major cyclotron subsystems, the magnet and the accelerating system, have thus both evolved significantly in this process relative to the structures originally contemplated.

The K500 magnet and cryogenic system have now been in operation for nearly three years, and extensive operating experience has been accumulated. This has facilitated the handling of routine scheduled maintenance on the refrigerator and has also led to development of techniques

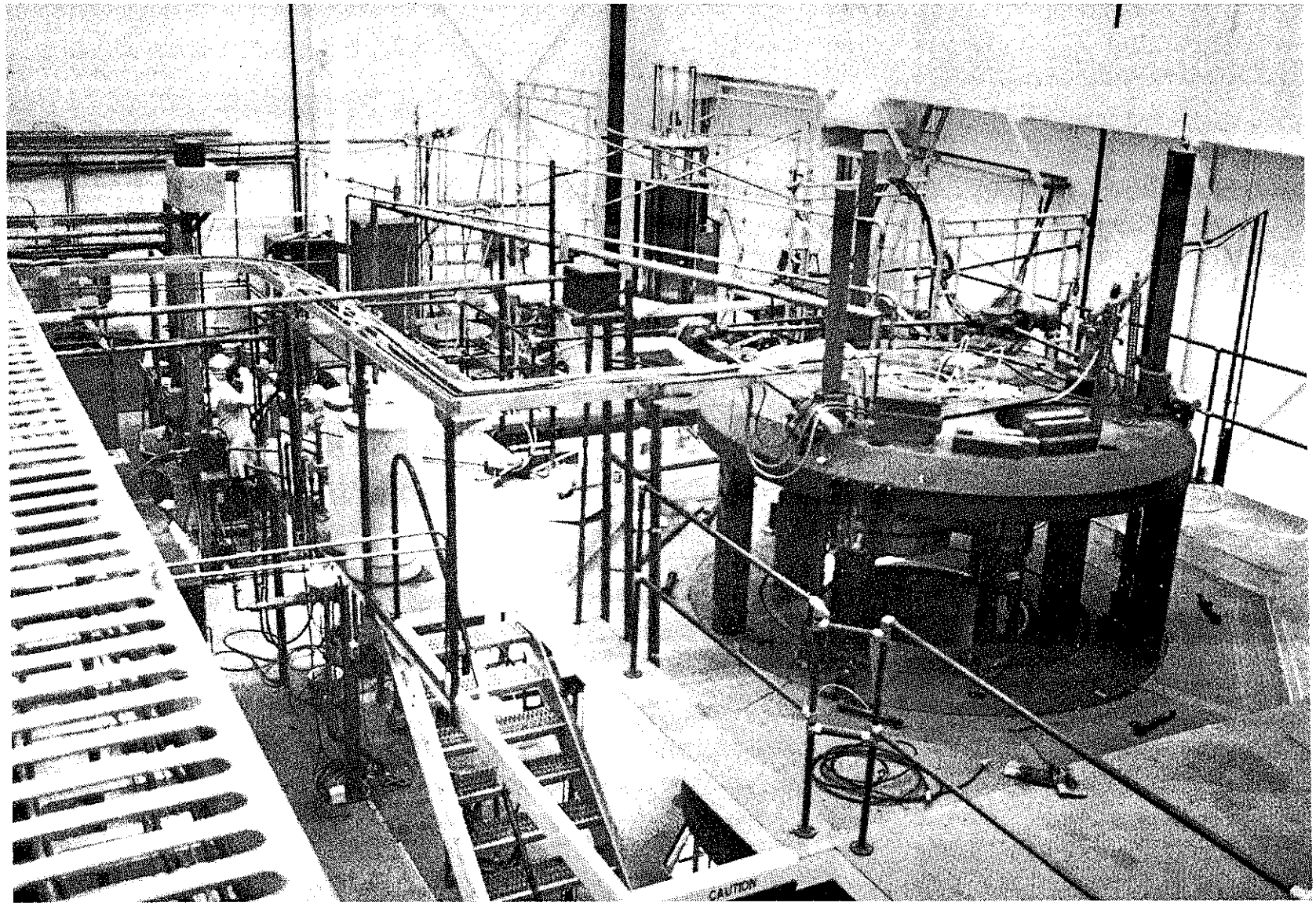


Fig. II. 4. View of the magnet of the K500 from the upper level with top raised for access. Shielding walls will later be installed at the locations defined by the edges of the metal deck.

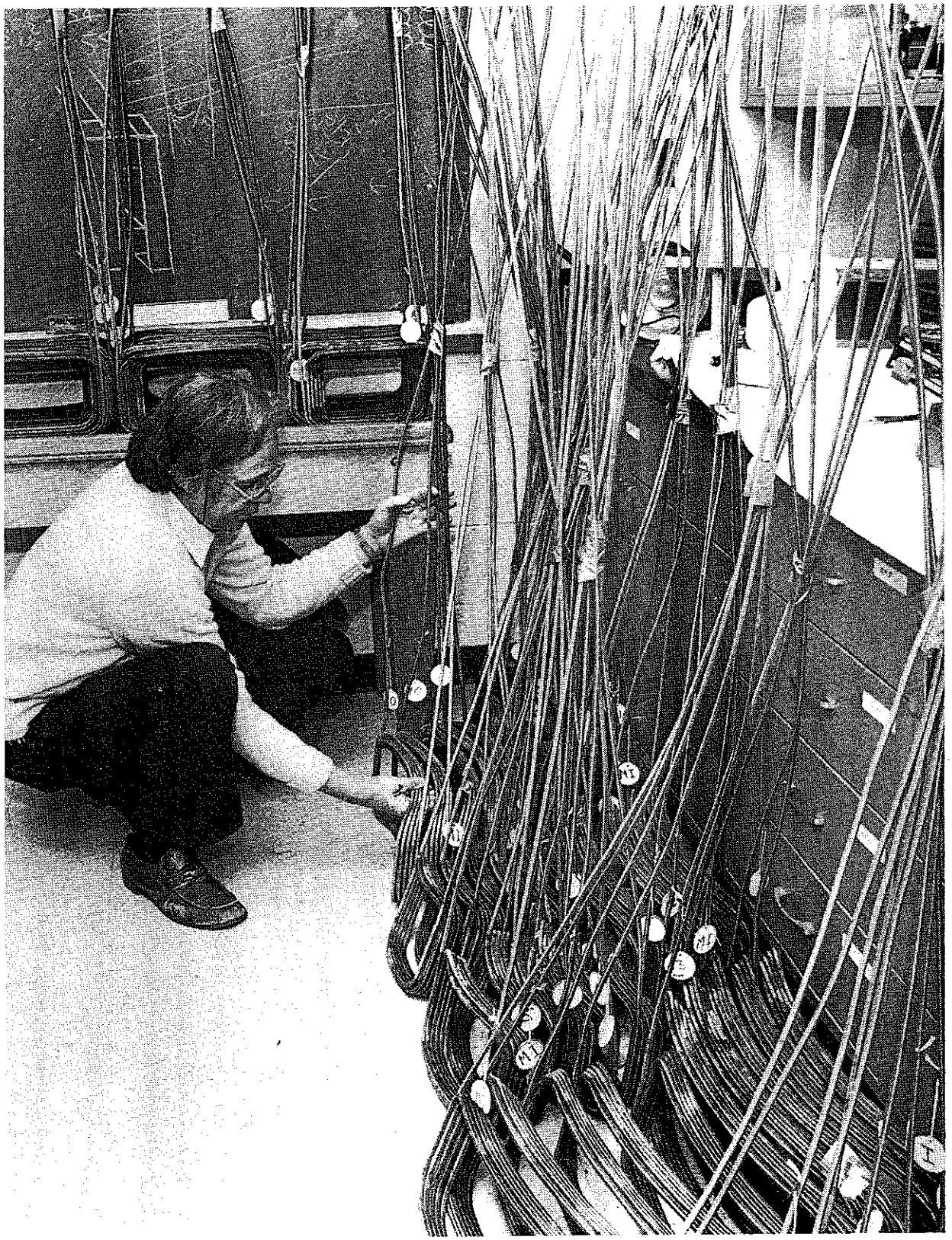

Fig. II. 5. Room temperature trimming windings for the cyclotron waiting to be installed on the pole tips.

Fig.II.6. An outer pole tip section with its seven trimming windings as it is being lowered into the vacuum potting fixture.

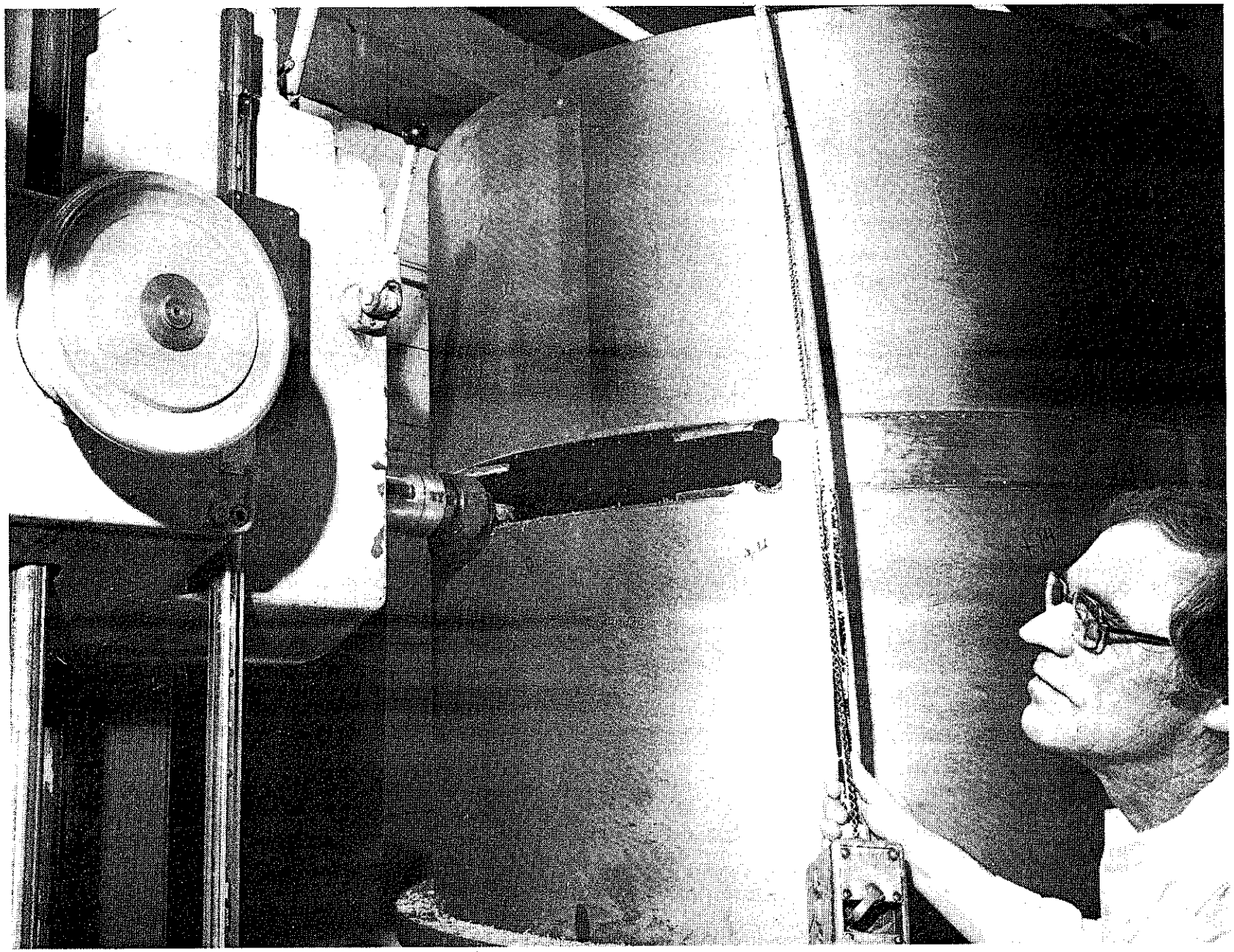

Fig.II.7. Milling the extraction channel opening in the inner cryostat wall.

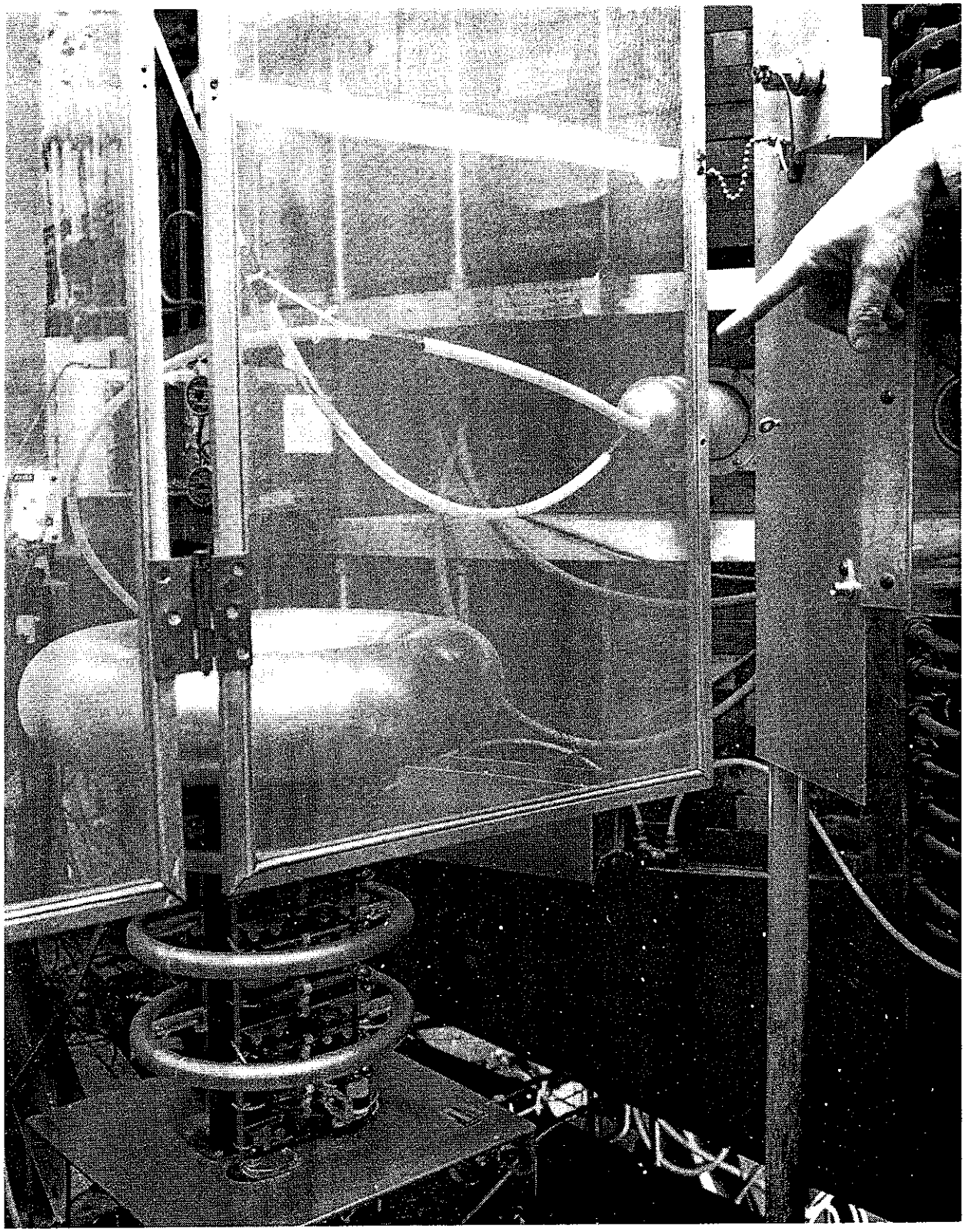

Fig.II.8. One of the two, 150 KeV deflector power supplies for the K500 under test on the deflector of the 50 MeV cyclotron.

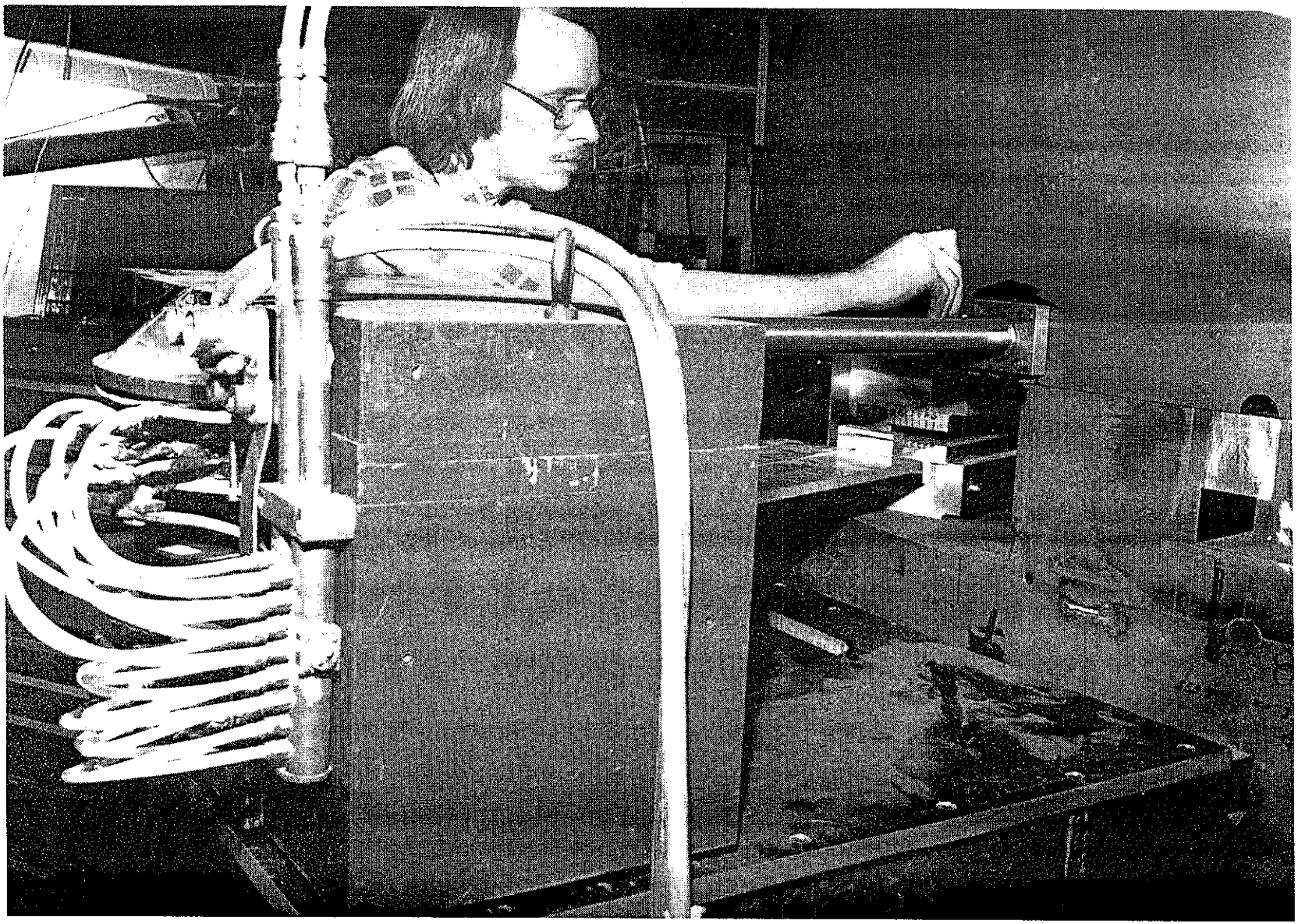

Fig. II. 9. Mapping of the fringing field of the K500 magnet in the vicinity of the extraction channel. The final set of"focusing bars"is located in the hole in the magnet yoke just below the worker's hand. The steering magnet at left center is the first element of the beam transport system.

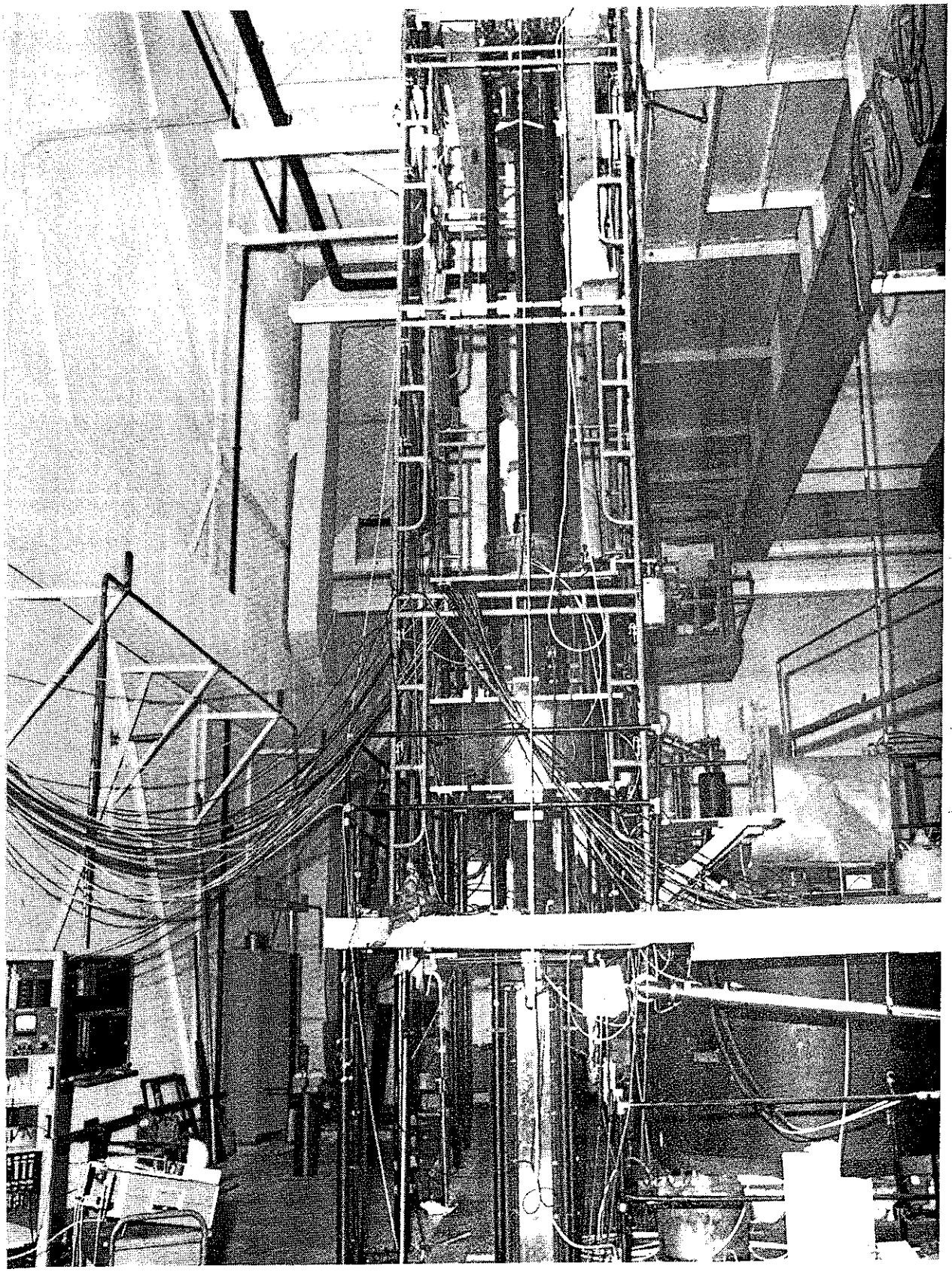

Fig. II. 10. Photograph of the prototype resonator set up for high power RF tests. The prototype dee is housed in a dummy aluminum vacuum chamber, the exterior of which is visible just below the center of the picture.

Fig. II. 11. Power amplifier No. 1 with access doors open to the grid box at the top and the plate box at the bottom.

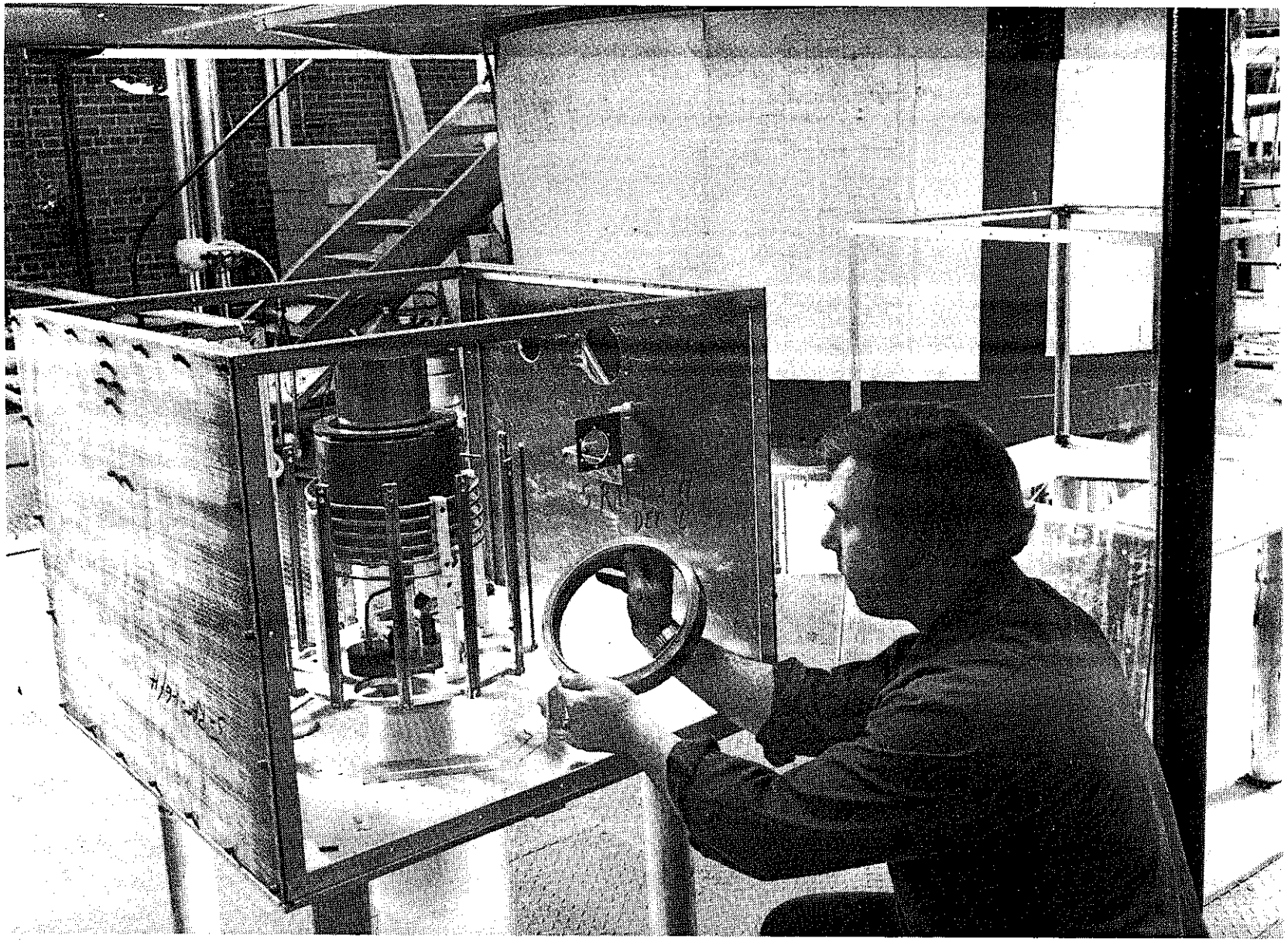

Fig. II. 12. Power amplifier No. 2 in the process of assembly with a plate circuit contact ring about to be installed. The frame for power amplifier No. 3 is visible to the right with assembly operations just beginning.

Fig.II.13. Parts for power amplifiers Nos. 2 and 3 waiting to be installed.

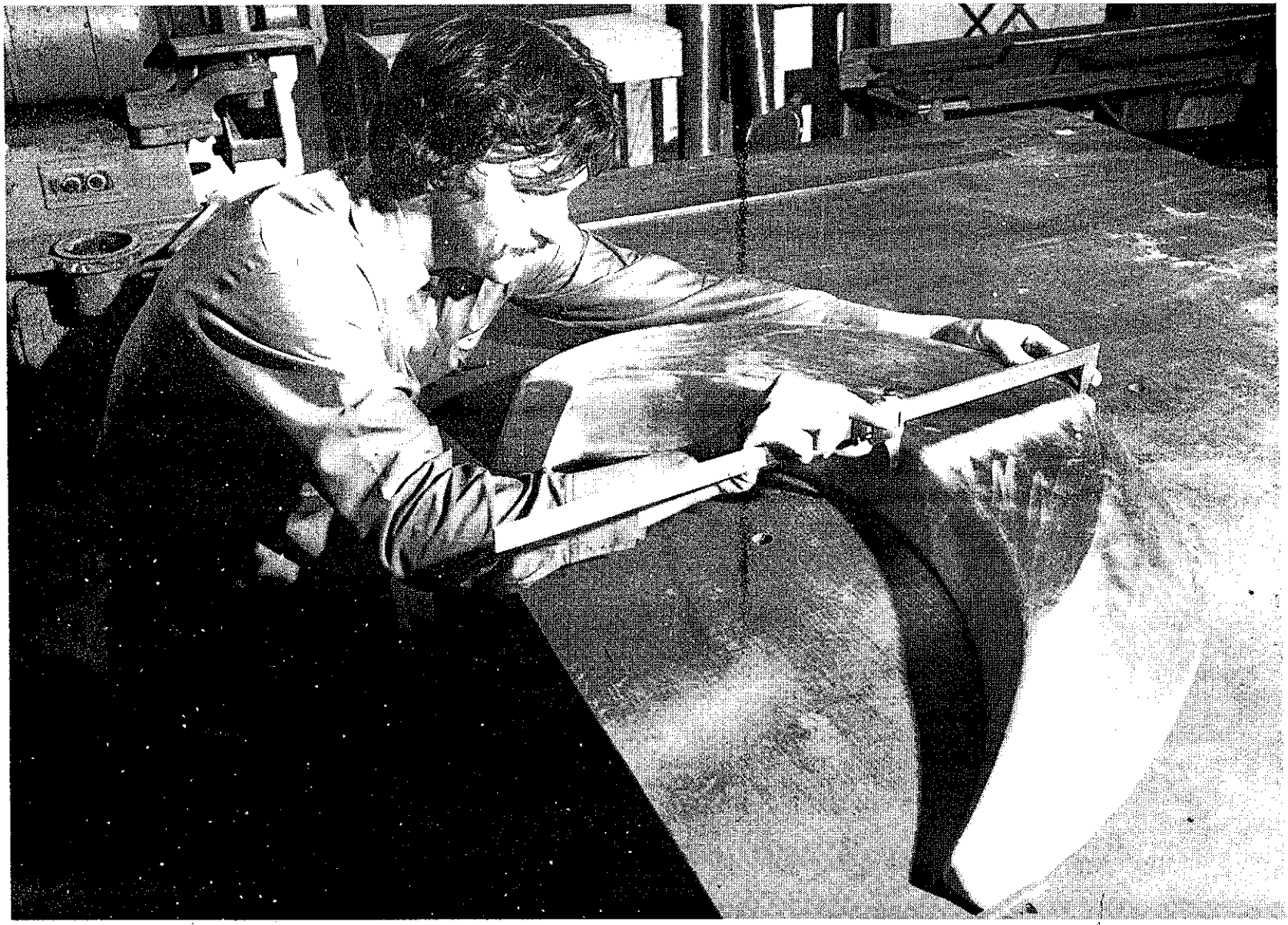

Fig.II.14. Upper half of the No. 2 dee with measurements in process in preparation for locating the dee stem attachment collar.

Fig. II. 15. Prototype cryopumping panel being set up for tests in a rectangular dummy aluminum vacuum box. The panel will ultimately mount inside the dee, the outer crescent shaped box in the figure being at 80°K with the chevron in the worker's hand facing the beam space and protecting the 4.5°K surface.

Fig. II.16. The set of aluminum pole tips which will be used as a "hammer form" in fabricating the copper liner structure. This liner will completely cover the poles and isolate the trimming coils in a separate vacuum envelope.

for coping with a variety of unexpected minor problems. The years of operation of the magnet include a lengthy period of use as an ion source testing facility and several long periods of magnet measurements. In the course of this work the operating range of the superconducting coils has been modestly extended from the original design value of 700 amps/turn (3,500 amps/$cm^2$ average current density) to 800 amps/turn (4,000 amps/$cm^2$). With this added range, the two independent sections of the superconducting coil can be used as supplemental field trimming elements at all field levels, and the power requirements on the room temperature correcting coils have been reduced to the very attractive level of approximately 20 kW total power for all coils.

The prototype rf resonator was first operated at full design voltage in May of 1979 and has since operated over the full frequency range of the system confirming basic design features. Important improvements in a number of design details have also been introduced, including improvements in the contact finger system on the "sliding short" tuning structure and replacement of an original leak-prone vacuum seal system on the dee stem insulators with a new ruggedly reliable system. The dee stem insulators themselves were a subject of considerable anxiety in the original design, but have proved to be completely reliable throughout the testing period.

Extensive additional work on orbit calculations has also been performed using the detailed field information

obtained from the magnet mapping. Generally these calculations indicate excellent beam quality, matching the levels achieved in the 50 MeV cyclotron, and with focusing along the extraction path significantly improved relative to the 50 MeV machine. One uncertainty not yet resolved, concerns operation of the machine with doubly charged $^3$He, due to a focusing resonance which occurs as a consequence of the low magnetic field which is needed for this ion. A technique for avoiding this resonance has not yet evolved, but exploration of possible mechanisms continues. Pending solution of this problem the energy maximum for $^3$He is at 133 MeV, which corresponds to the single charged ion. This resonance also cuts off the possibility of proton acceleration except as singly charged molecular ions.

Substantial prototype tests have also been made on other cyclotron sub-systems including the ion source, the cryopumping system. the deflector high voltage system, and a considerable number of less important systems. The overall testing program should, we feel, lead to a smooth turn on of the complete cyclotron. We then expect the cyclotron to be able to take up its role as a "black box" for the nuclear science program after a relatively brief debugging period on the overall system.

## B. BEAM TRANSPORT AND ANALYSIS SYSTEM

The layout of the experimental floor as shown in Fig. II.1 includes an arrangement of beam transport elements

designed to accomodate the wide variety of beams expected from the K500 cyclotron. Calculations to design this system include ray tracing in the fringing field region of the cyclotron(where special measurements were made) and conventional matrix methods for the rest of the beam line. A major design feature of the system is the provision for a variable linear and angular dispersion at the magnetic spectrograph target in order to accomodate matching conditions in the "energy-loss" mode for the wide variety of reactions and detection systems which will be utilized.

The basic configuration for the Phase I experimental floor includes a fanning out from a large existing dipole and a shielding system which separates the experimental area into two large rooms designated North and South. The North vault houses the present Enge split-pole spectrograph, a new, low-resolution spectrograph capable of bending the most rigid beams, a high resolution scattering chamber from the University of Minnesota, a low rigidity beam line (which can also be used for full rigidity beams by stripping after acceleration) and the counting apparatus for the cryogenic helium-jet apparatus. The South experimental room will house the 60 inch scattering chamber, an initial version of the recoil mass separator, a gamma ray goniometer, and the target for the cryogenic helium-jet apparatus.

The design of the beam transport system is strongly influenced by an unusual feature of the extraction system of the K500 cyclotron, namely that the extraction system

consists entirely of inert focusing elements. This feature greatly simplifies design and construction of the extraction system itself but at the cost of a variability in direction and focusing conditions for beams leaving the cyclotron. (The basic cause of this phenomenon is the fact that the inert extraction system focusing elements stay at fixed absolute strength whereas bending and focusing effects of the fringe field vary in proportion to main field strength.) The first section of the transport system must then be used as an active element to compensate for this variability in order to bring all beams to an approximately identical phase space condition at the location of the first slit. Figure II.17 shows an example of two extreme beams tracked through this portion of the optical system, the quantity plotted being the horizontal and vertical envelope of the beam as a function of path length through the system. As the figure shows, the beam transport system in this region includes sufficient optical elements to allow compensation for the variable emittance condition from the cyclotron while at the same time keeping hte beam evelope within reasonable limits ($<\pm 2$ cm). Figures II.18 through II.20 are envelope plots similar to II.17 for beams going forward from the first slit to the various experimental devices. Table II.1 summarizes major optical parameters of the system for each beam line.

With respect to the actual beam line hardware, we have elected to use an aluminum system because of its

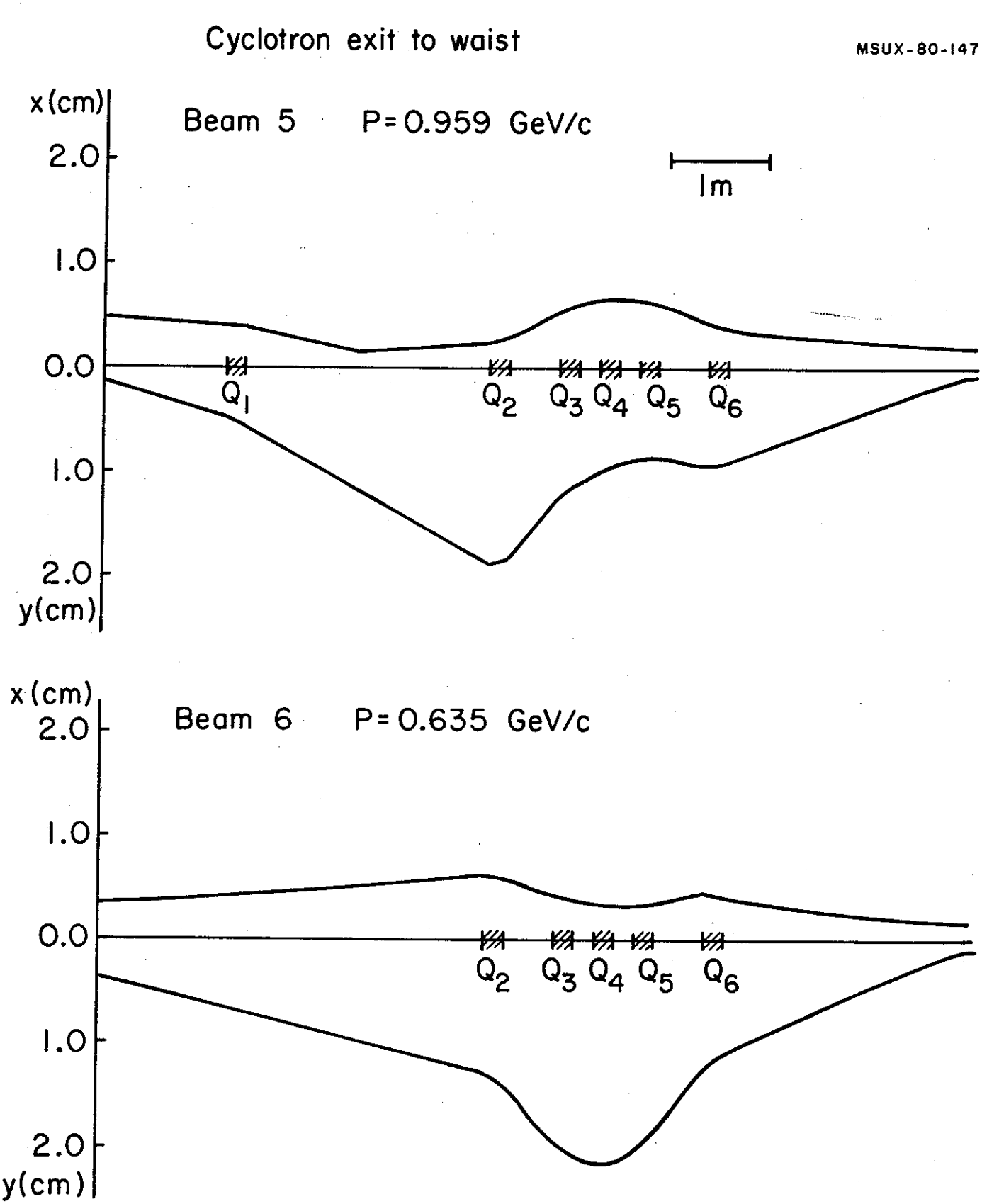


Fig. II. 17. Plot of horizontal and vertical beam envelopes from the cyclotron exit to the waist located at the first defining slit. The two beams represent the extreme limits of the distribution of focusing conditions for beams leaving the cyclotron. With appropriate adjustments of the six quadrupoles, the beams are brought to an approximately identical focusing condition at the first slit which would be located at the right edge of the figure.

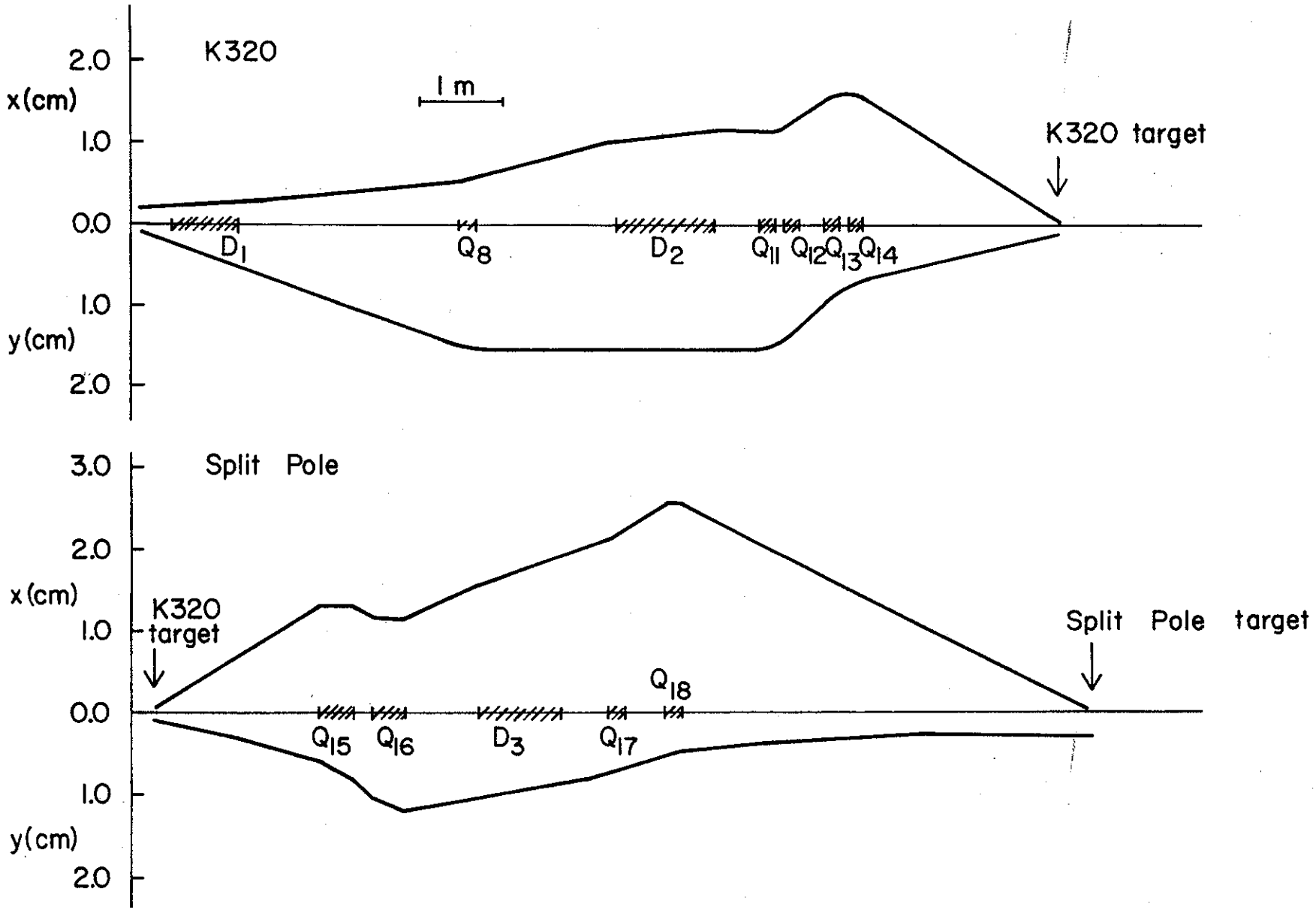


Fig. II. 18. Top--Plot of horizontal and vertical beam envelopes versus distance, for the beam line from the first slit to the K320 spectrograph. Bottom--similar plot for the beam line continuing from the K320 to the split pole. (When the split pole is in use, the K320 is used as a part of the beam transport system.)

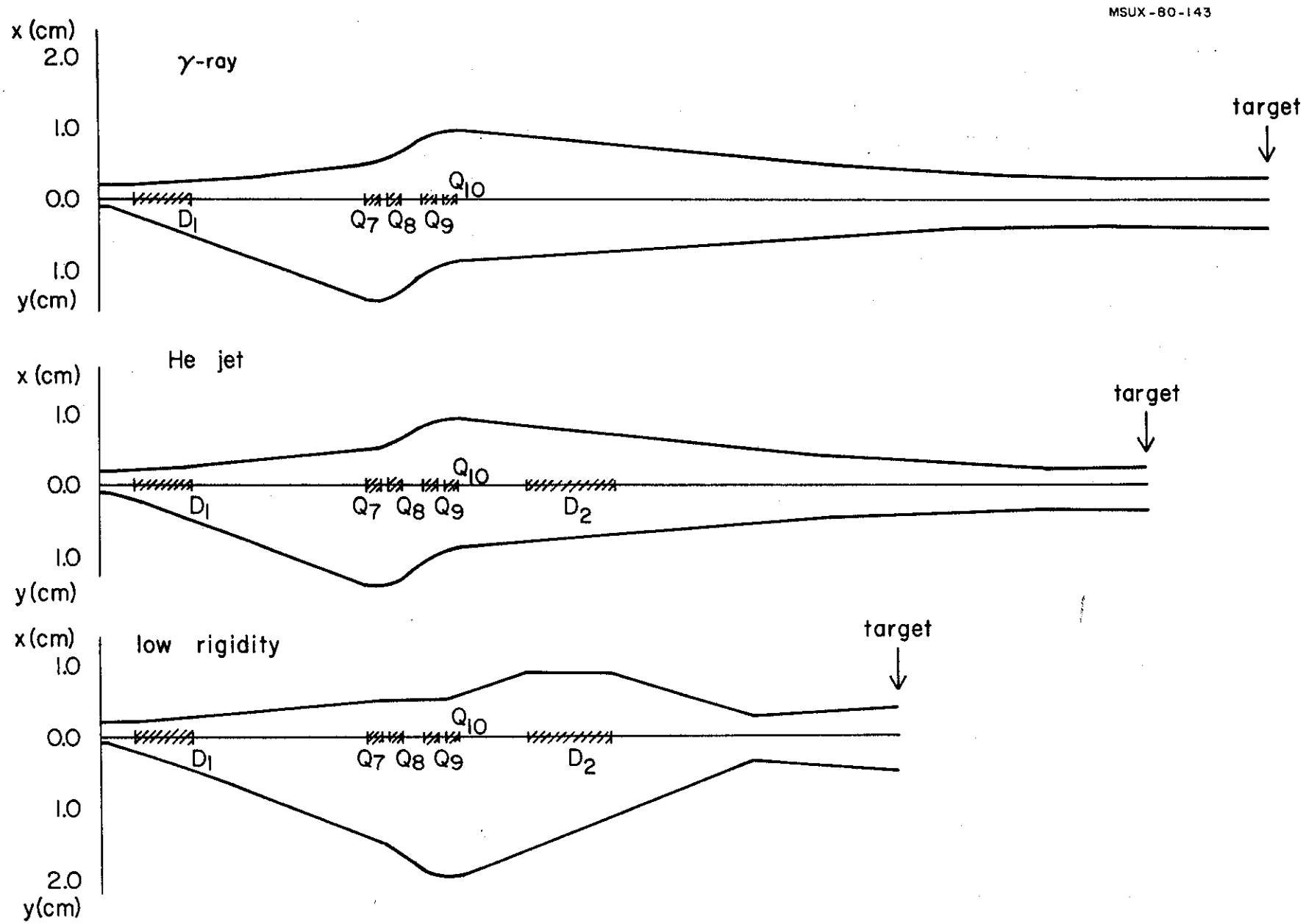


Fig. II. 19. Plot of horizontal and vertical beam envelopes versus distance for beam lines from the first slit to the gamma goniometer, the cryogenic helium jet and the general purpose scattering chamber located on the so called low-rigidity beam line (the upper-most beam line in Fig. II. 1).

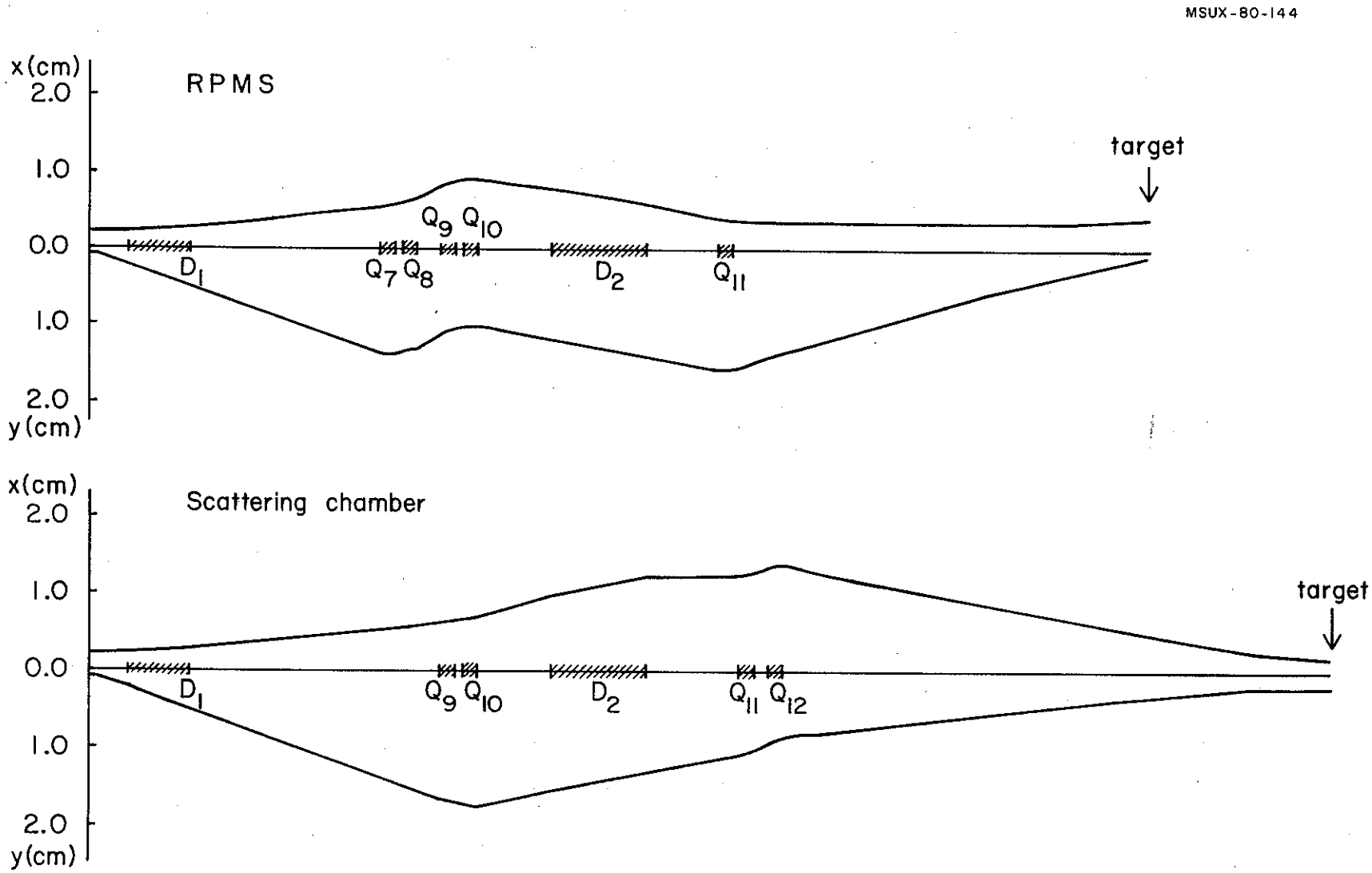


Fig. II. 20. Plot of horizontal and vertical beam envelopes versus distance for the beam lines from the first slit to the recoil product mass spectrometer and the 60 inch scattering chamber.

Table II. 1. Top--"Transport" parameters for the two extreme beams from the K500 cyclotron at the cyclotron exit location and at the initial waist location. "x" and "θ" are the maximum values of horizontal displacement and divergence for particles of a given energy, "y" and "ϕ" are the similar quantities for the vertical displacement and "$R_{16}$" and "$R_{26}$" give the displacement in direction and angle per % momentum variation relative to the central ray. "Beam 5" has a momentum of 0.959 GeV/c, "beam 6" has a momentum of 0.635 GeV/c and both have Q/A = 0.322. Bottom--Corresponding Transport parameters at each of the Phase I target locations.

Beam Parameters in First Section of Transport Line

| | x(cm) | θ(mr) | y(cm) | ϕ(mr) | $R_{16}$(cm/%) | $R_{26}$(mr/%) |
|---|---|---|---|---|---|---|
| Beam 5 | | | | | | |
| at cycl exit | 0.49 | 0.85 | 0.12 | 3.25 | -18.12 | 15.04 |
| initial waist | 0.20 | 1.41 | 0.08 | 3.77 | 7.32 | -22.21 |
| Beam 6 | | | | | | |
| at cycl exit | 0.34 | 0.89 | 0.36 | 2.5 | -0.96 | 21.37 |
| initial waist | 0.16 | 1.54 | 0.10 | 4.61 | 4.78 | -16.26 |

"On Target" Beam Parameters for Various Beam Lines (Beam 5)

| | x(cm) | θ(mr) | y(cm) | ϕ(mr) | $R_{16}$(cm/%) | $R_{26}$(mr/%) |
|---|---|---|---|---|---|---|
| Low rigidity | 0.40 | 3.24 | 0.49 | 4.00 | -2.64 | 28.9 |
| K=320 | 0.05 | 6.47 | 0.11 | 2.88 | -2.64 | 88.97 |
| Split Pole | 0.06 | 5.19 | 0.31 | 1.21 | 4.61 | -68.95 |
| He Jet | 0.28 | 1.13 | 0.34 | 0.97 | -11.67 | -2.34 |
| γ-ray | 0.34 | 0.97 | 0.39 | 0.85 | -12.75 | -2.99 |
| RPMS | 0.41 | 1.01 | 0.10 | 2.96 | -12.18 | -9.74 |
| Scatt Cham | 0.15 | 1.96 | 0.24 | 1.31 | -2.23 | 23.48 |

significant advantage in reduced activation and because of its lower cost. The system will be basically all metal in construction (with a few Viton O-rings in the seats of isolation valves). The high vacuum pumping system will utilize both commercial cryopumps and ion pumps. For roughing from atmosphere, two movable pumping stations will be provided, each consisting of a turbomolecular pump backed by a small mechanical pump. The basic beam line and pumping system and major bean line devices have been tested in prototype configurations. Operating vacuum on the basis of these tests is expected to be in the low $10^{-7}$ range.

Operator information on beam conditions will be provided by a combination of slits, beam scanners and scintillating screens (viewed with closed circuit TV). A prototype slit of all metal and ceramic design has been extensively tested, and remaining slits are now under construction. Scintillation screen viewers will utilize a multiple position system with a series of scintillators of varying sensitivity so as to accomodate the large variation in specific ionization and intensity of expected beams.

The shielding wall system utilizes the same concepts as in the earlier system for the 50 MeV cyclotron, namely walls stacked from small 4" x 8" x 16" concrete blocks and a roof consisting of multiple layers of 18" x 30" x 30' movable beams. Figure II.21 is a photograph showing student workers rearranging walls for Phase I. Shielding

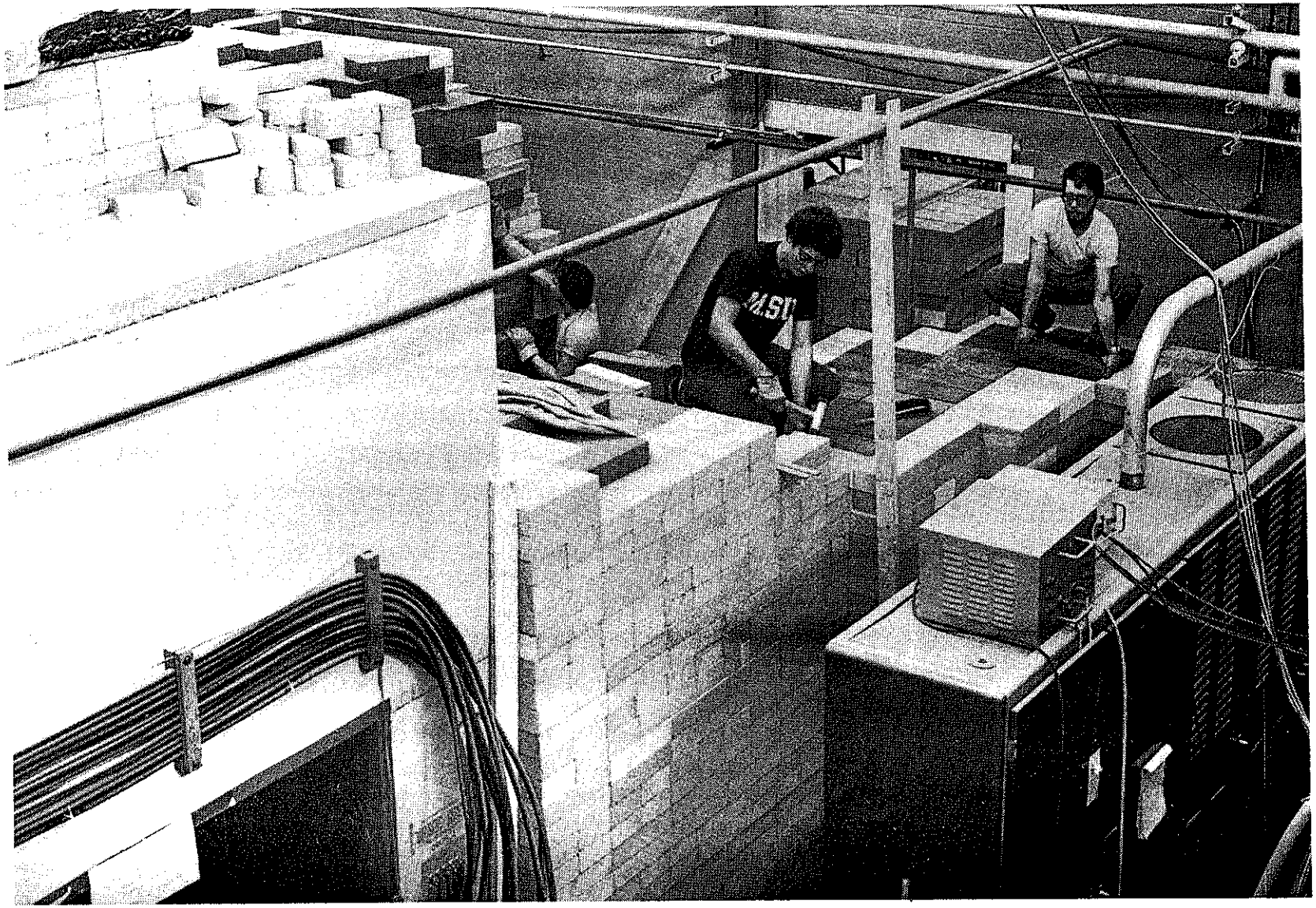

Fig.II.~~20.~~ 21. Student workers in the process of reconfiguring the shielding wall for the Phase I beam transport system.

isolation of one valut from another is provided by iron plugs, which are hydraulically positioned in and out of the beam line.

Work on setting up the beam transport system in the Phase I configuration is now in an advanced stage; shielding walls have been rearranged, the major bending magnet has been set in position, and most beam line components are on order. We expect no difficulty in bringing the system to ready-for-beam condition on the same schedule as first beam testing of the K500 cyclotron.

## C. EXPERIMENTAL EQUIPMENT

This section gives a brief review of the status of the main experimental devices which will be available for the Phase I program plus a review of plans for the large K800 spectrograph which is part of the Phase II program.

The K320 Magnetic Spectrograph. Our existing magnetic detection systems cut off at the bending limit of the Enge Split-pole spectrograph. (If expressed as a "K" value in the same notation as used for the cyclotron the split-pole limit is 120 MeV.) To remedy this deficiency, an interim "K320" spectrograph is being constructed out of a collection of existing elements which in part are magnets left over from the 50 MeV transport system and in part are magnets obtained from other laboratories as surplus property. This K320 spectrograph design is tailored

to take advantage of the excellent quality of the unique light heavy-ion beams (helium, carbon, nitrogen, neon...) from the K500 cyclotron. Possible applications of this spectrograph are described in the research section of the proposal and include systematic studies of elastic scattering, giant resonance phenomena, and transfer reactions.

The goals of the spectrograph design are to have a solid angle of approximately 1 msr, an energy range of approximately 60 MeV at 300 MeV, and an energy resolu tion of approximately 300 keV at 300 MeV. The K320 bending capability of the design is matched to that of the most rigid particles from the K500 cyclotron magnet (since partially stripped ions from the cyclotron have a higher charge after passing through the target and fully stripped ions from the cyclotron are limited to K320 rigidity by focusing limitations in the cyclotron). An additional consideration in the design emphasizes the capability of working at small scattering angles by the incorporation of design features which suppress spurious scattering from slits and pole faces.

A design consistent with these goals has been achieved, and the component layout and beam envelopes of the resulting QQDS System are shown in Fig. II.22. Major hardware elements of the K320 consist of an 8" aperture quadrupole doublet (obtained from SREL via Brookhaven), a beam-line switching magnet from the MSU 50 MeV cyclotron, and a 6" aperture x 8" long sextupole magnet under construction. The scattering

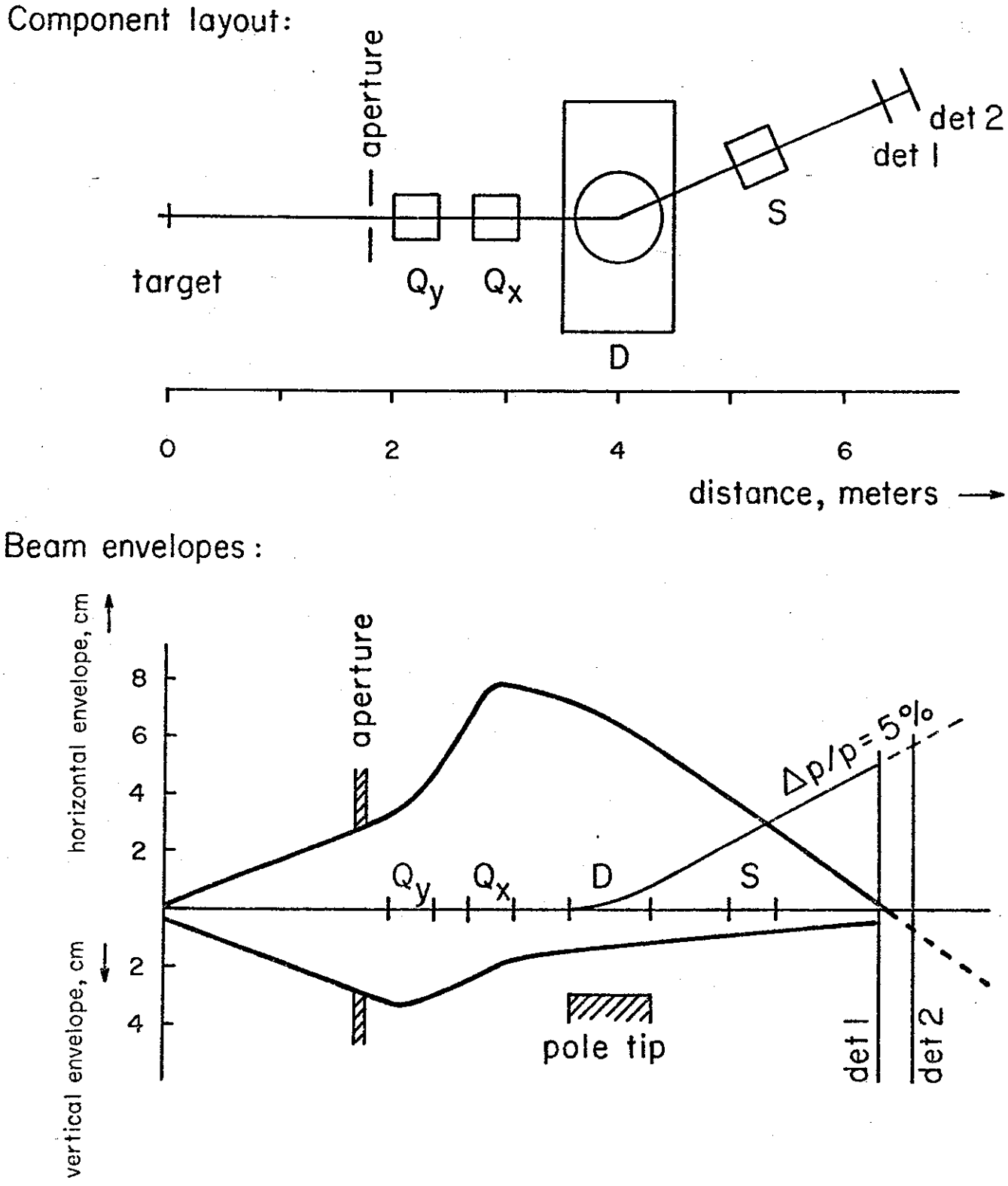


Fig. II. 22. Top--schematic layout of the optical elements of the K320 spectrograph. Bottom--horizontal envelope, vertical envelope and dispersion versus distance for the K320 spectrograph.

chamber to be used with the spectrograph is a precision chamber obtained from the University of Minnesota. Fig. II.23 gives a plan view of the system layout including the Minnesota chamber.

The spectrograph design has been optimized with the matrix search code "Transport" and the related code "Turtle", and the final design has been checked for higher order effects using the ray tracing program "Raytrace". The sectupole magnet serves to correct a steep focal-plane tilt associated with the small bending angle (which is in turn due to the relatively small dipole). The sextupole also greatly improves the resolution by correcting $(x|\theta^2)$ and $(x|\phi^2)$ aberrations. The remaining dominant aberration in the system is $(x|y\phi)$, which is related to the vertical spot size on target. The useful solid angle of the system is limited by higher order terms induced by the strong sextupole, giving an acceptance aperture of $1.5^{o}$ x $1.5^{o}$. With the large target-to-aperture drift distance available in the Minnesota chamber, the actual physical aperture will be large ($\simeq$1" x 1"), and slit scattering will therefore be small.

The spectrograph design assumes that the beam on target has an incoherent width of 0.5 mm and an incoherent height of 3 mm, which are the values predicted by cyclotron and beam transport design calculations. Dispersion matching will be used to eliminate the line-width contribution from energy spread in the beam, and kinematic compensation will be accomplished with the quadrupole doublet.

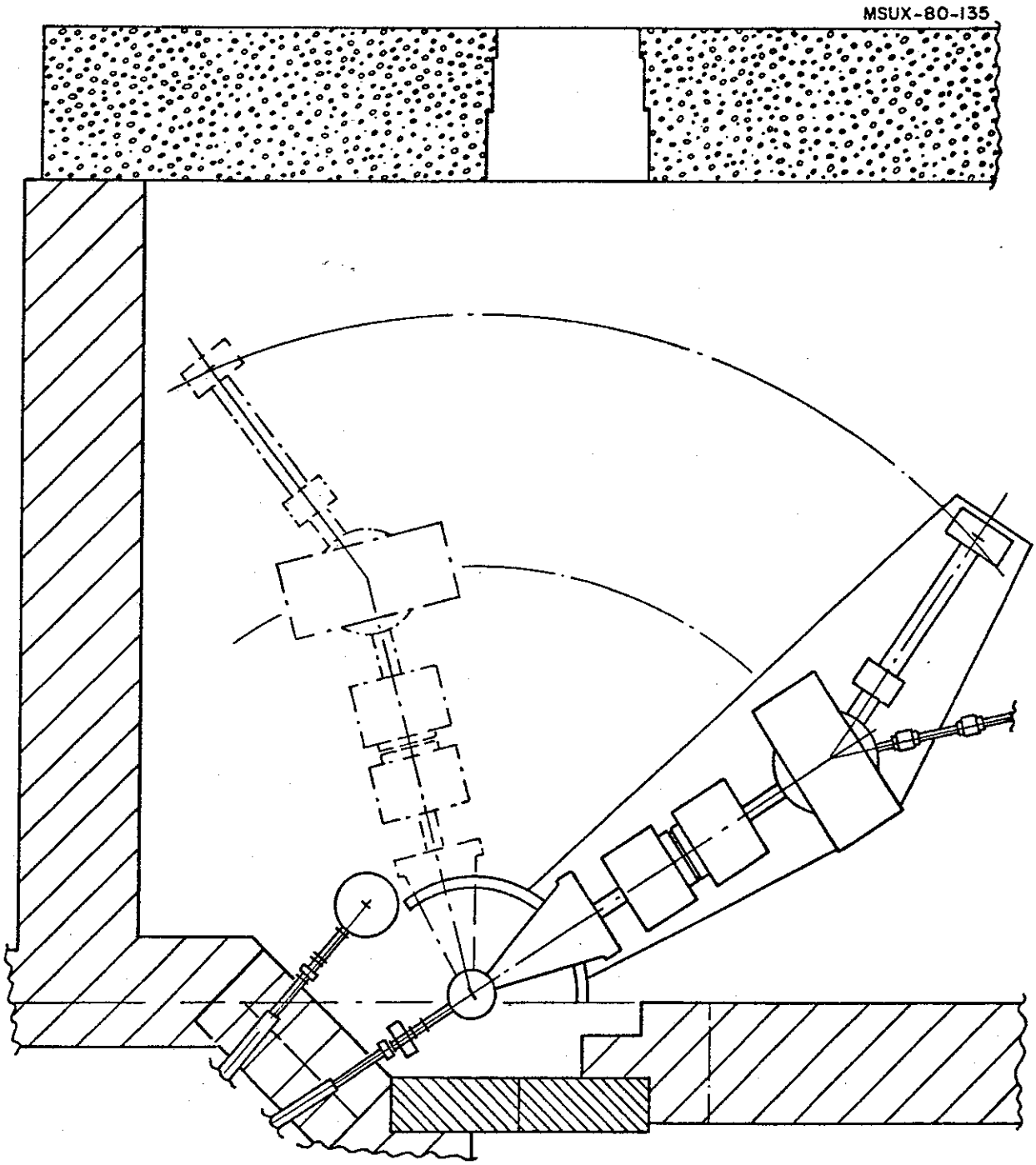


Fig. II. 23. Plan View of the K320 Spectrograph. The large triangular box just after the target is a part of the Minnesota scattering chamber. (This chamber will be used both for spectrograph experiments and for counter experiments.) With the spectrograph at zero degrees as shown by the solid lines, a rightward bending beam line from the dipole will be connected as shown when the K320 spectrograph is being used as a part of the beam transport system to feed beams to the split pole spectrograph. The dashed lines show the K320 at a scattering angle of $70^{\circ}$ which is the limit of its angular range. The second beam line entering at the bottom is the low rigidity line which connects to a small general purpose chamber.

Focal plane detector requirements for the spectrograph are modest. The required detector size is 10 cm long x 3 cm tall, and the particles will have normal incidence. The design energy resolution of 0.1% corresponds to a position resolution of 0.5 mm, which can be achieved with single-wire, resistive-division proportional counters. Particle identification for light ions will use the $\Delta E$ information from the proportional counter plus light output from a backup plastic scintillator. The scintillator signal will also be used for a time-of-flight measurement relative to the rf beam structure from the cyclotron. For heavier ions an ionization counter will be added to the focal plane detector for better total energy and energy loss information.

Enge Split Pole Upgrade. The Enge split pole spectrograph was the most frequently used experimental instrument in the 50 MeV research program, and we expect it to remain a very important instrument in the K500 program. The bending limit of the spectrograph corresponds to 30 MeV/nucleon for fully stripped N=Z ions (and at this energy stripping in the target will put most ions in the fully stripped state). The broad range and inherent high resolution of the split-pole make it an extremely useful device for experiments in the energy range compatible with its bending limit.

To prepare the spectrograph for heavy-ion experiments, a major upgrade of the vacuum system is in process. This

upgrade includes a change to a cryopumping system and a shift to Viton gaskets. The final system is expected to be oil free and should achieve a vacuum below $10^{-6}$ Torr.

The spectrograph focal plane apparatus is being modified to allow the use of large focal plane detectors at the full Bρ of the magnet. A doweling system is also being installed which will allow detectors to be inserted in accurately reproducible locations. The focal plane modifications have also been specifically tailored to provide for use of the heavy ion focal plane detector from the University of Minnesota (this detector is a version of a detector originally developed at Argonne); the location of the high energy end of this detector will correspond to a K value of 120 MeV.

The split-pole spectrograph will also function as an excellent pion spectrograph and is expected to be extensively used for this purpose in the Phase II program. Experiments exploring the near-threshold behavior of pion production phenomena are also contemplated in the Phase I program as discussed in the research section. The techniques developed in the 50 MeV program for measuring low cross section, transfer reactions are broadly applicable to both heavy ion and pion detection. These techniques, which employ both time-of-flight and redundant energy loss information to eliminate background, constitute a highly effective, already existing system. The 3 to 4 meter flight path of the split pole is also well matched

to the beam repetition rate of the cyclotron allowing good separation of particle groups (without at the same time encountering significant problems from accidental overlap of particles from different beam bursts which would occur for longer flight paths).

High resolution experiments in the split-pole spectrograph are clearly possible, the resolution limits coming dominately from target effects. A test run with the 50 MeV cyclotron explored the intrinsic system limitations using a 77 MeV $^{12}C$ beam. Running without a target, a focal plane line width of 1/8 mm or 9 KeV was obtained (vividly demonstrating the effectiveness of the on-line resolution optimization techniques which have been developed). Taking account of target effects, we expect to be able to obtain overall resolutions of better than 1 in 1000 which would for example allow elastic scattering experiments with 1 GeV $^{40}Ar$ beams (25 MeV/nucleon) from many targets, and these would be the first such experiments in this energy range for ions in this mass range.

Reaction Product Mass Spectrometer. An element of the Phase II Program which is expected to have important beneficial impact on the Phase I program is a prototype section of the Reaction Product Mass Separator (RPMS). Both the prototype and the final device have the same basic goal, namely to take reaction products as they are emitted from the target and focus them on a mass dispersive, energy non-dispersive focal plane. (Such a system differs

from the usual "on-line" mass separator in that no intermediate ion source is used in the RPMS; this has the important benefit of decreasing the delay time between production and detection from several milli-seconds for on-line separators to a few microseconds for the RPMS.) The final RPMS is designed to collect reaction products over a relatively large solid angle, and an incident beam steering system will allow this collection angle to be centered at scattering angles from $0^{o}$ to $30^{o}$. With proper selection of reaction kinematics, a large fraction of the yield from any desired reaction should thus enter the RPMS. Many studies of previously unobserved isotopes and isomers will then be possible with this device.

The configuration of the prototype RPMS is shown in Fig. II.24. The system will be constructed mainly of components presently in the laboratory and is therefore expected to be ready for use on roughly the same schedule as the K500 cyclotron. The heart of the device is a "Mark VI" Wien filter which was loaned to us by the Lawrence Berkeley Laboratory. This filter is five meters long and for 20 MeV/u particles will operate with an electric field of 36 kV/cm over a 10 cm gap and a magnetic filed of 570 gauss. Focusing will be provided by four 8" aperture quadrupoles (obtained from SREL via Brookhaven) and a magnetic dipole (from the 50 MeV cyclotron beam transport system) will be used to cancel the energy dispersion introduced by the Wein filter so that for ions of given mass the

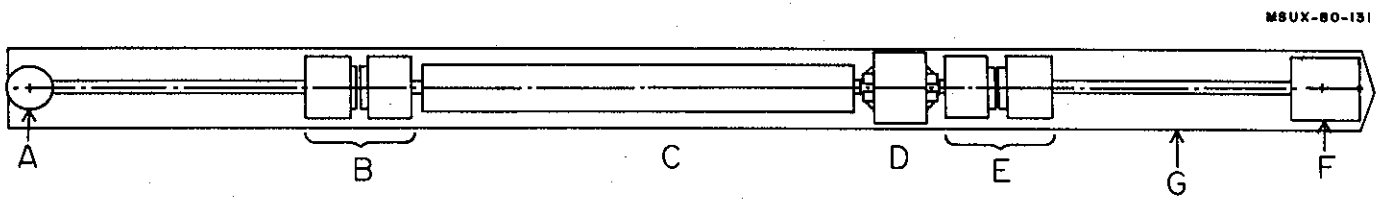


Fig. II. 24. Plan View of the Recoil Product Mass Spectrometer in the prototype configuration which will be initially used in the Phase I program. "A" is a scattering chamber, "B" and "E" are quadrupole doublets from SREL, "C" is a Mark VI Wein filter on loan from the Lawrence Berkeley Laboratory, "D" is a dipole from the MSU 50 MeV transport system, "F" is a detector box and "G" is a support rail for the total system. Scattering angles from zero to 30° will be available by shifting the left hand end of the rail horizontally so as to move the scattering chamber relative to an immediate upstream dipole, this dipole being adjusted to give the bending needed for the particular scattering angle.

dispersion of the complete system is zero. The complete protype RPMS system will be 14.3 meters long and will have a solid angle of ≃1 msr. The system is designed to work up to a momenta of 800 MeV/c which corresponds to 80 MeV/u for fully stripped N=Z nuclei. (For neutron rich nuclei, this of course, decreases to, for example, 35 MeV/u for $^{18}C$.) Slits before the first quadrupole will define the solid angle, and a slit between the Wein filter and the magnetic dipole will define the energy bandpass.

The mass resolution of the RPMS depends critically upon the energy bandpass and the solid angle. When the prototype system is operated at 20 MeV/u with 16% energy acceptance and a solid angle of 1.2 msr, the mass resolution will be $m/\Delta m \simeq 50$ (base to base). At the same energy, if energy acceptance is reduced to 6% and solid angle to 0.3 msr, the mass resolution is increased by a factor of 10, i.e. $m/\Delta m \simeq 500$.

After sufficient experience has been accumulated with the operation of the prototype RPMS, the design for the final Phase II device will be fixed, and at an appropriate point the final device will be substituted for the prototype. This device as presently envisaged will be 18.2 m in length. the additional length allowing aberration compensating unit cells to be inserted, which will have the effect of increasing the mass resolving power, $m/\Delta m$, to 200 at a solid angle of 1.6 msr with an energy bandpass of 8%

at 20 MeV/nucleon. As in the prototype an additional factor of 10 in mass resolution will be available by reducing the solid angle (to 0.1 msr). This final version of the RPMS will also have the capability of being able to focus all particles and energies which can be produced with the cyclotron.

A wide variety of focal plane detection systems are liekly to be used with the RPMS, reflecting the broad scope of possible experiments, and the focal plane configura tion will be appropriately flexible.

Fusion evaporation reactions are an example of one class of reactions which the RPMS should handle with great effectiveness. Reactions such as $^{40}Ca + ^{64}Zn \rightarrow ^{100}Sn + 4n$ in general provide potential access to heavy,very proton-rich,nuclei. Yields are concentrated near $0^{\circ}$ relative to the beam, and the RPMS is specifically designed to function at $0^{\circ}$. (The incident beam is intercepted at the entrance to the first quadrupole, so that the beam is prevented from entering the Wien filter -- this is in fact, necessary since the relatively large dispersion of the device could easily cause the beam to strike the electrostatic plates leading to voltage breakdown and possible plate damage.)

The RPMS should also be an excellent device for studying products of deep inelastic reactions, in which the peak cross section is generally displaced from $0^{\circ}$ but usually is contained within the 0 to $30^{\circ}$ angular range of the system.

High Precision Goniometer for In Beam γ-ray Spectroscopy. The laboratory's existing high precision goniometer will be located on a beam line in the South experimental hall and will provide capability for in-beam gamma-ray spectroscopy experiments. The major arm of the goniometer is four feet long and is capable of supporting a Ge(Li) detector system complete with cryostat and dewar, while maintaining an angular precision of approximately $0.1^{o}$. A second two foot arm has a similar capability. The goniometer system includes a number of interchangable target chambers including chambers with sliding seals for particle and low energy photon experiments as well as large circular chambers for precision angular correlations. A narrow, flat-sided, thin-window chamber for gamma-gamma coincidence experiments is also available. The chambers include provision for automatic target changing and positioning, and a variety of slits of various materials are available for collimation and monitoring of the beam. A heavily shielded beam dump will also be provided as a part of the overall facility.

Sixty Inch Scattering Chamber. A large sixty inch diameter general purpose scattering chamber has been ordered,based on a design which uses the base plate and hub from the laboratory's existing forty inch scattering chamber. The new chamber will have a hemispherical dome, and the overall increase in size will allow relatively large detectors to be used, and the detector assemblies can function at more forward angles. In addition the

larger size will make it possible to carry out time-of-flight measurements within the chamber, and detectors can be placed out of the horizontal plane as is often important in complicated coincidence experiments. The precision hub from the 40" chamber provides two independent angular motions, namely a table with a full $360^{o}$ rotation capability with motion accurate to $\pm 0.03^{o}$ and an arm, 6" in width, also movable through the full $360^{o}$ with accuracy of $\pm 0.03^{o}$. The hub also contains a target holder mechanism with a rotational accuracy of $\pm 0.1^{o}$ and an independent 6" vertical motion. All movements are controlled by stepping motors with digital read-out and control both locally and at a remote location. In its new configuration the system will be connected directly to the data processing computer to allow automatic recording of parameters and to premit programmed operation of the chamber.

The pumping system for the chamber will consist of two large cryopumps on the chamber proper plus an ion pump in the beam line immediately adjacent to the chamber. This system, in combination with an oil free roughing module, is designed to pump the system to $5 \times 10^{-6}$ torr in one hour and to reach an ultimate vacuum in the $10^{-7}$ range.

Cryogenic Helium Jet. The liquid nitrogen cooled helium jet system which was constructed and used with the K=50 cyclotorn will also be used with the K500 machine.

This apparatus consists of a target assembly which can be cooled to 77 K, a He capillary which runs through the shielding wall (into the North experimental vault) and a detector chamber. At low temperatures, reasonalbe transport efficiency for radioactive atoms can be obtained without the need for impurities in the helium. The device is thus, for example, suitable for recoil time-of-flight measurements on delayed proton and alpha emitters, and the first use of the device was in fact in observing the delayed proton emitter $^{24}$Si. In this application the alpha particle passed through the catcher foil, stopped in a silicon detector, and was detected in coincidence with the residual nucleus ejected by the decay. The time delay and the proton or alpha energy was then used to calculate the mass of the nucleus responsible for the decay. Such a technique is only practical if there is no microscopic buildup of impurities on the surface of the catcher foil, a condition satisfied by the cryohelium jet. Beams from the K500 cyclotron will open up a broad category of interesting new studies with this device.

K800 Spectrograph. The Phase II project, as previously mentioned, provides for the addition of a number of major new experimental facilities One of these, the reaction product mass separator, or RPMS, has already been discussed since a prototype section of this device will be brought into operation for concept testing and ititial experimental use during the Phase I years. Two other major magnetic

devices are included in the Phase II funding, namely 1) a superconducting solenoid reaction product collector, and 2) a large high-resolution spectrograph with bending power matched to that of the K800 cyclotron. These and other Phase II devices will for the most part not be available for use during the period covered by this operating proposal, but we nevertheless include here a brief description of present plans for the largest of these devices, the K800 spectrograph, in order to give a reasonably complete picture of long range plans for the facility.

Design work on this spectrograph is in fact proceeding rapidly in response to the need to fix space and foundation requirements for the spectrograph in the early Spring of this year so that the preparation of architectural specifications for building construction can proceed. Design goals are listed in Table II.2. The actual design of the spectrograph utilizes many features from the HRS

Table II.2. Design Goals for the K = 800 Spectrograph.

| | | | |
|---|---|---|---|
| 1. | Magnet Rigidity: | 4 t-m | (K = 800, 200 MeV/A $^{40}Ca$) |
| 2. | Energy Resolution: | 1 in $10^4$ | (800 keV at 8 GeV) |
| 3. | Solid Angle: | >5 msr | |
| 4. | Energy Range: | 10% | (100 MeV at 1 GeV) |
| 5. | Angular Resolution: | 2 mr | |
| 6. | Angular Range: | $-20^{\circ}$ to $130^{\circ}$ | |

at LAMPF, including the major decision of using a bending plane perpendicular to the scattering plane. This arrangement has the important advantage of decoupling the energy loss compensation system from the scattering angle so that settings which are tuned for high resolution at one scattering angle should hold for all scattering angles. The focal plane coordinate perpendicular to the spectrograph dispersion plane also becomes a scattering angle coordinate with good angular resolution. Also as at the HRS a phase space rotater will be provided in the beam line feeding the spectrograph in order to achieve the most favorable emittance matching for given reactions.

The useful solid angle of the spectrograph will be 20 msr with energy resolution and angular resolution at the values indicated in Table II.2. At this solid angle a four parameter focal plane detector system is required measuring position and direction both along the dispersion plane and perpendicular to the dispersion plane. If the spectrograph is operated with reduced solid angle (5 msr) the energy and angular resolution goals can be achieved with a two parameter detector system, (measuring position both along and perpendicular to the dispersion plane). There will also clearly be a large class of experiments in which the spectrograph will function as a filter in order to separate rare events from intense backgrounds. For these experiments it will be most advantageous to use the full solid angle and reduced resolution, and a

single two dimensional detector will adequately handle this situation.

The geometrical arrangement of the spectrograph is shown in Fig. II.25, and beam envelopes are indicated in Fig. II.26. Quadrupoles 1,2 & 3 will include adjustable multipole components which will be adjusted for optimized resolution.

A prototype of the four dimensional focal plane detector system will be constructed in the coming year and tested in the K320 spectrograph. This will provide experience and verification of an important element in the high resolution spectrograph design. It should also, at the same time, improve the resolution of the 320 MeV spectrograph.

## D. AUTOMATIC DATA PROCESSING SYSTEM

The effectiveness of a nuclear laboraotry is always stongly dependent on the reliability, convenience, and power of its data processing system. Our laboratory has had a tradition of strength in this area beginning in early days with the original acquisition of the Sigma-7. This system over the years evolved into innumerable revised configurations, in the hands of a creative and responsive computer staff reacting to the needs of the nuclear science program. Now, the Laboratory's data processing capability is entering a major new phase as a consequence of a) the Sigma-7 nearing the end of its useful life and b) the

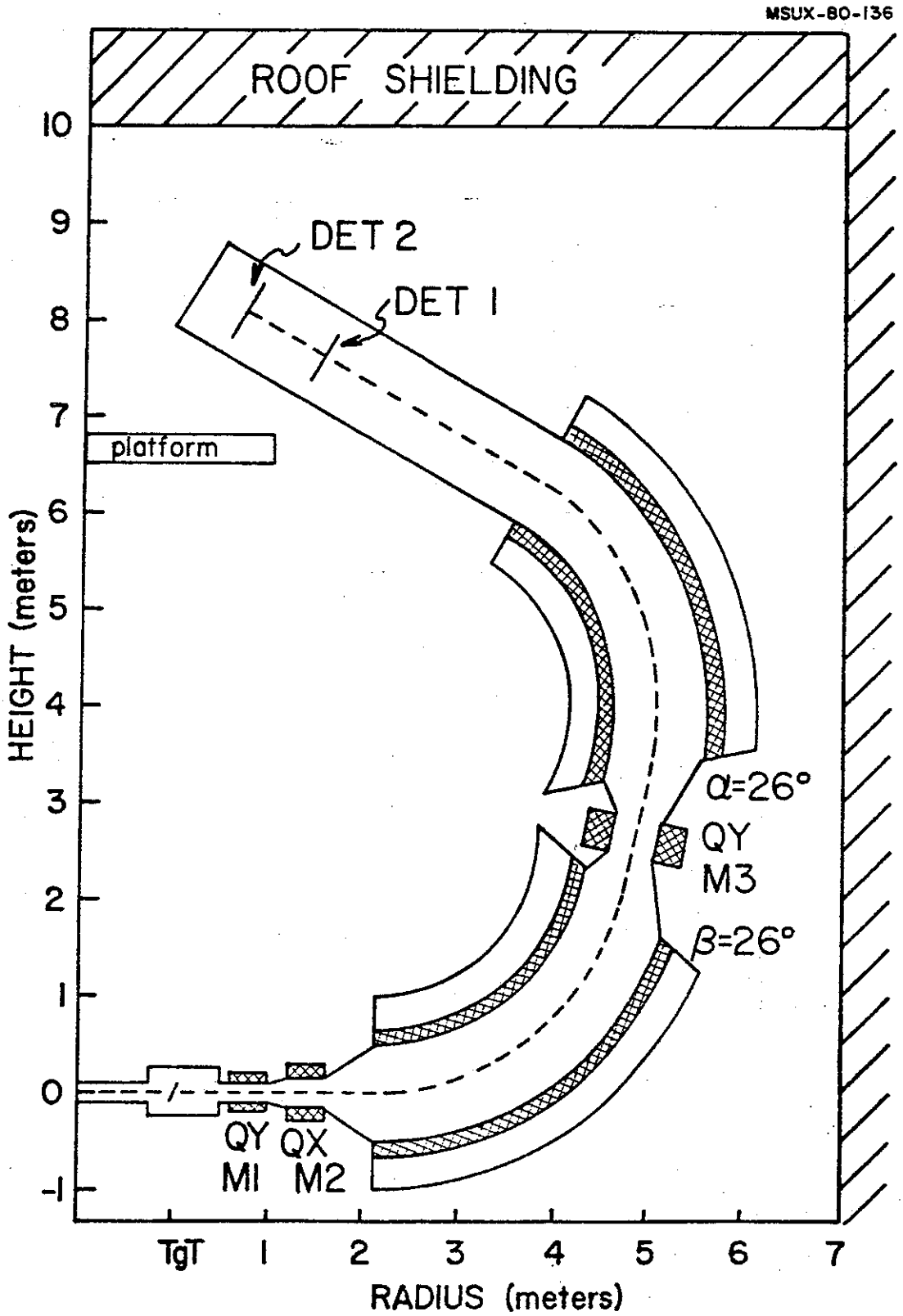


Fig. II. 25. Spatial arrangement of major elements of the K800 Spectrograph. The spectrograph is located in a depressed pit and bends the beam vertically in the fashion of the HRS at Lampf. The platform at the upper left is at the level of the main floor of the Laboratory.

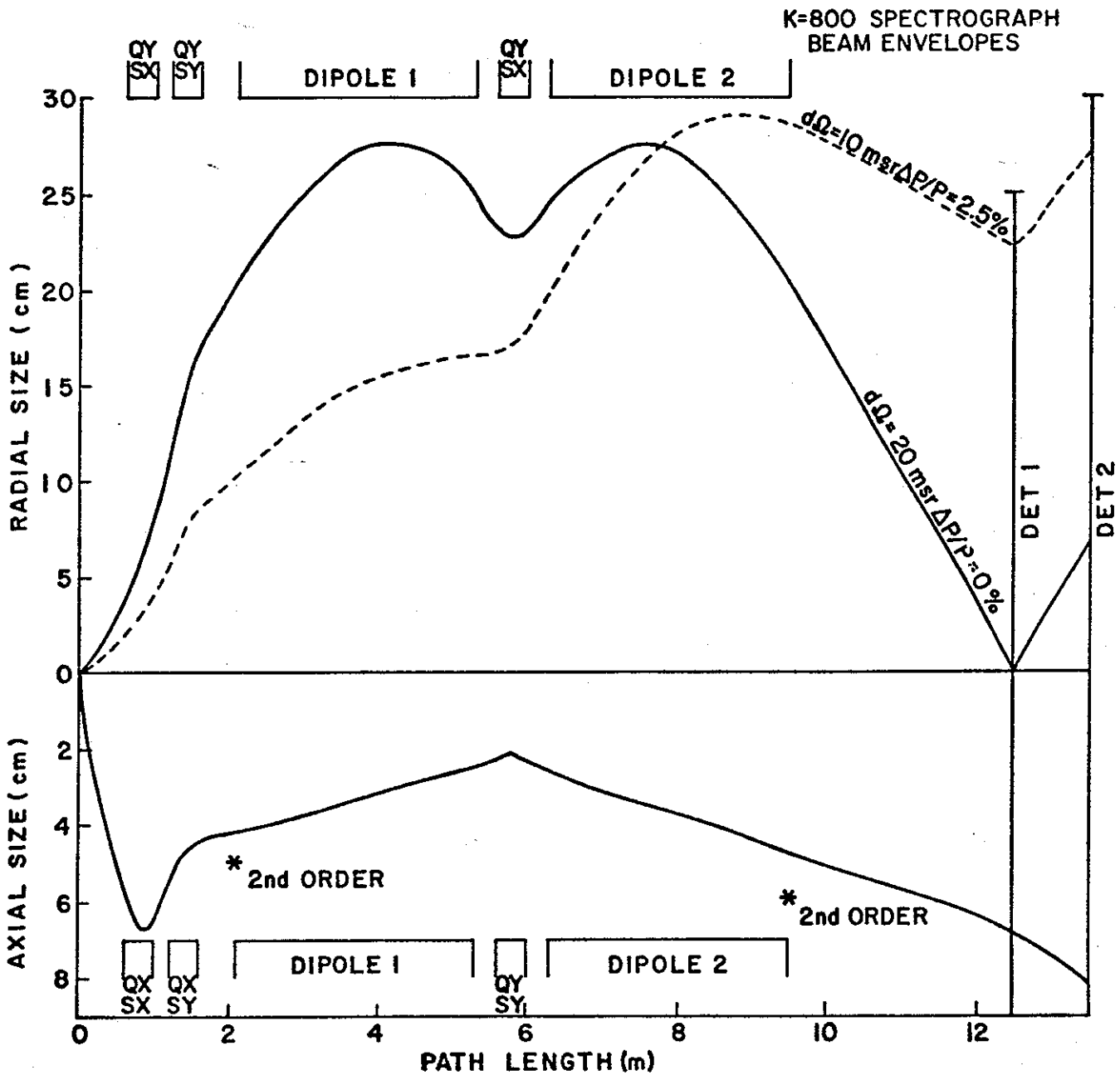


Fig. II. 26. Top--plot of the in-the-bending-plane beam envelope and dispersion versus length for the K800 spectrograph. Bottom--plot of the perpendicular-to-the-bending-plane beam envelope.

need to begin phasing in the much more powerful data processing system which is provided as part of the Phase II project. This transition will include a major shift in the basic architecture of the computer complex, namely a change away from the present "master" plus "satelite" system to a configuration consisting of a cluster of basically identical"master"computers each operating independently and each able to communicate with its neighbors via a high speed interconnecting network.

The Phase II processing system is then envisaged as consisting of six 32 bit master computers (each having capabilities approximately corresponding to the Digital Equipment VACS series). Five of these six computers would be attached to five experimental console units, each console unit connecting through a mini-computer and CAMAC to a fixed subset of the experimental devices. At a given time, one of these console/computer units would be serving the primary running experiment, a second might be serving a background experiment, a third would probably be involved with a setting-up experiment, and the remaining systems would be available for playback and analysis of data from previous experiments. The sixth master computer would have the same basic mainframe, but would have a larger memory and file structure and would both handle the general computing needs of the laboratory and serve as a library and storage facility for all computers in the system.

The procurement plan for this system is divided into two steps, the first step involving procurement of three

of the central processor units. These will be set up in the configuration shown in Fig. II.27, i.e. two of the computers will serve experimental console units for the North vault and South vault respectively, and the third will take on general purpose computing and library functions. This first stage system then involves all basic functions of the final system and allows a testing of the concepts prior to committing the full package and also allows software development for the final system at an early date.

Moving forward with this plan, two console units are presently being set up in the data acquisition room. Each of these will be completely self sufficient in terms of the NIM and CAMAC modules necessary to service the associated experimental apparatus, and each will also have a control module which will allow the experimentalist to monitor the beam and control various items of apparatus. Each console will also have a dedicated mini-computer, which will process all events, execute validity checks, block, label and address the data and finally, transfer the data to the master computer associated with that console unit for further processing and storage on disc or tape.

The advantages of employing the mini-computers as intermediaries include the decoupling of detailed hardware considerations from the general purpose analysis program and a very significant reduction in the interrupt rate

on the main system. Hardware dependent aspects of data acquisition are also removed from the main system so that the main system is able to work with advanced general acquisition routines which are easily modified as research interests evolve. A final advantage of the procedure is that the general codes can be made machine independent and hence easily transferable to computers at the home institutions of users, the issue of maximizing compatibility between the lab's data processing equipment and that of the potential user's, being a point of major concern in the design of the overall system.

Commenting on the status of procurement arrangements, a Request for Proposals package for the equipment needed to implement the plan shown in Fig. II.27 has been completed and submitted for DOE review in accord with procedures stipulated in the Phase II contract. When this review is completed, the package will be issued to vendors, after which proposals will be received, evaluated and an order placed. Finally, sometime in early 1981, the system should be available for use. In the meantime data processing and computing will continue to use existing facilities of the Laboratory.

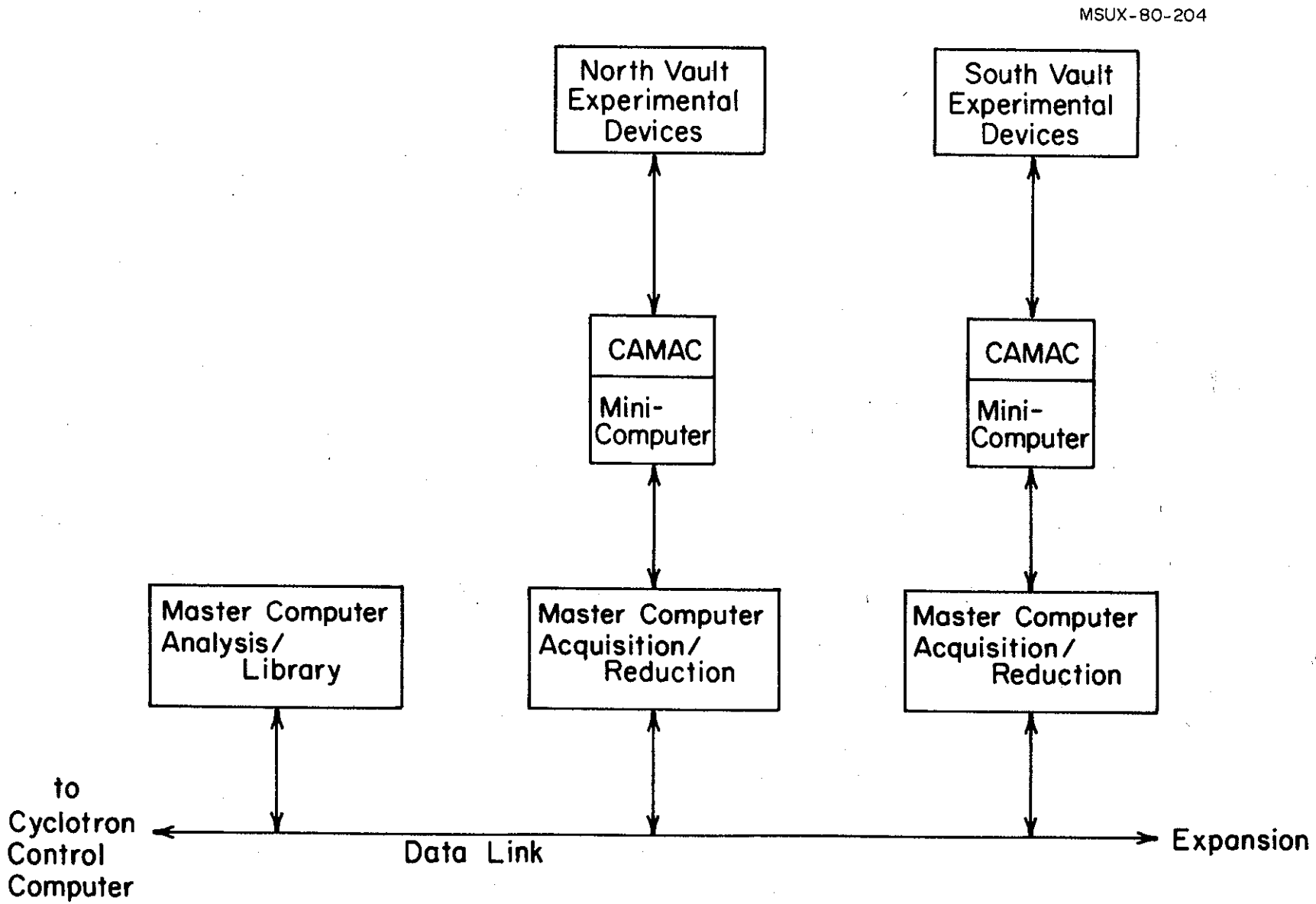


Fig. II. 27. Block Diagram showing major elements of the three-master-computer prototype arrangement of the Phase II data processing system. This prototype system is expected to come into use in the first half of 1981.

# III. PROGRAM OF RESEARCH IN NUCLEAR SCIENCE

## INTRODUCTION

The K500 cyclotron will give access for the first time to a new region of incident energy with beams of high quality and high intensity. The production of the lighter ions up to 80 MeV/u and of ions with mass 50 up to 20 MeV/u permits experiments which will test the extrapolation of current theoretical approaches which have been developed for both higher and lower energies. Furthermore, this energy region holds many possibilities for the study of exotic phenomena. For heavier ions, of mass 50-100, the energies up to 10 MeV/u will allow the continued detailed study of heavy ion reactions which at present can be pursued at very few accelerators. The range of research topics accessible with the new cyclotron is therefore extremely broad. In the discussion of our proposed research, we have selected areas which we believe will make imaginative use of the new facility and for which we have the appropriate experimental equipment. Some of these topics are continuations and extrapolations of previous research efforts by MSU staff. We therefore expect a smooth and rapid transition into the new areas of nuclear science provided by the K500 cyclotron. There will, of course, be many other areas of interest pursued by the community of outside users.

The scientific material presented in the proposal is divided into three major sections - Nuclear Reaction Mechanisms, Nuclear Strucuture, and Exotic Processes - though, of course, there can be no hard dividing lines between them. In reaction mechanisms we discuss mainly the new possibilities for heavy ion processes. The main emphasis in nuclear structure is on the excitation of new structures at high excitation. The section on exotic processes deals with nuclei far from stability, fundamental processes of astrophysics and weak interactions, as well as phenomena related to high energy studies, like critical opalescence and pion production.

The discussion of each topic usually consists of a combined review of the highlights of previous work and an anticipation of future directions. We hope that this approach will provide a brief overview of the current and future program, with sufficient detail for reviewers to assess the overall quality and vitality.

## A. NUCLEAR REACTION MECHANISMS

### A1. ELASTIC SCATTERING

a. Background at MSU

b. Heavy Ion Optical Potential

c. Heavier Projectiles ($A \gtrsim 50$)

d. Reaction Cross Sections

e. Backward Angle Elastic Scattering

f. Nuclear Josephson Effect

### A2. NUCLEON TRANSFER REACTIONS

a. One and Two Nucleon Transfers

b. Cluster Transfers

### A3. HEAVY ION REACTION MECHANISMS

a. Energy Dependence of Peripheral Reactions

b. Isotope Production with Peripheral Reactions

c. Central Collisions

## A. NUCLEAR REACTION MECHANISMS

### A1. ELASTIC SCATTERING

Elastic scattering is the simplest and, perhaps, the most fundamental interaction between two colliding nuclei. A thorough understanding of elastic scattering is a prerequisite for the perturbative description of more complex processes such as inelastic scattering, transfer reactions, and breakup reactions. Continuing studies of elastic scattering will, therefore, be a significant part of the MSU research program. One of the major objectives of such studies is the investigation and establishment of the optical potential between the two colliding nuclei.

#### a. Background at MSU

For several years there has been an active program at MSU to study details of the optical potential with lighter projectiles. As an example of recent work , Fig. 1 shows an angular distribution[1] for the elastic scattering of neutrons on $^{40}Ca$ at 30.3 MeV. The availability of such high quality neutron elastic scattering data (and corresponding proton elastic scattering data[2]) allows the determination of the isospin dependent part of the optical potential as the difference between the neutron and proton potentials. The results of such an analysis are summarized in Fig. 2. After the volume integrals are fitted with the linear energy dependences shown,

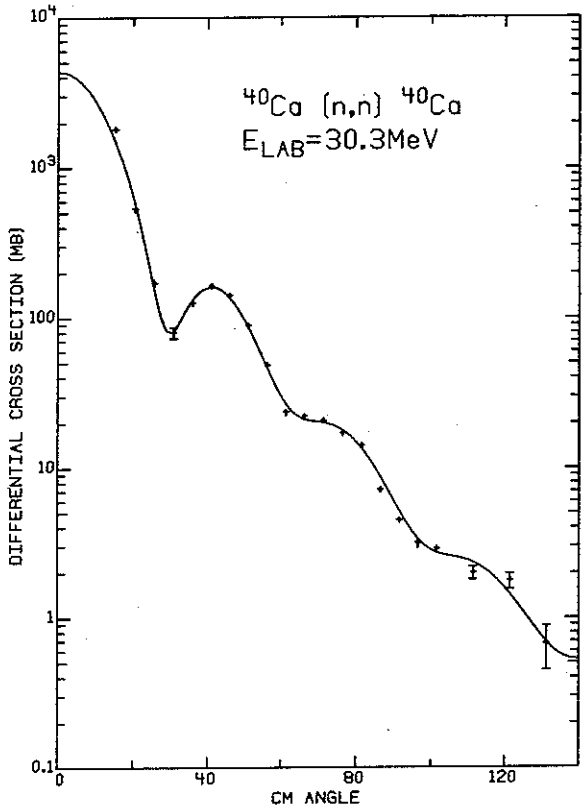


FIG. III.1. Cross sections for elastic scattering of 30.3 MeV neutrons from $^{40}$Ca. The curve is the optical model fit to the data.

the energy scale for the proton results is shifted by the mean Coulomb energy to account for the slowing down of the proton in the Coulomb field of the target. Then the volume integral per nucleon for the symmetry potential is obtained by straightforward subtraction:

$$\frac{J_{sym}}{A} = 2\left(\frac{J_n - J_p}{A}\right) = (135 - 1.46E)\ \text{MeV-fm}^3.$$

This value is somewhat smaller than previous extimates but larger than the prediction of Jeukenne, et al.[2]

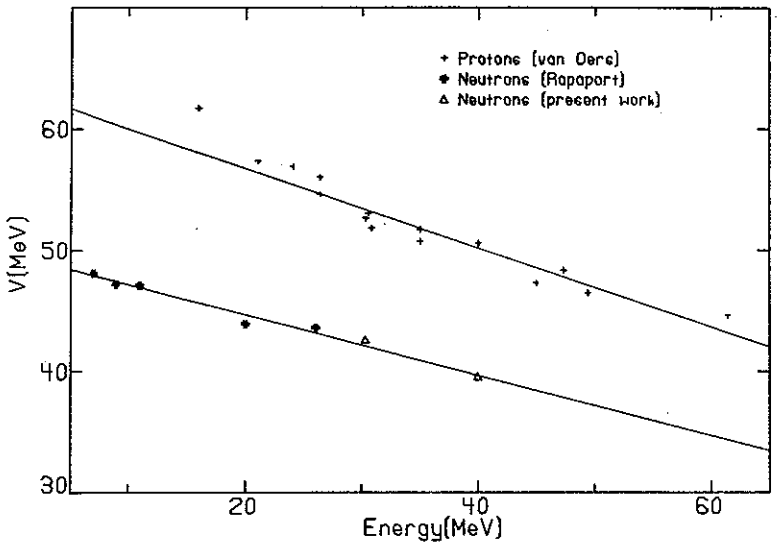


FIG. III.2. Energy dependence of the lead real potential with fixed geometry. The proton potentials are from ref. 2 and the neutron potentials at $E \leq 26$ MeV are from the Ohio University work.

In an analysis of the N=Z data (where the effects of the symmetry potential are absent) the resulting differences in $J_p$ and $J_n$ can be attributed to differences in the two body neutron-neutron and proton-proton interactions $v^{pp}$ and $v^{nn}$. Our results for $^{40}Ca$ are:

$$\frac{J_{nn}-J_{pp}}{A} = (-0.2 \pm 5) \text{ MeV-fm}^3.$$

This value is consistent with zero; the one-standard-deviation upper limit is substantially smaller than the value

of 19.4 MeV-fm$^3$ introduced by Negele[4] to explain the Coulomb energy anomaly.

As another example of recent elastic scattering studies performed at MSU, Fig. 3 shows data that were taken in a systematic study of the elastic scattering of $^6$Li on a variety of target nuclei.[6] We plan to pursue these and similar elastic scattering investigations with heavier projectiles and at the higher energies of the K500 cyclotron for the next few years.

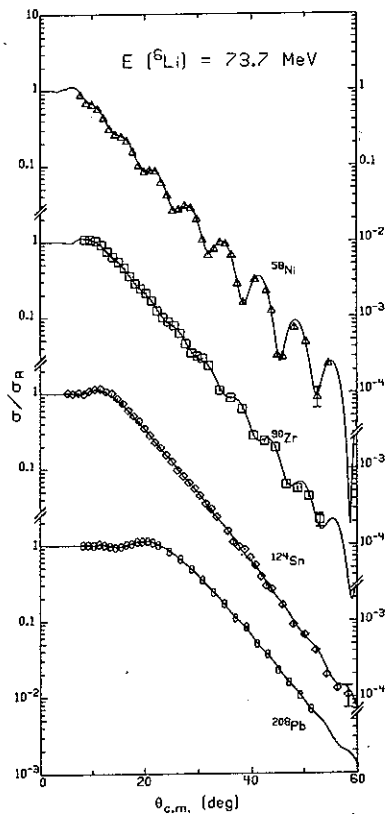


FIG. III.3. Elastic scattering of $^6$Li. The curves are from one of the families of Woods-Saxon potentials which fit the data.

The elastic scattering of heavy ions is qualitatively different from the elastic scattering of nucleons and, consequently, different problems will be addressed in our future research. A few selective examples are given below.

b. Heavy Ion Optical Potential

The elastic scattering of heavy ions is dominated by two physical effects: 1) a strong Coulomb repulsion of the colliding nuclei and 2) a strong absorption into non-elastic reaction channels. The strong Coulomb potential acts like a diverging lens and produces rather smooth Fresnel diffraction patterns[7] in the angular distributions, in contrast to the strongly oscillating Fraunhofer diffraction patterns that are characteristic of the elastic scattering of nucleons. (See the transition to pure Fresnel diffraction for heavier targets in Fig. 3.) Because of the strong absorption, the angular distributions are generally insensitive to the interior part of the optical potential and determine the optical potential only at the rather large inter-nuclear distances[8] where the density overlaps are less than about 10% of the central nuclear densities.

An extensive study of the elastic scattering of $^{16}O + ^{28}Si$ over a large range of energies has shown[9] that the optical potential ambiguities can be reduced significantly by extending elastic scattering measurements towards higher energies. However, it has been demonstrated

that the energy range investigated (33-215 MeV) is still not sufficient to allow unambiguous conclusions about the depth of the interior part of the optical potential. A distinction between the proximity potential (which is repulsive at small distances) and the folding potential (which is strongly attractive at small distances) could not be made on the basis of existing data.[10] Quite clearly, it will be very important to extend elastic scattering studies towards even higher energies in order to restrict the range of existing ambiguities. The cyclotron will provide $^{16}O$ beams up to about 1 GeV and will be a unique facility for extending the investigation of heavy ion elastic scattering.

c. Heavier Projectiles ($A \gtrsim 50$)

Only sparse information is available[11,12] on the elastic scattering of heavier projectiles ($A \gtrsim 50$) since most experiments have been performed with insufficient energy resolution to separate the inelastic scattering to low lying states. Very recently, the GSI magnetic spectrograph has provided data[13] of better quality. A significant contribution in this area can be made through the use of the Enge spectrograph to obtain good energy resolution. Quite dramatic deviations from the simple Fresnel diffraction pattern are expected for the elastic scattering between heavy nuclei since the strong coupling to inelastic channels by Coulomb excitation effectively

acts as a long-range absorptive potential,[14] as seen in Fig. 4. This long range absorption causes a decrease of the elastic scattering cross section at large impact parameters and destroys the Fresnel diffraction pattern that normally results from the strong short range nuclear absorption. Similar effects have already been observed in the elastic scattering of $^{16}O$ on deformed nuclei.[15,16] However, effects as dramatic as those predicted for Kr + Be in Fig. 4 clearly call for investigations with heavier projectiles.

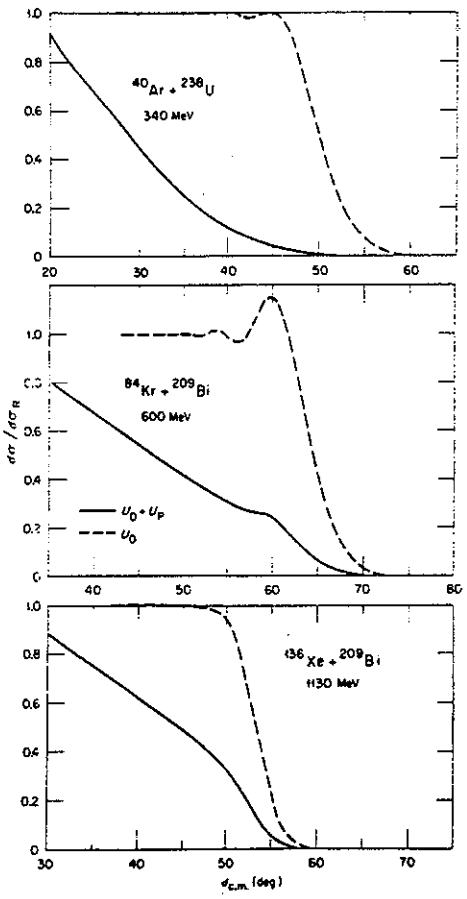


FIG. III.4. Predicted elastic scattering cross sections for very heavy systems[14] including (solid curves) or omitting (dashed curves) the effect of E2 Coulomb excitations.

d. Reaction Cross Sections

In spite of existing parameter ambiguities it is possible to obtain the reaction cross section from the optical model analysis of elastic scattering measurements.[17,18] Recently, DeVries et al.[19] have suggested that the heavy ion reaction cross section should not simply approach the geometric cross section as the energy per nucleon increases from the Coulomb barrier toward a few hundred MeV but should, rather, exhibit an energy dependence similar to the nucleon - nucleon cross section, i.e. a pronounced minimum at about 250 MeV/nucleon. There are practically no cross section data for heavy ion reactions at energies above 10 MeV/nucleon. The new facility will permit the acquisition of an extensive body of such data for $A \lesssim 12$ up to about 80 MeV/nucleon.

Precise studies of reaction cross sections as a function of energy could also reveal the onset of exotic effects in nuclear collisions. The changes in nucleon-nucleon scattering cross sections brought about by a phase transition in nuclear matter could show up as a deviation of the reaction cross section from the trend predicted by the superposition of nucleon-nucleon cross sections.

e. Backward Angle Elastic Scattering

One of the most surprising discoveries in recent heavy ion scattering studies has been the strong backward rise of elastic cross sections for systems such as $^{16}O + ^{28}Si$ and the concurrent existence of pronounced structures

in the backward angle excitation functions.[20,21] A recent example[22] is shown in Fig. 5. At present, it is not known whether such a dramatic backward rise of the elastic scattering will persist at higher energies. Since back-angle measurements are generally best performed[20] by use of the heavier nucleus as the projectile and detection of the recoiling target nucleus at small laboratory angles, a magnetic spectrograph is required. Furthermore, relatively high projectile energies are needed since the major fraction of the projectile energy ends up as kinetic energy of the center-of-mass system. Both conditions will be ideally met at MSU, thus allowing the extension of studies of back-angle elastic scattering to higher energy.

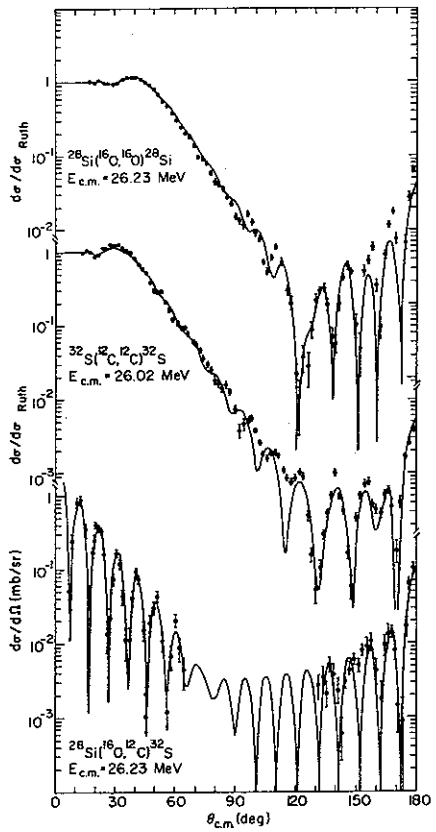


FIG. III.5. Angular distirubtions for the reaction $^{28}Si(^{16}O,^{12}C)^{32}S$ and the entrance-and exit-channel elastic scattering at $E_{cm}(^{16}O+^{28}Si)$ = 26.23 MeV. The curves are the results of a Regge-pole parameterization.

A related and similarly interesting problem involves the search for "quasi-molecular" structures in the $90^{o}$ c.m. excitation functions for the elastic scattering of identical nuclei such as $^{40}Ca + ^{40}Ca$. Although very pronounced structures have been observed[23] with nuclei having $A \lesssim 28$, e.g. $^{28}Si + ^{28}Si$, no such structures have been seen[24] with $^{40}Ca + ^{40}Ca$ for energies up to 240 MeV. The energies that have been investigated until now may still be too low to reveal quasi-molecular resonances which, quite possibly, will appear at the higher energies accessible with the K500 cyclotron.

f. Nuclear Josephson Effect

The elastic scattering of a pair of heavy ions differing by only a few nucleons can lead to characterisitc interference patterns between a "direct" elastic scattering amplitude and an "elastic transfer" amplitude.[25] If the two colliding nuclei have strong pairing correlations (as observed for Sn isotopes) there could be an enhanced probability for the transfer of nucleon pairs from one nucleus to the other.[26] Such a "Josephson" current should be observable - if it exists[27] - in the elastic scattering of two similar nuclei with good BCS wave functions, such as $^{64}Zn + ^{66}Zn$ or $^{120}Sn + ^{122}Sn$. Although doubts[27] have been raised concerning the existence of the "nuclear Josephson effect", an experimental investigation is still a challenging problem that can be attacked at MSU.

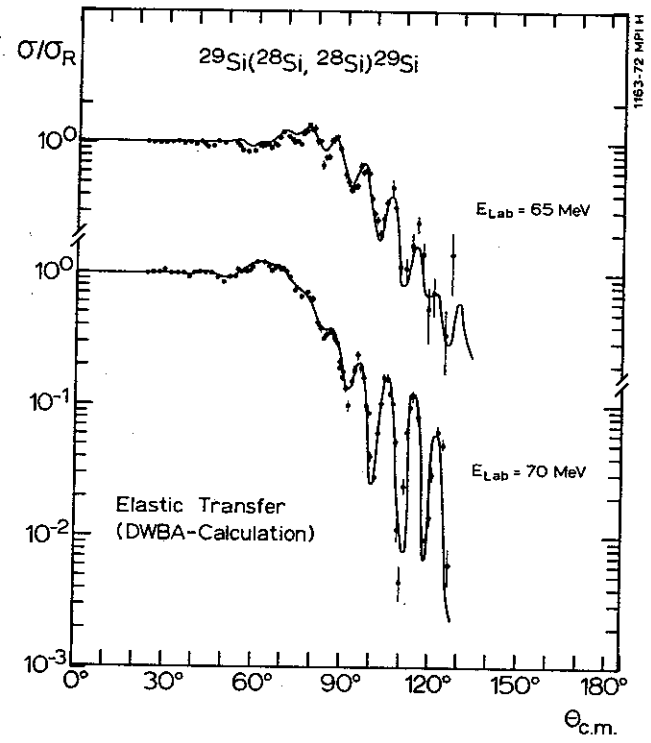


FIG. III.6. Elastic scattering of $^{28}Si+^{29}Si$ at 65 and 70 MeV.[25] The theoretical curves include the coherent contributions from the "elastic transfer" process.

## A2. NUCLEON TRANSFER REACTIONS

Transfer reactions have always made important contributions to our knowledge of nuclear structure. The wide range of high energy precise beams from the new cyclotron is certain to lead to additional refinements of our models of nuclei. We plan to study multinucleon transfer reactions for the spectroscopy of exotic nuclei and for the excitation of simple cluster configurations that are inaccessible in light ion reactions. The traditional difficulties associated with heavy ion spectroscopy such as the effects of target thickness on the attainable resolution, will be alleviated in experiments at higher energy. For other reasons, the high energies will be valuable even in the study of simple one and two-nucleon transfer reactions. Our recent work with pick-up reactions, for example, in which deep hole excitations appeared as new, high lying structures in the continuum can be enhanced and extended. (See Sec. III.B3.h. )

### a. One and Two Nucleon Transfers

Traditionally, single nucleon transfer using light ions, through its relative simplicity, has made major contributions to our knowledge of shell structures and to the dynamics of the reaction mechanism. In heavy-ion induced transfer there remain some outstanding problems at the highest presently available energies of 20 MeV/nucleon. The cross sections for transitions to single particle

states in $^{208}Bi$ are shown in Fig. 7 for the $^{208}Pb(^{16}O,^{15}N)$ reaction.[28] The comparison of experiment and theory, using absolute spectroscopic factors, gives a discrepancy of up to a factor of 7. We are faced here with an apparent failure of direct reaction theory. Since the discrepancy increases at high energies, the effects of multistep and polarization processes are unlikely to be the explanation. Clearly an extension of these experiments up to 60 MeV/nucleon will be extremely interesting.

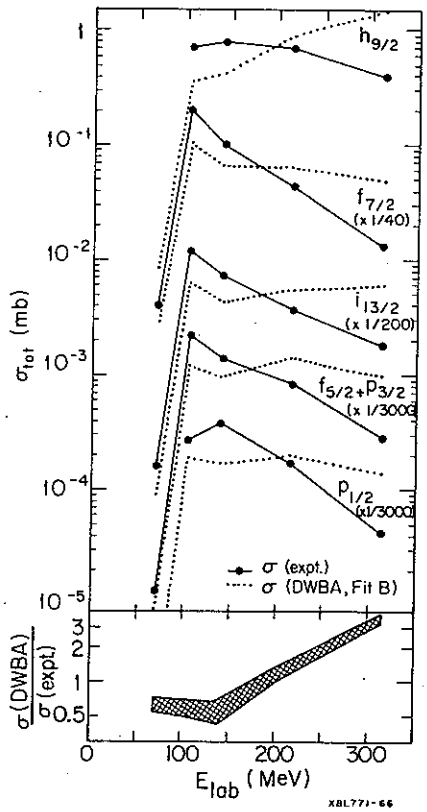


FIG. III.7. A comparison of experimental and theoretical cross sections for the reaction $^{208}Pb(^{16}O,^{15}N)^{209}Bi$ leading to different single particle states as a function of incident energy. The ratio of theoretical and experimental cross sections for all the states is encompassed by the hatched region at the bottom.

Two-nucleon transfer reactions with heavy ions offer some interesting possibilities for the spectroscopy of new nuclei, e.g., for the two proton transfer ($^{12}C$,$^{10}Be$) which we have used[39] to produce $^{146}Gd$. A completely different aspect is the study of "time-reversed" stripping and pick-up reactions, like ($^{18}O$,$^{16}O$) and ($^{16}O$,$^{18}O$), in which the sensitivity to constructive and destructive interference between direct and indirect amplitudes has already refined our knowledge of the wave functions of deformed nuclei.[30] As in the case of one nucleon transfer, an investigation over a wide energy range, in which the relative contributions of direct and multistep processes change, will make a stringent test of the theories.

The comparison of spectra in which two nucleons are transferred from different incident projectiles, can provide useful clues to nuclear structure, as in the recent comparison[31-34] of the reactions ($^{18}O$,$^{16}O$), ($^{14}C$,$^{12}C$), ($^{4}He$,$^{2}He$), and (t,p). Figure 8 shows a spectrum for $^{26}Mg(^{14}C,^{12}C)^{28}Mg$ in which the unnatural parity states are not excited, collective states are only weakly populated, and there is high selectivity compared to the analogous (t,p) reaction for exciting high angular momentum states. The same nucleus can also be formed in a variety of different transfer reactions.

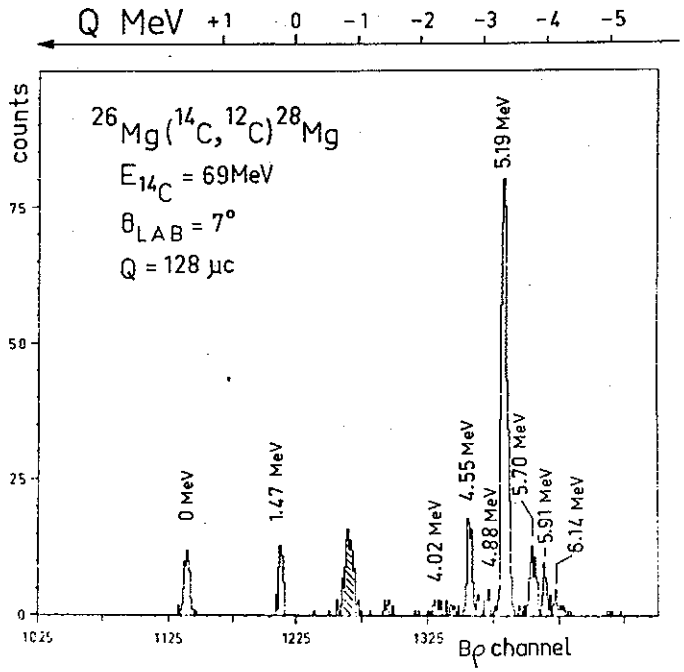


FIG. III.8. Energy spectrum for the $^{26}Mg(^{14}C,^{12}C)^{28}Mg$ reaction at incident energy of 69 MeV.

b. Cluster Transfers

The comparison of one, two, three, four and higher nucleon transfers should lead to the location of a hierarchy of simple configurations in the final nucleus. However, the greatest attraction of heavy ion transfer remains the possiblility of locating new types of cluster configurations at high excitation. The remarkable selectivity

at 10 MeV/nucleon has already been demonstrated.[34] The experiments have stimulated the development of literal cluster models for four nucleon transfer, convoluting an α-particle with the target core in phenomenological and folding potentials.[35] We shall undertake new experiments with light projectiles like $^{20}Ne$ and $^{24}Mg$ at energies of ~50 MeV/nucleon where we expect greater selectivity, the excitation of higher angular momenta, and an even greater surface dominance of the reaction mechanism. Having available a wide range of energies for each of a variety of projectile types should be very useful in examining cluster configurations under differing kinematic conditions; definitive identifications should result.

The possibilities are also encouraging[36] for producing quasimolecular configurations as residual states by direct multinuclear transfer in reactions of the type $^{12}C(^{16}O,\alpha)^{24}Mg$. Hitherto these states have been observed as resonances in the excitation function of elastic and inelastic scattering.[37]

Three or more neutron pick-up and stripping reactions, such as $(^{3}He,^{6}He)$, $(^{13}C,^{10}C)$ and $(^{18}O,^{14}O)$, will also be studied. In addition to reaching new nuclei which are either neutron rich or proton rich, we shall see whether these reactions are selective in exciting simple stretched configurations in light nuclei, like the counterpart $^{3}He$, t, and α transfers. There are also interesting unresolved questions about the nature of reaction mechanisms, e.g., in the $0^+$ and $2^+$ excitations in the $^{13}C(^{3}He,^{6}He)^{10}C$ reaction. Both states are strongly excited but with very

different angular distributions.[38] Calculations have been carried out assuming a direct cluster transfer,[39] and it is clear that data at higher energies will be needed to understand the reaction mechanism better.

## A3. HEAVY ION REACTION MECHANISMS

The major part of heavy ion research performed up to this time has been devoted to the investigation of nucleus-nucleus collisions at low energies, i.e. at only a few MeV/nucleon. Detailed experimental information is available in this energy range.[40-43] Since the relative velocity of the colliding nuclei at these low energies is small compared to the Fermi velocity of nucleons inside the projectile and target, the reactions are dominated by phenomena ranging from non-equilibrating direct, quasi-elastic, and deeply inelastic processes to fusion reactions in which complete statistical equilibrium of the composite system is finally attained. During the last few years the first experimental results have become available for heavy ion induced reactions at relativistic energies.[44,45] At these energies the reaction is unlikely to proceed via an equilibrating dinuclear system but rather by a fast abrasion stage followed by an equilibration phase for the reaction products. However, very little is known about heavy ion reactions in the intermediate energy range, i.e. between about 10 and 100 MeV per nucleon. The energy domain of a few tens of MeV per nucleon is particularly interesting since the relative velocity of the two colliding nuclei becomes comparable to the Fermi velocity and to the velocity of sound in nuclear matter in this domain. As a consequence, the transition from low-energy equilibration pheonmena to high-energy fragmentation and abrasion processes

is expected to occur in this energy range. The first evidence[46] for such a transition was obtained from the study of $^{16}O$ induced reactions over a large range of energies.[46-48]

The K500 superconducting cyclotron will provide beams of heavy ions with energies up to several tens of MeV per nucleon (for $^{16}O^{6+}$ the maximum value of E/A is 60 MeV) and will, therefore, permit the first intensive exploration of the range of intermediate energies. Because of this capability, the study of heavy ion induced reactions up to the highest possible beam energies will constitute a major part of our research program. In the following we give some examples of our recent research on heavy ion reaction mechanisms at intermediate energies, and we discuss some of the interesting questions that will be addressed by our future research. We will divide our discussion into two parts, dealing separately with "peripheral" and "central" collisions, although no sharp boundary can be drawn. We define as "peripheral" those reactions in which the projectile and target retain part of their identity. Consequently, "peripheral" reactions comprise elastic and inelastic scattering and, less trivially, transfer reactions and, at low energies, deeply inelastic reactions. At higher energies "peripheral" includes fragmentation. On the other hand, complete fusion reactions at low energies and "total explosion" reactions at high energies are classified as central. (For very heavy projectile - target combinations complete fusion has not been observed and our definition cannot be applied.)

a. Energy Dependence of Peripheral Reactions

At low incident energies peripheral reactions, such as deeply inelastic collisions, have been shown[49] to be primarily two body reactions followed by the statistical decay of the fully accelerated reaction products.[50,51] There is a growing body of evidence that the two-body aspect of the reaction is lost at higher energies ($E/A \gtrsim$ 10 MeV) where breakup reactions[52] and "projectile splitting"[53] have been observed. This loss has been demonstrated at an energy per nucleon of 20 MeV in the reaction $^{16}O+^{238}U$. The results are illustrated in Fig. 9 where the mean momenta of coincident target and projectile residues are plotted. Since the momenta of projectile-like and target-like fragments do not add up to the beam momentum, two-body kinematics do not apply.

Evidence for a rapid transition from low energy, two body reactions to high energy, projectile breakup reactions has come from single-particle inclusive measurements of projectile fragments in $^{16}O$-induced reactions.[56] Figure 10 shows the widths of the energy spectra of projectile residues over a large range of beam energies. These widths increase rapidly up to about 20 MeV/u but then change by less than 30% between 20 MeV/u and 2 GeV/u. We plan to extend these studies into the interesting transition-energy region between 20 MeV/u and 60 MeV/u.

Of course, complicated multi-particle correlation studies will be necessary in future experiments in order to discriminate between various existing models. An example of results from such experiments was given in Fig. 9.

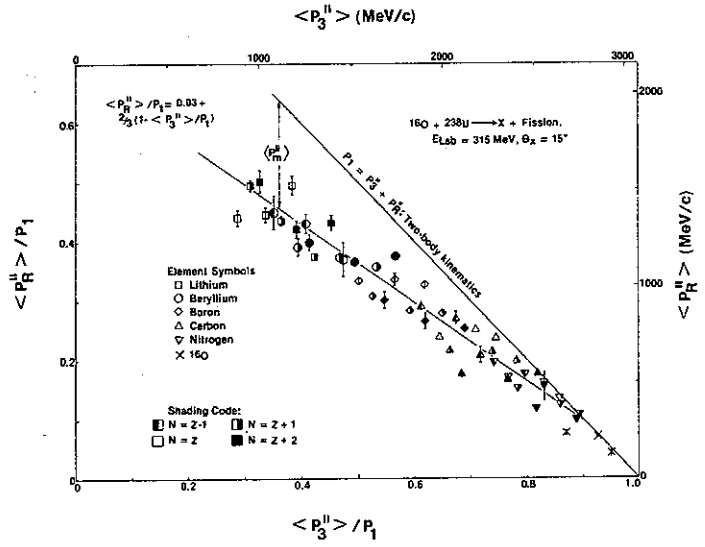


FIG. III.9. Dependence of the average parallel recoil momentum of the target residue, $\langle p_R^{\parallel} \rangle$ on the average parallel momentum of the projectile residue, $\langle p_3^{\parallel} \rangle$ for $^{16}O$-induced reactions on $^{238}U$ at 315 MeV. The momentum $p_R^{\parallel}$ has been measured with the correlated fission fragment technique.[54,55]

Another approach involves the measurement of coincidences between projectile residues and energetic light particles in order to test the multitude of proposed reaction mechanisms for the production of energetic light particles in peripheral heavy ion reactions. Some of these mechanisms are called the "piston model"[57], sequential decay,[58] "hot spots"[59], and "promptly-emitted particles"[60]. As an example, Fig. 11 shows projectile-fragment-alpha particle angular

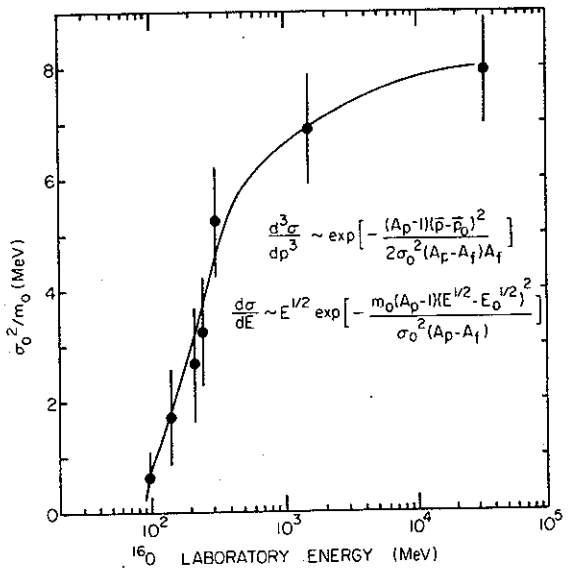


FIG. III.10. Energy dependence of the width parameter $\sigma_0$ for $^{16}O$-induced reactions. (From Ref. 56)

correlations that have been measured[52] for $^{16}O$-induced reactions. The observed correlations were shown to be consistent with projectile breakup or breakup following nucleon transfer. The measurement also showed that any contributions from more exotic reaction mechanisms are difficult to extract from this dominant breakup process. The identification of these mechanisms may become easier with beams of heavier ions (such as $^{40}Ar$) that will become available with energies up to 20 MeV/u, that is, up into the transition region.

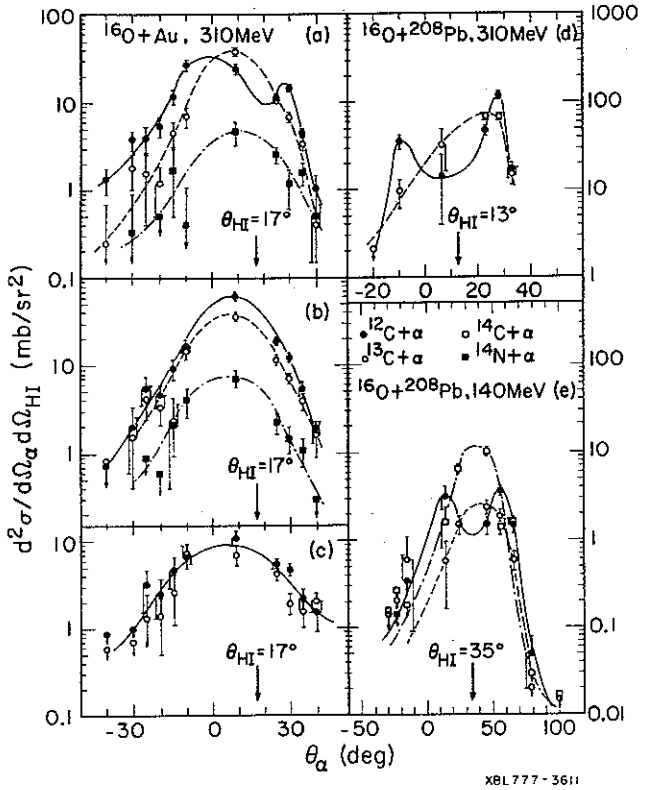


FIG. III.11. In-plane angular correlations[60] for $^{16}O$ induced reactions on $^{197}Au$ at 310 MeV (parts a-c) and on $^{208}Pb$ at 310 MeV (part d) and 140 MeV (part e). Three different regions of $Q_3$-value, the three body reaction Q-value, are displayed: Group I (parts a,d,e), Q (C+α)$\geq$ -20 MeV, Q (N+α)$>$ -30 MeV. Group II (part b), -60 MeV$>$ Q (C+α) $<$ -20 MeV, -80 MeV $\leq$ Q (N+α) $<$ -30 MeV. Group III (part c), -100 MeV $\leq$ Q (C+α) $<$ -60 MeV. The curves in the figure are drawn to guide the eye.

Since the beams delivered by the K500 cyclotron will have good time structure, we also plan to extend the correlation studies to the measurement of neutrons in coincidence with projectile and target residues. It is expected

that neutrons will provide a better probe of the detailed reaction mechanism than charged light particles since neutrons are insensitive to the long range Coulomb forces that complicate the interpretation of charged-particle correlations. Additional useful information will be obtained from γ-ray coincidences. High resolution Ge(Li) detectors will be used to identify residual target nuclei and to measure the alignment of their angular momenta. An array of NaI detectors will be used to measure the associated γ-ray multiplicities in order to provide information on the angular momenta of the reaction products. These experimental techniques have been applied with great success to the study of deeply inelastic reactions at energies below the transition region. (See, e.g., Refs. 61-65.)

b. Isotope Production with Peripheral Reactions

Heavy ion induced reactions can be used as a special tool for the production of nuclei far from the valley of stability (See also Sec. III.C1.). Both deeply inelastic reactions and projectile fragmentation reactions have been used with great success.[66-68] An example of this success is given in Fig. 12 which shows the isotopes identified (some for the first time) in a recent experiment on $^{48}Ca$ fragmentation at about 200 MeV/u.

At present, the optimal conditions for the production of a given isotope far from the valley of stability are, at best, poorly understood. For low energy, deeply inelastic reactions the charge asymmetry equilibrates so rapidly

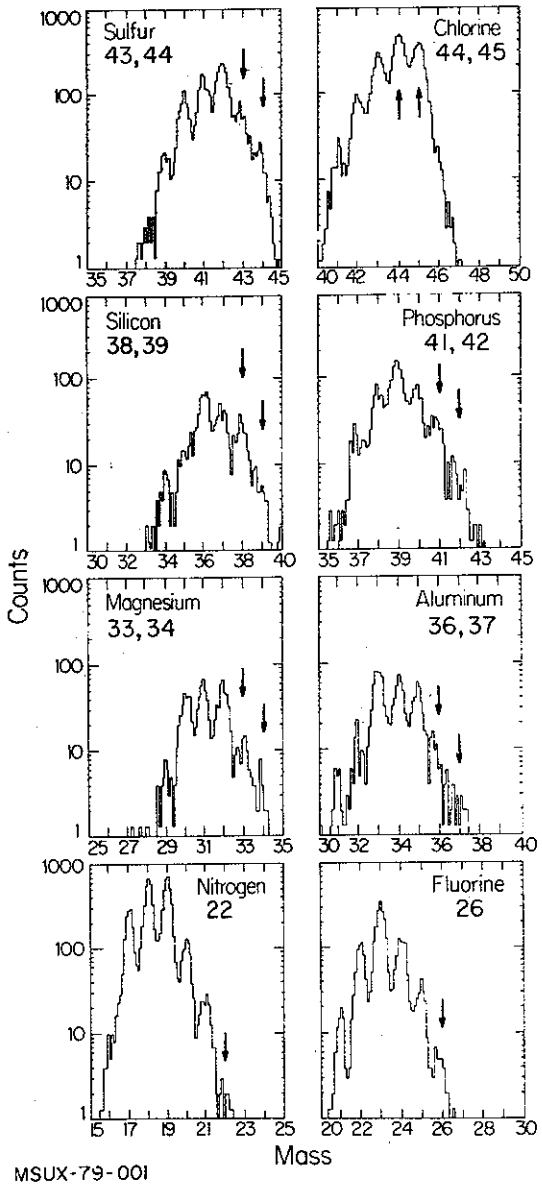


FIG. III.12. Isotopes identified[29] in fragmentation of $^{48}Ca$ at 212 MeV/u. Arrows indicate isotopes identifed experimentally for the first time.

that neutron rich primary projectile residues can be produced in reactions with heavy (i.e. neutron rich) target nuclei. These primary reaction products are generally highly excited and decay statistically.[69] At relativistic energies, on the other hand, equilibration of the charge-

to-mass ratio between projectile and target is probably unimportant. Instead, the primary reaction products are believed to be generated by a fast abrasion stage.[70,71] The primary fragments are, again, highly excited and decay statistically. At relativistic energies, however, very little is known about the excitation energies of the primary fragments, and rather different assumptions on the primary distributions can predict secondary isotope distributions that equally well reproduce the experimental data.[70,71]

Although models have been formulated which describe existing isotope distributions at low and high energies, no experimental information is available at intermediate energies. Furthermore, large uncertainties are encountered if one tries to predict cross sections for isotopes far from stability since many of the parameters that are relevant to these calculations (energies of the ground and low lying excited states) are not known. There is a definite need to make a systematic investigation of the energy, projectile, and target dependence of isotope production cross sections both for a better understanding of the evolution of the reaction mechanism and for an efficient use of heavy ion reactions in the study of nuclei far from stability (See Sec. III.C 1.).

One interesting aspect of these investigations is the determination of the importance of quantal and statistical fluctuations in determining the distribution of elements and isotopes.[72] In the high energy abrasion process, the suggested importance of quantal fluctuations[72,73]

of giant collective modes in the projectile and target needs further experimental clarification.[70,71] Similarly, where both statistical and quantal fluctuations in the composite system should play a role[69,74,75] in deeply inelastic collisions, their relative importance is still subject to controversy and needs further investigation.[75] We plan to study the interplay of these processes and their evolution with energy by using beams with $A \geq 30$ up to the highest accessible energies. The most useful instruments will be the Enge magnetic spectrograph for high resolution and, for a large dynamic range of mass and energy, time-of-flight, $\Delta E$-E telescopes.

c. Central Collisions

At low energies (for not too heavy target-projectile combinations) central collisions lead to formation and decay of the compound nucleus, a process which is well understood in terms of the statistical model.[76] However, at energies above 10 MeV/u, preequilibrium processes become important[61,77,78] and, at energies above several tens of MeV/u, it is not clear whether the compound nucleus is formed at all. At these higher energies, including relativistic energies, the investigation of central nucleus-nucleus collisions proceeds mainly[45] by the measurement of the light particles that are emitted. Since light particles are also produced in peripheral collisions, single particle inclusive experiments encompass a sum

over all impact parameters. This lack of discrimination could hinder the detection of the interesting phenomena that have been predicted to occur (e.g., hot spots[20] and shock waves[79,80]). It is, therefore, of vital importance to find adequate "coincidence filters" that allow a discrimination between central and peripheral reactions.

The observed light-particle multiplicity[81] has been used to "discriminate" between central and peripheral collisions at relativistic energies under the assumption that large multiplicities are associated with central collisions. It has been suggested that better discrimination between central and peripheral collisions can be made if the spatial symmetry of the light particle emission pattern is investigated on an event-by-event basis.[83] Such measurements require highly efficient, light particle detection hodoscopes (e.g., the "plastic ball" under construction at the Lawrence Berkeley Laboratory). We plan a feasibility study of such an approach with the highest energy beams of the cyclotron at the earliest possible time in order to be able to decide whether such an approach is warranted for the investigation of central collisions below 80 MeV/u. It is already known from emulsion studies that the probability for complete disintegration of $^{16}O$ increases rapidly in the region from 50 to 200 MeV/u and then remains fairly constant.[84]

For reactions on actinides, targets which have sufficiently low fission barriers, one can use the correlated fission fragment technique to discriminate between "central" and "peripheral" collisions.[78] An example for $^{16}O$-induced reactions on $^{238}U$ at 315 MeV is shown in Fig. 13. The folding angle $\theta_{AB}$ between two coincident fission fragments can be used to obtain information on the momentum transferred to the target residue prior to fission. For the inclusive

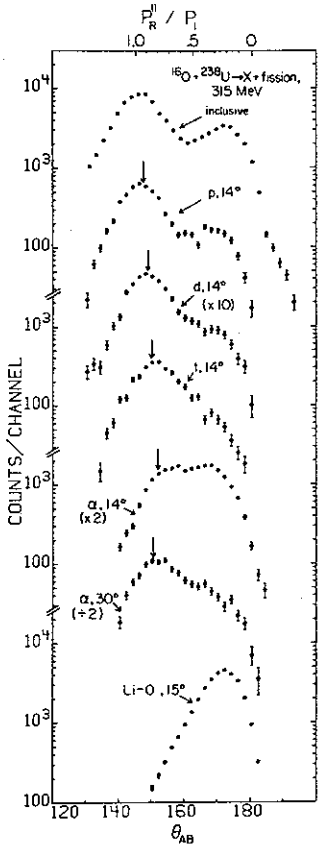


FIG. III.13. Folding angle distributions[65] for coincident fission fragments observed in coincidence with light particles. The arrows in the figure mark those values of $\theta_{AB}$ that are expected if the mean recoil momentum of the fissioning nucleus is equal to the difference between the beam-particle momentum and the mean momentum carried away by the coincident light particle.

spectrum, the maximum at $\theta_{AB} \simeq 150^{o}$ can be associated with "central" collisions in which the major part of the projectile momentum is transferred to the target residue, and the maximum at $\theta_{AB} \simeq 173^{o}$ can be associated with "peripheral" reactions in which only a small fraction of the projectile momentum is transferred to the target residue. The distributions labelled by p,d,t,... are observed in coincidence with the corresponding particle emitted close to the entrance channel grazing angle. By setting limits on the folding angle ($\theta_{AB} \leq 160^{o}$: "central collisions"; $\theta_{AB} > 160^{o}$: "peripheral collision") one can compare the light particle energy spectra for "central and "peripheral" collisions, as shown in Fig. 14. A remarkable similarity is observed for light particles emitted at small angles regardless of whether they are generated in central or in peripheral collisions. This has been taken as evidence that these energetic light particles are generated at an early stage of the reaction,[78] such as breakup in the entrance channel. We definitely plan to refine and continue these studies at higher energy.

Another technique for investigating the characteristics of light particle emission in medium energy, heavy ion collisions will be applied in our future investigations. By measuring light particle energy and angular correlations one can obtain information on the space-time distribution of the emitting source[85] (Hanbury-Brown and Twiss effect).

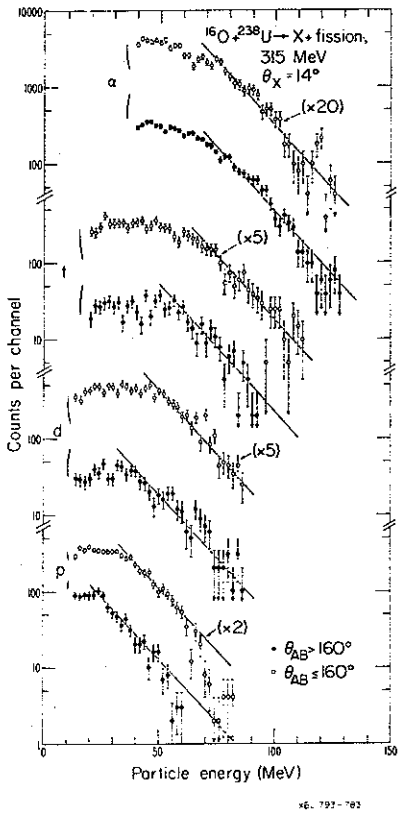


FIG. III.14. Energy spectra[65] of light particles detected at 14° in coincidence with fragments in "peripheral" ($\theta_{AB} \geq 160°$) and in "central" ($\theta_{AB} \leq 160°$) collisions. The solid lines correspond to the spectral shape exp(−E/T) with T=13 MeV.

These measurements could eventually substantiate or refute models that ascribe the emission of light particles to hot, localized substructures of the nucleus[59] such as "hot-spots" or the nuclear fireball. Experiments with beams varying in energy from 20 to 60 MeV/u should, in fact, enable us to determine if there is a connection between high energy and low energy concepts in central collisions similar to the relationships already discovered in peripheral reactions, such as displayed in Fig. 10.

## B. NUCLEAR STRUCTURE

### B1. THE SHAPES OF NUCLEI

a. Inelastic Scattering

b. Coulomb Excitation Measurements

c. g-factors and Quadrupole Moments of High Spin States

d. Electromagnetic Decay

### B2. NUCLEAR STRUCTURE CALCULATIONS

a. Intra sd Shell Structure

b. Mixing of sd Shell with p Shell and/or fp Shell Configurations

c. N=82 Nuclei and Their Neighbors

### B3. GIANT RESONANCES

a. Current Status

b. Investigations with High Energy Light Particles

c. Decay Modes of Giant Resonances

d. Excitation of Giant Resonances with Heavy Ions

e. Giant Resonances and Heavy Ion Discipation Mechanisms

f. Isovector Giant Resonances via Charge Exchange Reactions

g. Studies of Spin-Flip Strength with the ($^{6}$Li,$^{6}$He) Reaction

h. Deep Hole States in One and Two Particle Transfer Reactions

B4. AN EMPIRICAL INTERACTION FOR CHARGE EXCHANGE AND INELASTIC SCATTERING

## B. NUCLEAR STRUCTURE

### B1. THE SHAPES OF NUCLEI

Once the primitive notion that all nuclei are spheres was abandoned, the question "What are the shapes of nuclei?" had to be answered. That answer, in experiment and in theory, has been coming for three decades. The deviations from sphericity are described by a sum of components, or moments, much the way deviations on a string are described by a Fourier series. Inelastic scattering is an excellent means of selectively examining these moments of non-sphericity. If the nuclear physicist can find pleasure in learning of the non-sphericities of nuclei in their ground states, he can absolutely delight in the shapes of excited nuclei. With high angular momentum comes large deformation, and with heavy ion collisions one can excite states in which the limit of deformability of nuclear matter is closely approached In addition to inelastic scattering various types of $\gamma$-ray observations will be referred to in this section since electromagnetic decay gives most of the clues in these studies of nuclear structure.

#### a. Inelastic Scattering

One of the most direct ways of obtaining nuclear shape information is through inelastic scattering. Since nuclei have electric charge as well as mass, it is possible to investigate both the charge and the matter distributions; probes involving both Coulomb and strong interactions

must be employed. The K500 cyclotron will be well-suited to nuclear shape studies as it will make available a large variety of high quality beams and it has a variable energy capability. For example, the 320-MeV α-particle beam can probe the nuclear matter distribution, whereas the Kr beams (E/A=1-6 MeV) can probe the Coulomb interaction. This laboratory has carried out many studies to obtain nuclear shape information using the K50 cyclotron, and we expect nuclear shape studies to be a significant part of the program for the K500 cyclotron.

We have performed[86] high resolution inelastic proton scattering studies of deformed rare earth and actinide nuclei using protons of sufficient energy (35 MeV) to be sensitive to the strong interaction rather than to the Coulomb interaction. We have extended the conventional deformed optical model analysis to the deduction of moments of the matter distribution. These can then be compared to moments obtained by electromagnetic probes. Differences between moments obtained by these two kinds of experiments can point to possible differences between proton and neutron distributions or to some poorly understood reaction phenomenon. The determination of the moments of the mass distribution from the moments of the real part (that is, the part that determines the scattering) of a phenomenlogical, deformed optical model potential has been promoted by Mackintosh.[87] He has pointed out that those optical model potentials which can be derived

from folding realistic nucleon-nucleon interactions with the proton and neutron densities have the property that their moments are proportional to the underlying matter density moments. Figure 15 shows an example of our most recent study.[88] The quadrupole ($q_2$) and hexadecapole ($q_4$) moments deduced in our (p,p') studies agree better with the moments from Coulomb excitation and electron scattering that with those deduced from α-particle scattering. We do find the moments from (p,p') to be systematically smaller (≃7%) than those from Coulomb excitation. Whether this implies smaller neutron distribution moments than

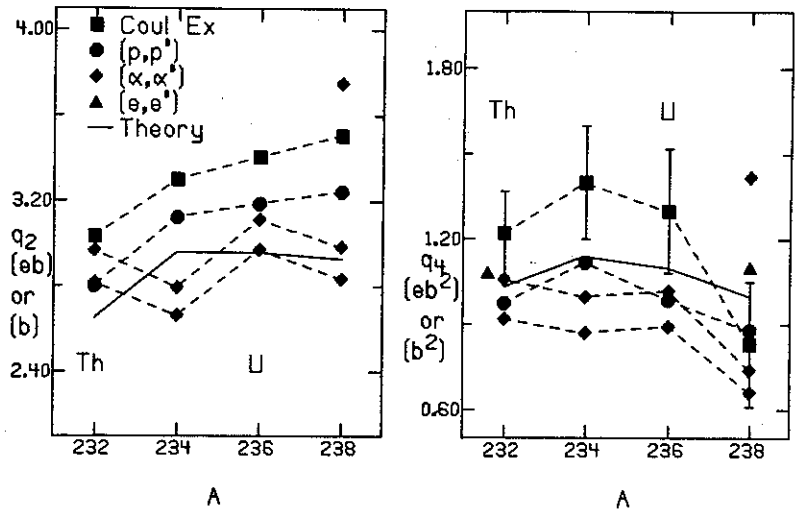


FIG. III.15. Comparisons of values of $q_2$ and $q_4$ from scattering experiments to theoretical values. The two curves for the (α,α') reaction result from two different optical model parameter sets.

proton distribution moments, or implies that the interaction contains effects which are not included in the phenomenological potential (e.g., a density dependent interaction) is not yet clear. We have demonstrated that the proton is a useful probe of the nuclear matter distribution. The inelastic proton scattering at 35 MeV has good sensitivity to higher order components of the matter distribution, and we are now investigating the $\lambda = 6$ multipoles. (See Figure 16).

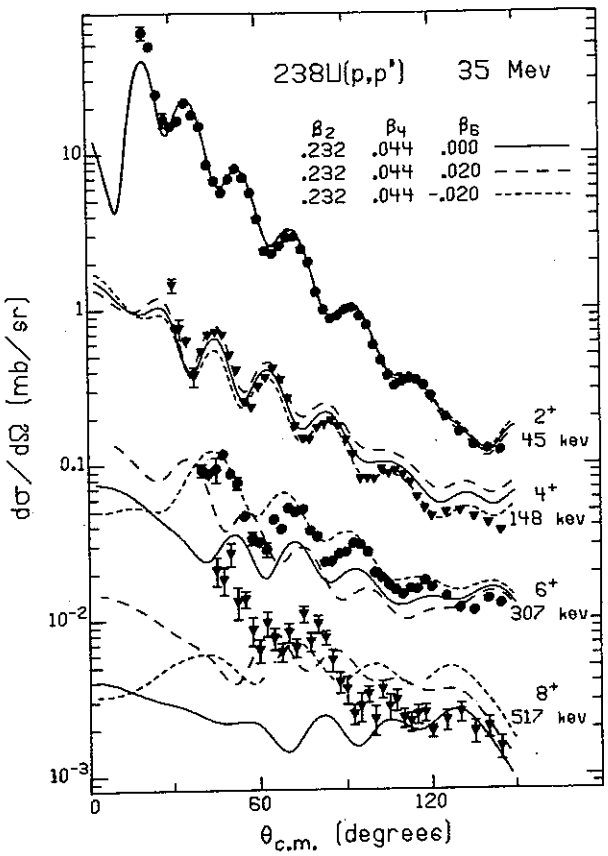


FIG. III.16. Angular distributions of inelastic proton scattering at 35 MeV from ground band states in $^{238}U$. Coupled channels calculations were performed for $\beta_6 = 0.0$ and for $\pm 0.02$.

We have extended shape studies to the transitional nuclei between the rare earths and the actinides. Using two nucleon transfer[89] and inelastic proton scattering[90] on $^{194,196,198}$Pt, we have tested a new collective nuclear model, the interacting boson approximation (IBA) model of Arima and Iachello.[91] Our (p,t) study[89] shows that the IBA model provides a qualitative explanation of L=0 and L=2 transfer strengths, especially for explaining the enhancement of the transfer to second-excited $0^+$ states over first-excited $0^+$ states. Our (p,p') study shows that the IBA model is one of two collective models (the other being the Davydov model extended to include hexadecapole effects[92]) to correctly predict the sign of the product, $P_3$, of three matrix elements that connect the first and second $2^+$ states and the ground state. For illustration, Fig. 17 clearly shows that in $^{194}$Pt the sign of $P_3$ is negative. Knowledge of the sign of this matrix element product is very important in quadrupole moment determinations using Coulomb excitation.

We have also performed elastic[93] and inelastic[94] $^6$Li scattering on $^{58}$Ni at twice the energy previously used for this projectile - target combination in an attempt to learn about optical model and shape parameters. Five optical model parameter sets were used, each giving equivalent fits over the angular ranges of the data for the elastic scattering and for inelastic scattering to different states. This is in agreement with the Austern-Blair prediction[95] for scattering of strongly absorbed particles,

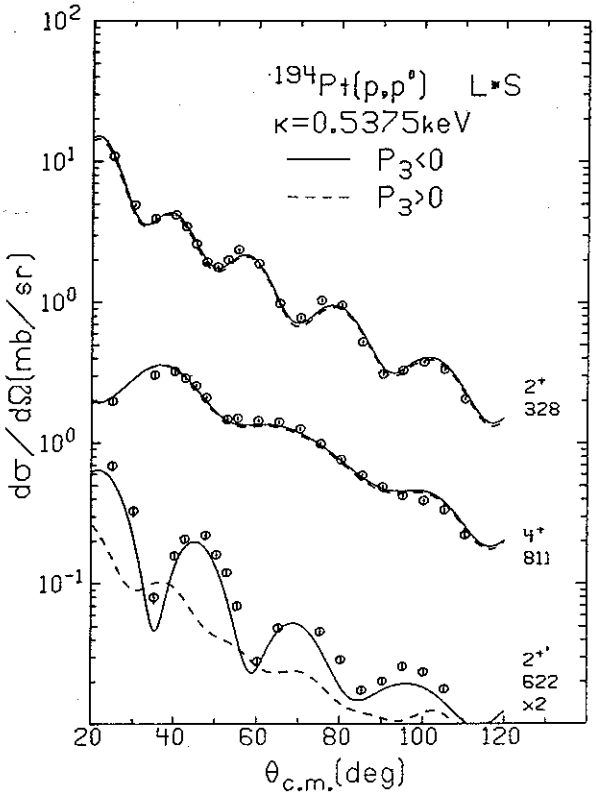


FIG. III.17. Angular distributions of inelastic proton scattering at 35 MeV from the first and second $2^+$ states and the first $4^+$ state in $^{194}$Pt. Two coupled channel calculation results are shown, for positive and negative values of $P_3$ (= $M_{02}\ M_{22'}\ M_{02'}$). The relative magnitudes of the matrix elements are from the O(6) limit of the IBA model (Ref. 91).

such as $^6$Li, that potentials producing the same elastic scattering will produce the same inelastic scattering. The values of the deformation parameters were relatively insensitive to the choice of optical potential.

The ambiguities of nuclear models can be better resolved through study of states of higher spin. Projectiles of high mass will be effective in exciting these states, and we intend to use such projectiles.

b. Coulomb Excitation Measurements

The use of heavy ions for Coulomb excitation is well suited to probing nuclear structure effects at high spin, because a high angular momentum, a large charge, and a long interaction time result in multiple excitation of the nucleus to a state of high spin via the well understood electromagnetic interaction.

The measurement of lifetimes provide a check on B(E2) values deduced using Coulomb excitation theory. These lifetimes are usually more precise than those which can be obtained in (HI, xn) reactions, because Coulomb excitation preferentially excites those states which are coupled strongly to the ground band. Thus, the complex problem of knowing side-feeding populations and their lifetimes is not a factor. Lifetimes of the order of 2 psec for states with I=20 have been measured[96] in the actinide region.

To measure level energies and $\gamma$-ray yields precisely, corrections for Doppler shifts and Doppler broadening of $\gamma$-ray lines must be made. This has been done[96] by detecting both the recoiling target and projectile nuclei using two two-dimensional position sensitive gas counters (see Sec. II.C) to measure the angle and velocity distributions. Time-of-flight measurements distinguish between the target and projectile nuclei in each detector so that proper particle identification is made and unwanted events are rejected. The experimental efficiency can be increased

by using several Ge(Li) detectors. The power of such a system is further enhanced by using several NaI(Tl) detectors to measure γ-ray multiplicities. The highest spin states will have the largest multiplicities.

Heavy ion Coulomb excitation has proved its power in the use of the above techniques. Spins up to I≈30 have been excited[97] in the actinide nuclei, and deviations from predictions of a simple rotational model for level energies and B(E2) values may have been seen. With high quality beams of heavy ions from the K500 cyclotron spins of I≈10-18 (depending on the target) could be excited with projectiles as heavy as Kr. It is in this region of spin that the first bandcrossing takes place, and measurement[98] of the interaction matrix element between the bands would provide a crucial test of nuclear models. The variable energy capability of the cyclotron will allow us to populate high spin states as a function of energy; hence, the influence of specific excitation paths can be studied. Many studies have been made of nuclei for which the rotational model is expected to work best. But few studies[99-101] have been made on transitional nuclei at high spin where specific predictions[91] of B(E2) values must yet be tested. Such a study would be a natural extension of our previous work.

The data of inelastic scattering of heavy ions are often difficult to analyze quantitatively because of the many partial waves required and the large radial distances

that must be included in the calculations. Also, one must account for the possibility of projectile excitation.

The computational ability to describe heavy ion elastic and inelastic scattering is now in the beginning of a new generation.[102-104] Interpolative, extrapolative, and iterative techniques are taking advantage of the smooth behavior of the heavy ion interaction S-matrix with angular momentum. An order-of-magnitude reduction of computational effort can be achieved over the direct application of light ion reaction techniques.

c. g-Factors and Quadrupole Moments of High Spin States

g-factors and quadrupole moments of high spin states are two of the most desirable spectroscopic quantities for deducing high spin structure. Experimentally they are difficult to obtain, but they are very sensitive probes of the nuclear wave function. For example, for a simple rotor the g-factor is constant in the band and is related to the moments of inertia of both the proton and the neutron distributions: $g = \frac{I_p}{I_p + I_n}$. We have measured[105] the g-factors of the $11/2^-$ and $19/2^-$ isomeric states in $^{115}$Sb using the time-differential perturbed angular distribution technique. The measured g-factors are sensitive to the level configuration. The g-factor for the $19/2^-$ state suggests a 3-particle configuration consisting of $\pi d_{5/2} \times (\nu h_{11/2} \times \nu d_{3/2})$ where $(\nu h_{11/2} \times \nu d_{3/2})$ is the $7^-$ state in the $^{114}$Sn core. Similar studies can be carried out

using rather heavy ions from the K500 cyclotron to excite even higher spins in odd-A or even-A nuclei using the following recently developed technique.

Coulomb excitation is used for selective population of collective states. The target nucleus decays while recoiling into a polarized ferromagnetic backing. A large ($\approx 10^6$ Gauss) transient magnetic field is produced when an s-orbital electron is captured by the recoil. The field is proportional[106-108] to the charge and velocity of the recoiling nucleus. The strong field perturbs the $\gamma$-ray angular distribution as a function of time, and the g-factor can be deduced from the time dependent $\gamma$-ray anisotropy. The higher the charge-velocity product, the shorter the lifetime to which the method can be applied, hence the value in having very heavy projectiles to do the Coulomb exciting in the first place. Such studies have been carried out[109] to spin 10 in some even-A Yb nuclei. The object was to look for changes in the g-factor for high spin states, changes which could signify[110] variations in the relative proton and neutron moments of inertia as one encounters "backbending" or other irregularities in band structure.

Traditionally, quadrupole moments have been measured with Coulomb excitation techniques. Studies of the angular distributions of the scattered ions and of the $\gamma$-rays in coincidence with the scattered ions have allowed the determination of quadrupole moments of first excited states.

The K500 cyclotron, having a wide range of projectiles of variable energy, can be used to continue these traditional measurements as well as to extend them to measure moments of higher spin states. But, an especially attractive feature of the K500 cyclotron is its ability to produce nuclei far from stability where targets for Coulomb excitation cannot be made. In such heavy ion collisions, highly excited, high spin states are populated in the product nuclei which can recoil into a crystal site of a host substance. There the quadrupole moments of the excited states are subject to strong ( $10^{17}$ V/cm$^2$) electric field gradients. The interaction between the quadrupole moment of the high spin state and the electric field gradient produces a time dependent anisotropy in the $\gamma$-ray distribution which de-excites the state. By measuring these quadrupole modulations of the $\gamma$-ray angular distribution, the Chalk River group[111] has recently deduced quadrupole moments of high spin states in $^{146,147,148}$Gd (to I = 59/2 in $^{147}$Gd). The quadrupole deformation parameters showed the tendency for these nuclei to become increasingly more oblate at high spins.

d. Electromagnetic Decay

A very active program in nuclear structure studies via on-line and off-line $\gamma$-ray and conversion electron spectroscopy has been an important component of the overall research program at MSU. The new capabilities of energy

and ion species which will be provided by the K500 cyclotron will, in conjunction with new detection apparatus, allow a major expansion in depth and breadth of these types of studies. Most simply put, the new cyclotron will permit essentially all investigations to be pursued up to the limiting angular momenta ( $\simeq 70\hbar$) which nuclear matter can sustain.

Many of the in-beam $\gamma$-ray spectroscopic studies we have carried out during the past few years have been concentrated in the region between Z=70 (Ytterbium) and Z=82 (Lead). Study of nuclei in this region is particularly instructive since their properties are influenced by changing nuclear shapes, shell effects, and strong Coriolis forces. These are the general features which dominate nuclear structure at high spins, and they are manifested in the transition from prolate to oblate deformation in the Os and Pt isotopes[112,113], in the appearance of high-spin, multi-quasi-particle yrast traps in certain Hf isotopes[114] and in the appearance of strong rotation-alignment effects in Os, Pt, and Hg isotopes.[112,115,116] The richness of the spectrum of nuclear states in this region derives from the fact that under sufficient stress from increasing angular rotation, virtually all nuclei exhibit the band structure characteristic of a deformed system. It is the study of this band structure, the interaction between bands, and the interplay between single particle and collective modes of motion that dominated the work on deformed

and shape-transitional nuclei before very heavy ions became available. The results of that work are now providing the basis for understanding the behavior of nuclei at very high spins.

Three separate thrusts which eventually coalesced to contribute to a unified picture of high-spin behavior were: 1) The shape transitions in Pt isotopes; 2) The interplay between particle-aligned and collective band structures (backbending); and 3) The occurence of very-high-spin isomeric structures in the Hf-W region. These isomers, in some cases, were demonstrated to be yrast traps, and their associated bands were found to form the yrast band structures at spins of 20$\hbar$. For the sake of conciseness, we refer the reader to Fig. 18, which contains the conventional "backbending" - style displays of the yrast band sequences in the Hf-Pt region. THe cases of $^{190-194}$Pt illustrate the intrusion of what are now understood to be aligned $i_{13/2}$ neutrons into the yrast sequence; such phenomena make this display something of a parody of the "backbending" plot. Also shown are the highest spins that were identified in the yrast sequence of each of the nuclei studied plus the spins and lifetimes of the numerous high-spin isomeric states which were identified or whose band structures were characterized.

The odd-A isotopes for the mass region of Fig. 18 were also studied. The purpose of these odd-A investigations was to provide insight into the behavior of band structures by way of the special interaction of collective

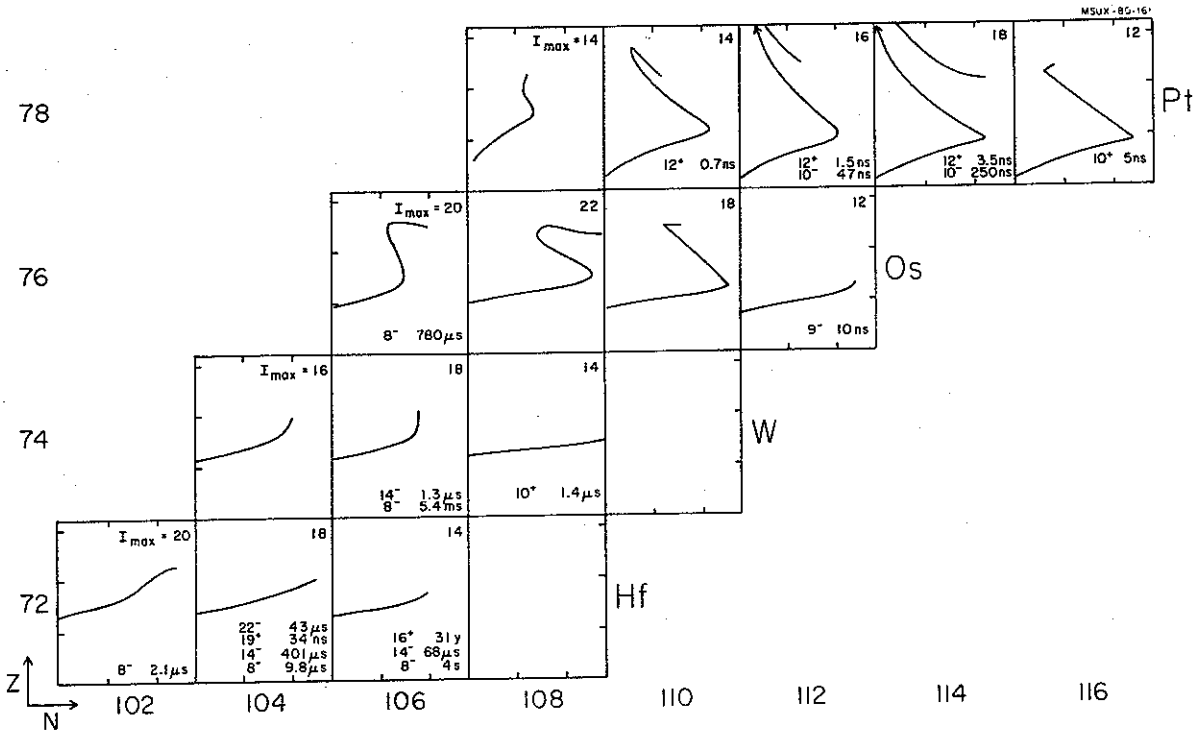


FIG. III.18. "Backbending" plots of the yrast bands in the even-A Hf, W, Os, and Pt nuclei studied at MSU. The maximum spin, $I_{max}$, observed in the yrast sequence is shown. Values of $I^{\pi}$ and $T_{1/2}$ are given for some high-spin ($I \geq 8$) isomers.

motion with an identifiable single particle in a deformed, or weakly deformed, potential. Such data have greatly enhanced our understanding of the important contribution of rotation-aligned intrinsic structures to the interactions between bands, and by implication, to the once controversial question of backbending itself. Our long-standing collaboration with Daly's group at Purdue concluded[117] with a systematic

study of the high spin structure of the Pb isotopes 195—203 and the identification of numerous isomers with spins up to (29/2). Walker and co-workers[118] have studied the effects of rotational alignment of a high-j particle on the negative parity band structure in even-A Yb isotopes 168-172. Other in-beam gamma-ray studies have been carried out on odd-Z systems just below the N=82 closed shell.[119]

The natural evolution of interests in this field is to even higher regimes of spin-energy space. This makes the transition to the new K500 facility a natural one, and the extension of our on-going work to spins well above our previous limitation of 20ħ will follow well-defined lines. Other areas of research in this general field which will be pursued are sketched in the remaining paragraphs.

Substantial progress has recently occured in techniques for extracting structure information from both discrete line spectra and from unresolved continuum spectra of nuclei at very high spins. The general features of the latter are now understood to be a low energy bump near 1 MeV, the "yrast bump", and a high energy tail of statistical transitions which serve primarily to cool the nucleus in the early stages of de-excitation from the entry line. The "yrast bump" is the feature of such spectra which contains the interesting information on nuclear structure. It and attendant features in continuum spectra have been studied by a variety of methods: angular correlations, multiplicity, total gamma-ray energy, linear polarization,

conversion coefficients, lifetime measurements by Doppler shift techniques, and most recently, energy correlation analysis. The picture that has emerged from such studies suggests substantial differences between prolate and oblate nuclear deexcitation paths at very high spins. Prolate systems are thought to decay primarily by enhanced E2 transitions within bands parallel to the yrast line. Oblate systems, on the other hand, which are likely to carry angular momentum about the symmetry axis by high-j particles, will have transitions in the "yrast bump" region which are less collective and fewer in number. Oblate systems will cool more rapidly and reach the yrast line at substantially higher spins.

The recent identification in the Argonne-Chalk River collaboration[120] of spins approaching 40$\hbar$ in discrete line spectroscopy of $^{152}$Dy is an example. Subsequent measurements of lifetimes in this nucleus[121] and of the quadrupole moments of an yrast trap in $^{147}$Gd at Chalk River[122] have confirmed the picture of oblate shapes with rotation about the symmetry axis for these weakly deformed nuclei.

A great deal of additional work remains to be done as the techniques for extracting information on moments of inertia, transition rates, multiplicities, and multipolarities associated with the "yrast bump" are refined. The Copenhagen group, especially, has been at the forefront of refining the techniques of continuum spectroscopy. Their method for high spin selection by total gamma-ray

energy detection led to the recent observation at Berkeley of the highest multiplicities yet observed for compound nuclear products.[123] Very recently, Andersen and coworkers[124] at Copenhagen outlined a method of gamma-ray transition energy-correlations, a highly promising new technique for isolating the energy-correlated cascades that form the signature of rotational nuclei. Application of this technique to gamma-ray continuum spectroscopy reveals the general rotational properties of the "yrast E2 bump", e.g. band-crossing (backbending) and the collective moment of inertia. Figure 19, from work done by the Copenhagen-Berkeley-GSI collaboration,[125] reveals these features in the two-dimensional γ-ray energy correlation diagram; the valley along the 45° diagonal is characteristic of

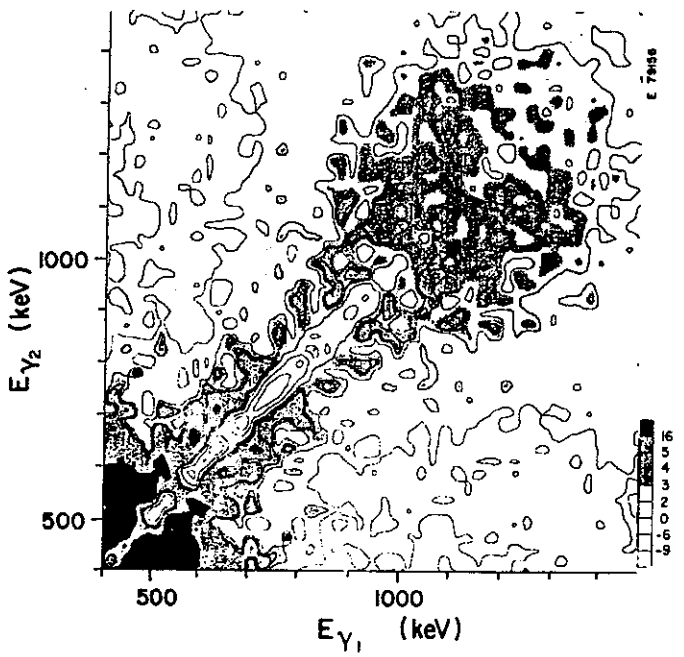


FIG. III.19. Contour plot of the two-dimensional correlation spectrum for $^{164-xn}$Er nuclei from the $^{124}$Sn ($^{40}$Ar,xn) reaction at 185 MeV (Ref. 14) using Ge(Li) detectors.

rotational-like band structures. The distance between the diagonal ridges is inversely proportional to the collective moment of inertia. Where regular rotational structure breaks down, as in band crossing, the energy correlations disintegrate, the diagonal ridges wash out, and bridges form between them, as the figure illustrates in the region of 1 MeV, for example. An excellent review of these techniques has been given by Garrett and Herskind.[126] By combining such data with multiplicity and energy measurements on the yrast bump, one can, in principle, extract information on the way angular momentum is shared by aligned particles and by the nuclear core at very high spins.

We expect our contributions to this wide-open field to take two directions. The first will be selected studies of very high spin systems in the N=86 and other regions of weak deformation, where structural considerations give the prospect of extending discrete line spectroscopy to very high spins. The immediate attraction of the N=86 region is the known occurence of high spin isomers.

At the same time, we will develop apparatus to permit an extension of those studies to well deformed, prolate nuclei by the methods already outlined for continuum spectroscopy. As the first step, we have designed a relatively simple but versatile assembly of two large NaI(Tl) crystals which can serve as a combination multiplicity filter and total gamma-ray-energy sum spectrometer. The apparatus, shown in cross-section in Fig. 20, is similar to devices which have already proved their utility elsewhere. The

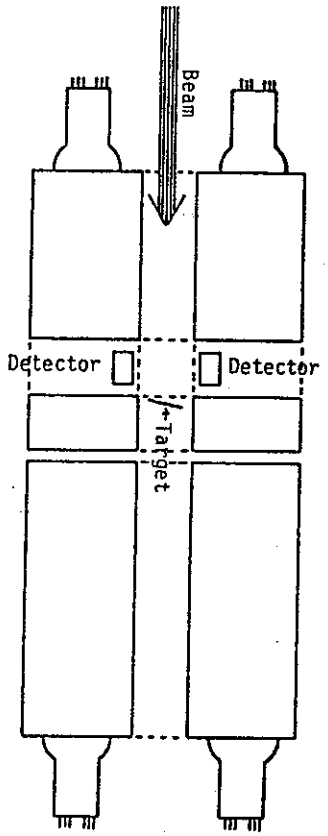


FIG. III.20. Cross sectional view of a 2-crystal $\gamma$-ray-energy sum spectrometer in one possible operating configuration. In this mode two detectors (e.g. Ge(Li)) are shown in the radial bore.

NaI(Tl) crystals will each be about 13" x 13", and will contain axial bores (for beam line and target). A radial bore near the end of the first crystal will permit coincident operation of one or two solid state or other detectors. The second crystal, down-stream from the first, completes the energy sum configuration, or can be replaced with smaller detectors in a variety of experimental arrangements. Specifications for both crystals are similar, with each split into four light tight sectors. This allows rough multiplicity selection to complement angular momentum selection from the energy sum feature. Each crystal can

also operate independently as a Compton suppression spectrometer when used in conjunction with a Ge(Li) detector.

While this initial device will provide a great deal of flexibility and capability for high-spin continuum and discrete-line spectroscopy, more ambitious developments are underway at other laboratories. In particular, it is clear that for nuclei which do not exhibit energy correlations characteristic of rotational systems, high selectivity in multiplicity measurements will be needed to tag well-defined regions of spin for detailed study. The large $4\pi$NaI(T$\ell$) "crystal balls" now under construction at Oak Ridge and Heidelberg will provide the first indication of just how useful very large arrays of 100 or more counters will be for such work. Their performance will certainly influence our plans for $\gamma$ray instrumentation.

In view of the special interest that attaches to isomeric structures, it is appropriate to add some comments on how one can best exploit isomers as tools for very high spin discrete line spectroscopy. From a structure standpoint, perhaps the most interesting new isomers that may yet be identified would be shape isomers at very high spins. In any case, the techniques are the same, and since isomeric lifetimes can vary over a wide range, beam pulsing (including the natural pulsed beam of the cyclotron), mass separation (using the velocity filter proposed in Sec. II.C), He-jet transport, and other techniques, may be required.

For lifetimes of the order of tens of psec, one can utilize the high recoil velocity from collision of an energetic heavy ion on a lighter target in two ways. First, the relatively large recoil velocity (23 μm/psec for, say, 600 MeV Sn on $^{44}$Ca) makes it feasible to shield γ-ray detectors from the target so that only delayed activity free from prompt contamination may be observed. Second, a recoil electron spectrometer can be constructed to observe only delayed electrons from recoiling products.[127] A suitable arrangement consists of a solenoid with one section blocked off and another free for a Si(Li) detector to observe atoms which have recoiled from the target located in the blocked section. The observation of psec-delayed electrons or γ-rays will significantly extend our ability to discover discrete ultra-high-spin states since one or more decay paths along the yrast region may be slightly retarded.

The recoil electron spectrometer proposed above may also be used for lifetime measurements in the psec range. For (HI,xn) reactions it offers an advantage over the usual Doppler-shift-plunger or Doppler-shift-attenuation methods in that the delayed spectra are free from the large, prompt, continuum radiation background. In addition, it is also suitable for Coulomb excitation measurements (see Sec. III.B1.b). Lifetime information on discrete high spin states, an important test of nuclear models, is presently very limited. The availability of energetic

heavy ions, coupled with the recoil electron spectrometer, appears to be a promising combination for providing vital lifetime information.

## B2. NUCLEAR STRUCTURE CALCULATIONS

The research activities described under this heading are directed towards providing the theoretical frameworks, in the form of microscopic wave functions of nuclear states, with which various individual experimental results can be analyzed and, thereby, their interrelationships clarified and their underlying meanings extracted. The concerns of this research encompass essentially all aspects of the structure of the valence states of atomic nuclei. The thesis of our approach to understanding nuclear structure is that fruition of such stuides is achieved only after the features of the widest possible range of phenomena are integrated into a self-consistent and predictive theoretical regime.

The description of the research which will be pursued in this area is organized according to the general microscopic structures presumed for various families of nuclear states and classes of phenomena. The first of these sections will deal with the sd shell and will concentrate upon phenomena that are of particular interest at present. The succeeding sections are briefer and concentrate upon outlining the development of new nuclear wave functions since most of the types of phenomena which are of interest in the sd shell retain their importance in the various other groups of nuclei.

a Intra sd Shell Structure

Research in this area will be based on the evolving family of Preedom-Wildenthal/Chung-Wildenthal Hamiltonians [128,129] These effective shell model interactions are matched to the complete $d_{5/2}$ - $s_{1/2}$ - $d_{3/2}$ model space, and study of their wave functions to date has indicated that the use of this type of empirically based Hamiltonian together with complete major-shell basis spaces yields predictions for many standard spectroscopic variables which agree well with both the specific details and the overall trends of experimental results. Thorough studies have now been carried out for static electromagnetic moments,[130,131] Gamow-Teller beta decay rates,[132] E4 inelastic excitations,[133] and some aspects of isovector M1 excitations.[134] Equally comprehensive studies of E2 and M1 transitions between low lying states are underway and will be followed by a survey of single nucleon transfer.

Future work with these wave functions will span a wide range of topics. Multi-nucleon transfer data originating from both light-ion- and heavy-ion induced reactions will be studied in conjunction with consistent and comprehensive reaction model analyses of these data. At present, the usefulness of the data existing in this field is severely impaired by lack of self-consistent analyses and by the failure to tie together the results of individual experiments in order to establish the systematic trends The clustering features which can be generated within the

sd shell space will be studied by comprehensive comparison of systematically reduced data to the Chung-Wildenthal predictions along the lines of our preliminary investigations in this area.[135,136]

The predicted properties of far-from-stability ("exotic") nuclei will be collected for comparison both to the presently existing data and to the wider range of data which should become available with the exploitation of new experimental facilities such as the K500 cyclotron and the RPMS These properties begin with mass defects, progress to energy level spectra, continue to the beta decay properties, and ultimately include such properties as isotope shifts and M1 and E2 moments. The masses of the T=5/2 and T=3 nuclei which have been measured over the past several years have provided the initial impetus for our interest in this area and it has been found that these data are completely compatible with the theoretical structures based upon "valley of stability" data. The first more extensive studies[137] in this area, which utilize the masses and magnetic moments of the Na isotope data from Orsay, have proven extremely interesting in illuminating the limits of validity of the pure sd shell basis space. (See Figs. 21 and 22.)

As one step towards a deeper understanding of total electromagnetic transition strengths, the separate neutron and proton components of individual nuclear transitions will be studied by making predictions for the relative strengths of inelastic scattering excitations induced

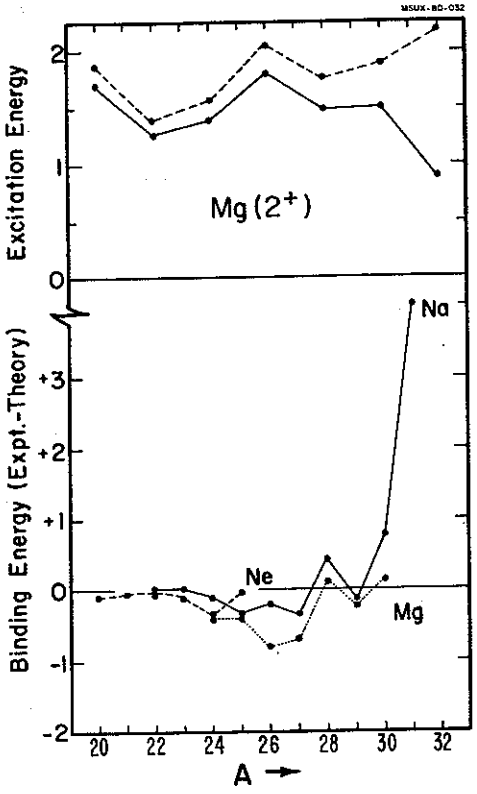


FIG.III.21. Plots of the deviations between calculated and measured nuclear binding energies for the N<Z isotopes of Ne, Na, and Mg (lower portion) and of the calculated and measured excitation energies of the lowest $J^{\pi}=2^{+}$ states of the even Mg isotopes (upper portion). Units are MeV.

by $\pi^-$ and $\pi^+$ projectiles. A preliminary study[138] in this field which utilizes existing electromagnetic decay data has shed some light on the empirically required isovector E2 effective charge, but has also illustrated the need for extensive scattering data. It is possible that comparative (e,e') - (p,p') data will prove competitive with the $\pi^-/\pi^+$ data in this area. Of course, the ongoing measurements of precise total decay strengths via heavy ion induced

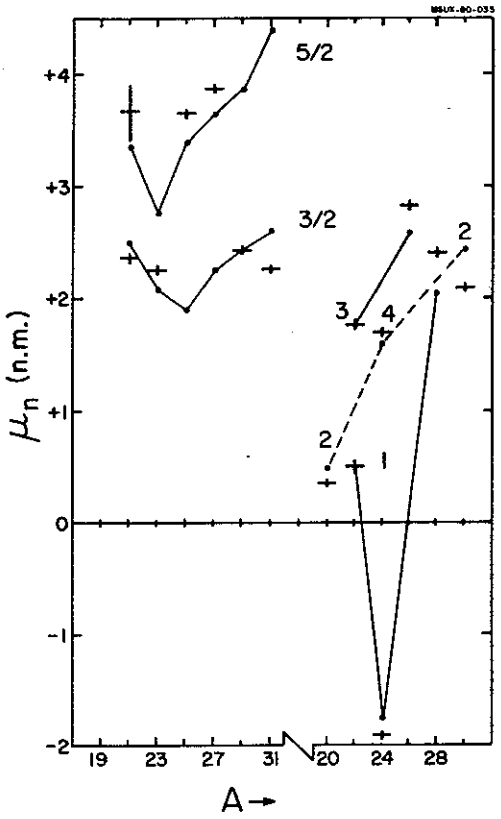


FIG.III.22. Plots of the calculated and measured magnetic dipole moments of ground and excited states of various Na isotopes. The lines connect the theoretical values. The spins of the various states are indicated by the notation 3/2, 5/2, 1, etc.

reactions and Doppler shift or recoil distance techniques wil continue to be vital in providing information on those states (the large majority) which are inaccessible to inelastic scattering studies.

Finally, all aspects of the nuclear structure data becoming available from the new electron accelerator facilities will be intensively studied. To some extent, these data provide information on transition strengths which are independent of rms radius and hence can yield information

on the character of the radial behavior of the single particle wave functions from comparisons of form factor peaks to B(E2) values as well as from the behavior of the form factors at high momentum transfer. The study of the form factors at high momentum transfer provides, in principle, information about the transition charge density as a function of radius. Various views about these data can be pursued, such as the relationship between the model space and polarization-charge contributions, the presence of explicit extra-model-space wave function components in the wave functions, the aforementioned radial shapes of single particle wave functions and, finally, the possible presence of non-nucleonic contributions to the scattering cross sections.

b. Mixing of sd Shell with p Shell and/or fp Shell Configurations

The thrusts of this component of the program are two-fold, one aimed at nuclei which are intrinsically a mixture of sd shell and p or fp shell configurations, such as $^{19}$N or $^{32}$Na, and the other at "intruder" states of either positive or negative parity within sd shell nuclei, such as the ground and first excited states of $^{32}$Mg or the $5^-$ and $6^-$ "stretched states" in $^{28}$Si The dominant interest in these studies will be the properties of exotic nuclei, with the phenomena exhibited by "stretched states" the other principal theme. The techniques developed

for determining empirical Hamiltonians within the sd shell space can easily be extrapolated to deal with these larger spaces; so the central problem will be that of determining the optinum model space truncations and evaluating the importance of spurious-state contaminations.

c. N=82 Nuclei and Their Neighbors

The region of nuclei encompassing those with the N=82 closed neutron shell are interesting from a variety of standpoints. Along with the tin isotopes, the N=82 isotones offer the clearest manifestations available of pairing phenomena in nuclei and the longest chain of existing isotones (isotopes in the case of tin). Immediately adjacent to the spherical, closed-shell-pairing structures of the N=82 nuclei themselves, nuclei swiftly develop strong rotational features. Also, of course, the nuclei around A=145-150 have been the focus of recent experimental studies of high-spin isomerism. Previous work[139] has shown that the N=82 nuclei themselves are exceptionally amenable to shell model analysis. We plan to take advantage of new techniques in shell model calculations[128] to expand our previous treatment of N=82 nuclei to incorporate the $h_{11/2}$ orbit and hence to provide for a detailed study of the minor closed shell at $^{146}$Gd. Proceeding from this basis, we plan to utilize the weak-coupling techniques developed by McGrory[13] to extrapolate from the N=82 line to the nuclei one and two neutrons removed. This would open up an exceedingly rich rield of phenomena for study, including not only high spin isomers, beta strength functions,

and pairing phenomena, but also some of the fundamental elements of the progression between spherical and deformed structures.

## B3. GIANT RESONANCES

During the past decade the focus of nuclear physics has begun to shift from studies of only the low lying excitations of the nucleus to consideration of modes which occur at higher excitation energy, but which may yet be considered simple modes of excitation. Until the shift began, only the giant dipole resonance (GDR) was solidly in this category. In addition to high excitation energy, the new resonances have in common with the GDR a large width and, sometimes, a universality of occurence in nuclei. In some cases the dependences of excitation energy and width on nuclear mass and, thus, the universality have not been established. It is in these cases - the monopole resonance, the magnetic dipole resonance, the deep-hole states - that much work remains to be done. In addition, one can hope that with high energy, lighter projectiles some of the predicted but heretofore unobserved giant multipole resonances, perhaps even unpredicted phenomena, will appear.

### a. Current Status

The giant dipole resonance has been studied with electromagnetic probes for many years, particularly with the (e,e') reaction. However, both electron and hadron scattering have proved useful in studying the properties of other giant multipole excitations. For example, one of the early papers showing the systematic behavior of

the isoscalar giant quadrupole resonance (GQR) was carried out using the 70 MeV $^{3}$He beam from the MSU K50 cyclotron.[140] Since then the dependence of the excitation energy and the dependence of the width of the GQR on mass have been established, and more recently the giant monopole resonance (GMR) has also been found. These successes have been reviewed recently[142-144] and will not be discussed in detail here.

Nevertheless, a number of important and interesting questions remain. For example, the detailed mass dependences of the excitation energy and width of the giant monopole resonance remain to be established, particularly for hte lighter nuclei. More work is needed in studying the decay properties of both the quadrupole and monopole resonances. These is presently an outstanding problem concerning the fission decay of the GQR in very heavy nuclei which is relevant to our understanding of the basic fission process. Perhaps the most interesing question of all concerns the observation of higher multipoles. These modes are predicted to exist with sufficient clustering of strength that they should be observable,[145] but, with the possible exception of the octupole resonance,[146] other multipoles have not been observed. One of the difficulties is to identify the higher mulitpoles when they are mixed into the GQR and GMR states. Some of these high lying excitations, e.g., the T=0 giant dipole mode, can give independent information on the compressibility of nuclear matter, for which at present the GMR is the only source of information.

The new K500 cyclotron at MSU, which will give high energy, good quality, and intense beams of a wide range of ions, will be a particularly suitable tool for the study of some of these problems, especially when used with the K320 spectrograph system. (See Sec. II.C.) This combination will allow experiments over a wide range of excitation energy with a variety of particles, including the highest energy, lightest ions available from the K500 cyclotron. The K320 spectrograph is particularly well suited to forward angle measurements without having the count rate problems associated with elastic scattering. Small angle experiments should therefore be possible This type of experiment has proved extremely useful in separating out various multipoles, particularly the GMR,[147,148] (See Fig. 23.) It is, therefore, anticipated that the following experiments will be carried out in the early years of operation of the K500 cyclotorn in order to help solve some of the problems mentioned above.

b. Investigations with High Energy Light Particles

One of the recurrent experimental problems in the study of giant resonances has been the separation of the broad resonances from the underlying background. Simple momentum matching arguments imply that the cross section for the excitation of giant resonances will increase at higher bombarding energies. For a well matched reaction at small scattering angles $k_f \simeq k_i - \Delta k$, where $k_f$ and $k_i$ are the final and initial wave numbers. Thus, the

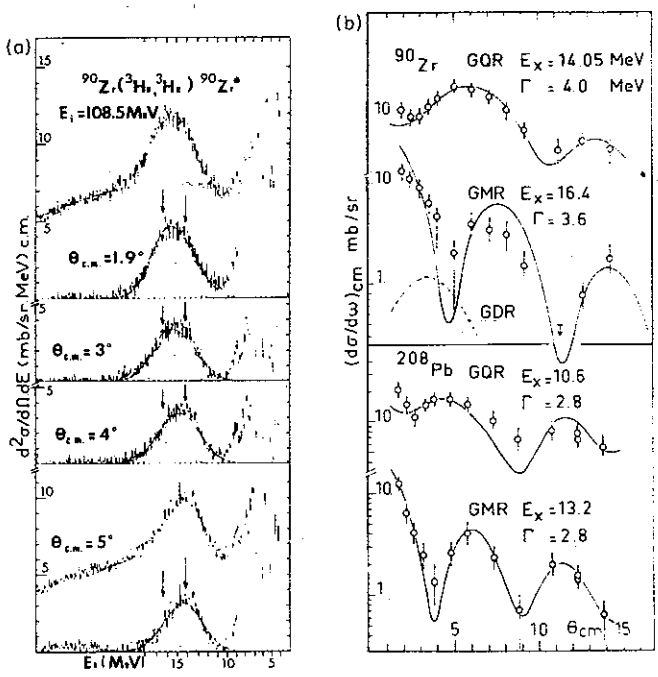


FIG.III.23. Energy spectra and angular distributions measured for inelastic He scattering. The decomposition of the energy spectra into two components is illustrated in part (a), and the resulting angular distribution, together with DWBA calculations, are shown in part (b) (from Ref. 148).

Q-value of the reaction can be written

$$Q = E_f - E_i = \frac{\hbar^2}{2m}(k_f^2 - k_i^2) \lesssim -\hbar v_i \Delta k.$$

Equivalently,

$$v_i \gtrsim |Qd/\hbar|,$$

where $v_i$ is the velocity of the incident particle and d is the distance along the particle projectory over which the reaction is localized.

Therefore, giant resonances are best studied at high beam velocities. For example, values of $Q \simeq -15$ MeV and $d \simeq 5$ fm give $v_i/c \geq 0.38$, which corresponds to a beam energy per nucleon of about 68 MeV.

These simple arguments are borne out by DWBA calculations.[149] The energy dependence of the cross section for E2 and E4 resonances at 11 MeV excitation energy in $^{208}$Pb for a variety of ions is shown in Fig. 24. At a bombarding energy of 40 MeV/nucleon the cross section for all ions is still calculated to be increasing.

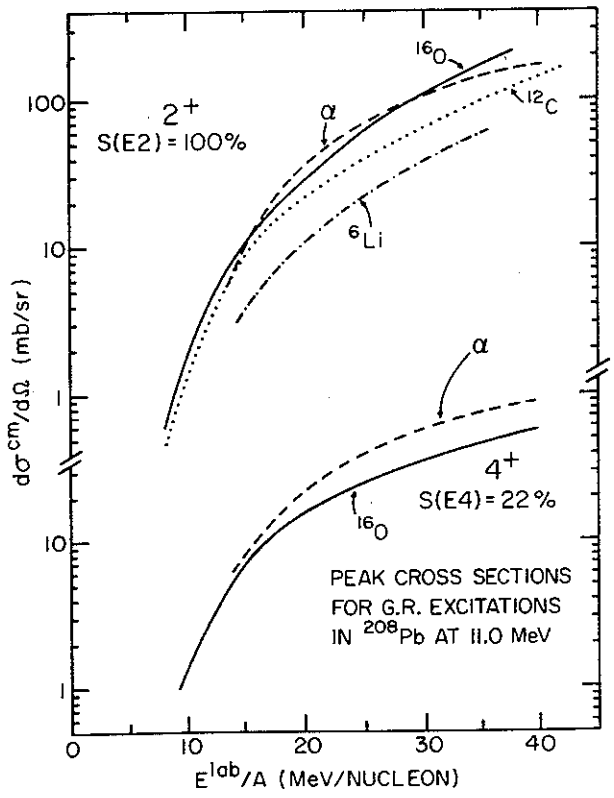


FIG.III.24. DWBA predictions [149] of the energy dependence of the peak cross sections for giant resonance excitations in $^{208}$Pb at 11 MeV.

This trend is also observed experimentally, where the ratio of peak area to background for the GQR increases, at least for α-particles, up to about 155 MeV.[150] The K500 cyclotron will produce α-particles of up to 320 MeV, which is a substantially higher bombarding energy than that of any previous investigation and will be an ideal tool for pursuing these studies

The different multipoles are likely to show different angular behavior, particularly at forward angles. Thus it will be important to be able to make measurements at very forward angles with these high energy, light ion beams. The K320 spectrograph is well suited for such measurements since it is a broad range device in which the elastic peak can be bent off the detector, thereby avoiding count rate limitations. In addition, theoretical calculations by Wambach et al.[151] imply that various L-multipoles are excited rather differently by different projectiles, such as deuterons and α-particles. Preliminary results from Marty et al.[152] at Orsay suggest that comparison of α and deuteron induced cross sections is a useful technique for untangling various overlapping multipoles. The new cyclotron would allow the comparison of, for example, inelastic scattering of 160 MeV deuterons, 160 MeV $^{3}$He, and 160 MeV α-particles with an identical experimental arrangement. By using the identical apparatus (K320 spectrograph) for all beams, a very accurate comparison of the spectra could be made at a variety of momentum transfers.

Two of the relationships which will be studied with these techniques will be the mass dependences of the position and width of the monopole resonance in light nuclei (A<40). At present, no information is available on these important questions.

c. Decay Modes of Giant Resonances

The earliest report of the decay of a GQR was an experiment on $^{40}Ca$ carried out using the K50 cyclotron at MSU.[153] Since then many decay studies have been done on a wide range of nuclei. An excellent review of this work was recently presented by G. Wagner.[154] The overall features of the decay of the GQR appear to be fairly well understood up to A≈90, with structure effects dominating in lighter nuclei and statistical decay being dominant for heavier nuclei (A≈40-90). The situation still remains to be clarified between mass 90 and mass 200. If, as expected, the cross sections for the GQR are larger at higher bombarding energies, these decay measurements could more readily be carried out.

In addition, practically nothing is known about the decay of other multipoles such as the monopole. The singles experiments suggested in a) and b) should give an indication of a suitable projectile and bombarding energy at which to carry out such decay studies. The monopole resonance is a particularly interesting case since this mode is related to the compressibility of nuclear matter and a

further understanding of the structure of the giant monopole state, which would be obtained from decay studies, would be most interesting.

Perhaps the most significant problem in the decay of giant resonances is related to the fission decay of very heavy nuclei. Two recent experiments which investigated this problem gave quite contradictory results. In one experiment[155] the fission decay of the GQR in $^{232}$Th and $^{238}$U was reported to be inhibited by at least a factor of 5 compared to the fission decay of the continuum. The other experiment[156] found that the fission probability in the region of the GQR in $^{238}$U was strongly energy dependent and higher than given in the former report. This situation needs further clarification. If an anomalous fission width does survive further experimental scrutiny, this would have serious implications for our understanding of the statistical theory of fission.

In particular, these experiments can give information about the release in fission of the collective energy injected into the nucleus through the various giant modes. An important question concerns the time scale of this energy release - whether it takes place from a statistically equilibrated compound nucleus on a slow time scale, or by prompt fission.[156]

d. Excitation of Giant Resonances with Heavy Ions

One of the earliest attempts to excite giant resonances with particles heavier than α-particles was an experiment

on $^{90}Zr$ using a 74 MeV $^{6}Li$ beam from the MSU K50 cyclotron.[157] One of the $^{6}Li$ spectra is shown in Fig. 25. While this experiment did succeed in exciting the GQR, it also pointed

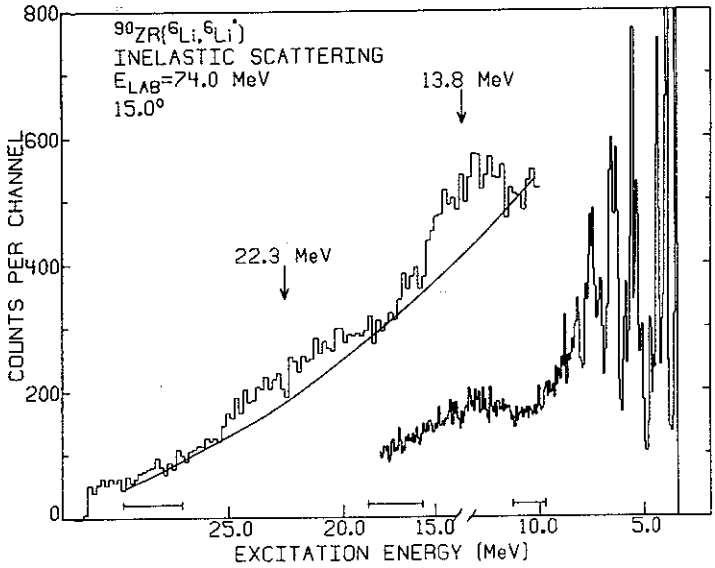


FIG.III.25. Energy spectrum observed[157] for the reaction $^{90}Zr(^{6}Li,^{6}Li')$ at E = 74 MeV and $\theta = 15^{o}$. The peak at 23.8 MeV is due to the break-up of $^{7}Li^{*}$.

out one of the problems with these experiments; namely, the production of spurious structure in the spectra due to the breakup of short lived nuclei formed by transfer of a single particle. This problem, observed for some years in $(\alpha,\alpha')$ experiments, is even more severe for heavier bombarding particles. Perhaps the most serious problem of giant resonance studies with heavy ions is the insensitivity, because of the strong Coulomb force, of the

(structureless) angular distributions to the angular momentum transfer. Nevertheless, there appears to be a number of potential advantages in using heavy ions at higher energies.

The first advantage is the fact that knock-out processes do not make a contribution to the underlying background, thus giving an improved peak-to-background ratio. Just as for α-particles, this ratio is also expected to improve at higher bombarding energies.

One might also expect that heavy ion experiments would be more likely to excite higher multipole resonances because of better angular momentum matching conditions. In fact, in an experiment with $^{16}O$ scattering from $^{208}Pb$ the observation of additional structure at higher excitation energies has been reported.[158] However, calculations for this reaction have shown that multi-step processes can also give rise to structure in the spectrum[159] at approximately the excitation energy observed. Thus, the evidence for the observation of higher multipoles is certainly not conclusive, but such experiments should be pursued with a variety of ions and bombarding energies to help separate out any reaction mechanism effects.

At higher bombarding energies, provided the target projectile combination is not too heavy, the angular distributions should show an increased sensitivity to the L-transfer compared to the situation at lower energy. Figure 26 shows calculations of $^{6}Li$ scattering from $^{90}Zr$

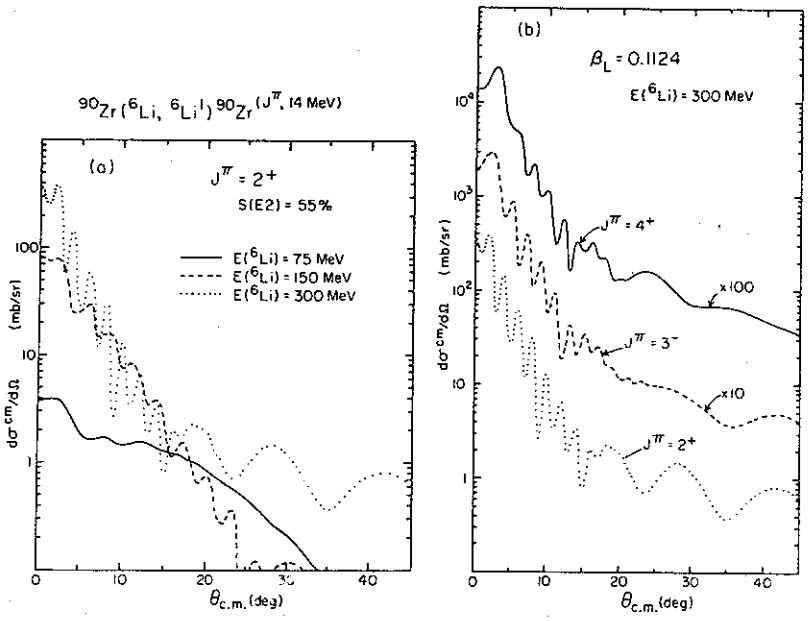


FIG.III.26. (a) Energy dependence of angular distributions for inelastic scattering of $^6$Li on $^{90}$Zr calculated[160] with the DWBA. (b) Dependence of the angular distributions on angular momentum transfer for 300 MeV $^6$Li scattering on $^{90}$Zr calculated[160] with the DWBA.

at a variety of bombarding energies.[160] At 300 MeV the angular distributions are quite structured and show very large differences for different L-transfers. The new cyclotron and the K320 spectrograph should make an excellent combination for carrying out these higher energy experiments.

The comparison of excitation functions obtained with light and heavy ions is likely to be an important means of untangling the contributions from various overlapping multipoles. At 80 MeV/nucleon, and at small scattering

angles, the excitation of giant resonances with $^{16}O$ is dominated by Coulomb excitation processes which can excite the quadrupole resonance strongly but which will not excite the nearby monopole. On the other hand, alpha particles at comparable energies will preferetially excite the monopole mode at small scattering angles.

e. Giant Resonances and Heavy Ion Dissipation Mechanisms

The previous sections focus on the intrinsic interest of continuing studies of giant resonances in nuclei. However, the role of these modes as a mechanism for damping the collective degrees of freedom in deeply inelastic collisions[161] is also interesting. Recent studies of $^{40}Ca$ - $^{40}Ca$ collisions show that gross structures may be observed in inelastic and transfer reactions with over 100 MeV excitation. These structure have been interpreted as giant resonances of very high multipolarity.[162] Clearly, if this interpretation is correct, the multiple step excitation of these modes can account for very large energy losses by mechanisms quite different from those contained in transport theories of dissipation. At present, the interpretation is not unambiguous since gross structures can also be generated from sequential transfer and decay processes.[163] A clear experimental distinction which could be made in a study at several different energies would be possible with the beams of mass 40 up to 20 MeV/nucleon. A study of giant resonance excitation and deeply inelastic scattering over the energy range from 10 to

20 MeV/nucleon should also provide good tests of current theories of deeply inelastic scattering, for the reason that these energies encompass a region where the deeply inelastic process is likely to be decreasing in importance, but where the cross section for giant resonance excitation is increasing.

## f. Isovector Giant Resonances via Charge Exchange Reactions

Inelastic scattering, the major tool in giant resonance studies, is so effective in exciting isoscalar resonances that isovector resonances are hard to find. Charge exchange reactions, on the contrary, can excite only isovector states. The isobaric analog states (IAS) discovered by Anderson and Wong[164] in (p,n) reactions are an example of giant isovector resonances. In transitions to these states the strength of the (non-spin-slip) Fermi operator is concentrated into a very narrow energy interval. A broad peak observed in neutron spectra from the $^{90}$Zr(p,n) reaction was interpreted[165] as a concentration of strength of the (spin-flip) Gamow-Teller operator in a $0^+ \rightarrow 1^+$, $T = 5 \rightarrow T = 4$ transition.

A corresponding peak has now been seen in experiments at MSU in neutron spectra produced by bombarding 17 targets from $^{90}$Zr to $^{208}$Pb with 45-MeV protons.[166,167] Spectra from targets of four Sn isotopes are shown in Fig. 27. The features common to all of the spectra are denoted on the topmost one. The Gamow-Teller peak is designated M1. This notation comes from the alternate interpretation[165] of that peak as the antianalog, or T-1 component (T=target isospin) of the analog, of the giant M1 resonance in the target. In the target, where $T_z$=T, only the T and T+1 components may exist, but in the nucleus produced in a (p,n) reaction, where $T_z$=T-1, we can also have a T-1 component. Indeed, isospin vector geometry greatly favors the (p,n)

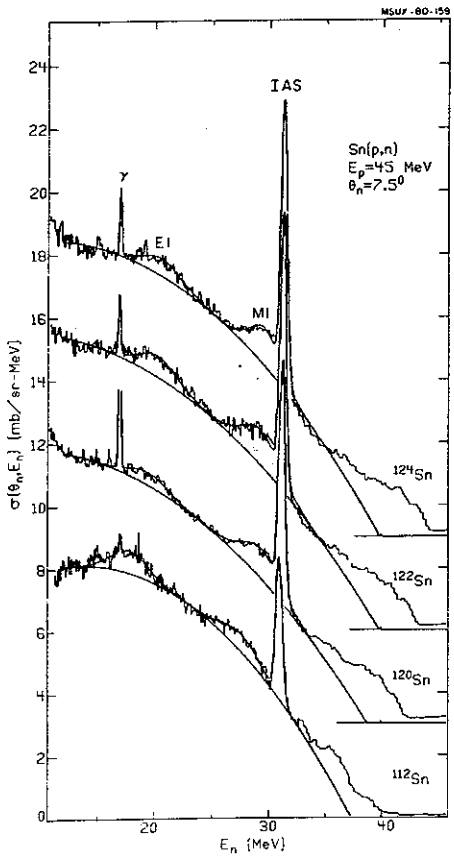


FIG.III.27. Neutron spectra resulting from proton bombardment of four isotopes of tin. The labelled features of the spectra are interpreted to be: "γ"-gamma rays from the target; "E1"(T-1) component of the giant electic dipole resonance in the target; "M1"(T-1) component of the giant magnetic dipole resonance in the target; and "IAS"- isobaric analog of the ground state of the target.

transition to the T-1 component over the T component. (For a $^{90}$Zr target, for example, the closed-shell model of $^{90}$Zr leads to a ratio of 9:1 for these two transition rates.) The excitation energy of the giant M1 or of its analog may be expected to have a weak mass dependence, $A^{-1/3}$, but the antianalog, being split from the analog

by an amount proportional to N-Z should move noticeably in a string of isotopes such as those in Fig. 27. Indeed, we do see a shift of the M1 peak to lower excitation energy with increasing neutron excess, i.e. from $^{112}$Sn to $^{124}$Sn.

The same bump has been seen at Indiana with 80, 120, and 160 MeV protons on a few isotopes of Zr, Sn, and Pb.[168] The prominence of the broad bump, presumably a $0^+ \rightarrow 1^+$ spin-flip transition, increases so rapidly with proton bombarding energy that the weaker M1 analog is visible in some of the higher-energy spectra. The two broad peaks labelled $1^+$ in Fig. 28 correspond in this interpretation to the analog and antianalog of the giant M1 state in $^{90}$Zr, $^{92}$Zr, and $^{94}$Zr. The isospin splitting, $E_T - E_{T_1}$, is about 4.5 MeV in $^{90}$Nb (topmost spectrum) and can be seen to increase slightly as N-Z increases. This behavior favors the interpretation given.

There is one difficulty with the above description, namely, the non-observation in backward electron inelastic scattering of the M1 state itself. The spin-isospin operators for the $0^+ \rightarrow 1^+$ (p,n) and for the $0^+ \rightarrow 1^+$(e,e') reactions are essentially the same. It is therefore difficult to see how the transition could be very strong in one reaction and very weak in the other. The strengths of the (p,n) cross section and of the M1 transition in the target should be strongly correlated. The (p,n) cross section exhausts the possible strength, yet the most detailed (e,e') work[169] has revealed only 15% of the expected M1 strength in $^{90}$Zr

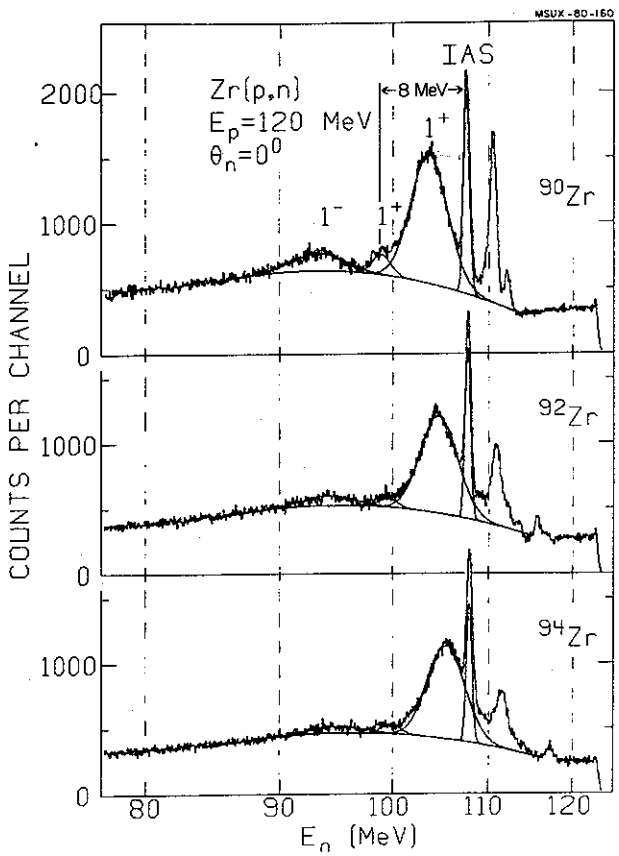


FIG.III.28. Neutron spectra resulting from proton bombardment of three zicronium isotopes. The labelled peaks are interpreted to be: $1^-$-(T-1) component of the giant E1 resonance in the target; $1^+$ (small peak) - T component of the giant M1 resonance in the target; $1^+$ (large peak)-(T-1) component of the giant M1 resonance in the target; and IAS - isobaric analog of the ground state of the target.

and no strength in $^{208}$Pb. Now that the original conjecture[165] has been confirmed in many experiments, the lack of M1 strength is indeed puzzling. A search for M1 strength with another particle probe seems the next logical step. Cecil, Garvey, and Braithwaite[170] searched in $^{90}$Zr with (p,p') but with rather low-energy protons (24 MeV). The

(p,n) work shows very clearly that the spin-flip part of the effective interaction increases rapidly with energy in comparison to the non-flip part. It therefore seems sensible to search for these transitions at Indiana with protons of energy 120 MeV and higher. For the Zr isotopes we believe that the region of interest in excitation energy is centered around 8 MeV. Angular distributions of states in that region should reveal those which may have $J = 1^+$. We will also search on other targets such as $^{208}Pb$.

A second broad bump, labelled E1 and $1^-$ in Figs. 27 and 28, respectively,occurs in the spectra of all targets at approximately 10 MeV higher excitation energy than the M1, $1^+$ bump. Particularly at 120 MeV, where we have good data on the Zr isotopes, the angular distribution of the $1^-$ peak is very different from that of the $1^+$ and IAS peaks. The latter fall off from $0^o$ with an L=0 shape, while the $1^-$ peak has its maximum around $8^o$, in agreement with the expectations for an angular distribution characteristic of an L=1 transfer.

It is then tempting to associate this bump with the well known giant dipole resonance (GDR). The association can be made, but not with the analog of this resonance. The known GDR excitation energies and Coulomb displacement energies always predict a peak several MeV higher in excitation energy than observed. Also, the bumps shift much faster towards the IAS with increasing (N-Z) than is expected from an $A^{-1/3}$ dependence. The most natural interpretation is that we are again seeing an antianalog, or

T-1 component in this case of the GDR. Estimates of the T, T-1 energy splitting[171] are generally in agreement with our observations, but now we have for the first time a substantial body of data (in 17 nuclei) for testing theories of the isospin splitting of the GDR. $E_T$ is obtained by Coulomb displacement of the GDR from the parent nucleus. $E_{T-1}$ is the energy of the observed neutron group above the IAS. Unlike the M1 analogs, where we can marginally see the analog $1^+$ peak at 120 MeV (Fig. 29), we do not expect to see the analog $1^-$ peak; the well known collective effects reduce the splitting for the GDR,[172] whereas the same isospin geometry effect as in the M1 case greatly inhibits transitions to the T component relative to the T-1 component.

Considering the success of the charge-exchange program in studying isovector giant resonances, we plan to continue these investigations by using beams from the K500 cyclotron. Two beams which will have obvious use are the $^3$He beam and the $^6$Li beam.

The first observation of the E1 bump was made in the $^{90}$Zr ($^3$He,t) reaction at 130 MeV.[173] Both the (p,n) and ($^3$He,t) reactions on $^{90}$Zr have produced a very noticeable structure in the region of the giant Gamow-Teller resonance, and some success was achieved in untangling the structure in an experiment with $^3$He at 80 MeV.[174] With normal use of the K320 spectrograph both high intensity and high resolution will be avaialble for observation

of tritons up to 107 MeV. Up to the highest energy $^3$He beams, 320 MeV, the factor-of-two difference in rigidity between t and $^3$He of the same energy can be exploited to make a clean separation of the two ions and to continue these studies up to 320 MeV.

The ($^6$Li,$^6$He) reaction produces the same charge change as the (p,n) and ($^3$He,t) reactions, and is therefore suitable for the study of isovector resonances. Furthermore, it is even more selective, because to first order it excites only those isovector transitions in which there is a spin flip. At high bombarding energies it should be ideal for studying $0^+ \rightarrow 1^+$ transitions. Since $^6$He is 50% more rigid than $^6$Li at the same energy, the K320 spectrograph can be used as with $^3$He and t to carry these studies to the highest energies of the $^6Li^{++}$ beam, that is, to 320 MeV. As discussed below, this reaction has the promise of opening several lines of investigation, most, but not all, of them related to giant resonances.

g. Studies of Spin-Flip Strength with the ($^6$Li,$^6$He) Reaction

Recent work has established that high energy charge exchange reactions observed at low momentum transfer (small angles) are an especially sensitive and selective probe for spin flip strength of low multipolarity. This sensitivity rests on the strong forward peaking of L=0 cross sections and on the increase with increasing energy of the relative strength of the spin transfer part of the effective interaction $V_{\sigma\tau}(\bar{\sigma}_1 \cdot \bar{\sigma}_2)(\bar{\tau}_1 \cdot \bar{\tau}_2)$. These properties have made it possible to locate and determine the strength of the giant Gamow-Teller resonance in many nuclei (see preceding section). It appears that the ($^6$Li,$^6$He) reaction will permit an extension of such studies to many other nuclei and to lesser transition strengths. The high energy, high intensity $^6Li^{++}$ beam from the K500 cyclotron, coupled with the K320 spectrograph, has many advantages for such studies.

The ($^6$Li,$^6$He) reaction is uniquely suited for studying spin transfer strength. Because of the projectile-product spins and isospins: $^6Li(1^+,T=0) - {}^6He(0^+,T=1)$, all reactions transfer one unit of spin and isospin, i.e., S=T=1. Hence, from $J=0^+$ targets only unnatural parity states can be reached, and only the $V_{\sigma\tau}$ component of the effective interaction (and possibly the tensor component at high momentum transfer) contributes to the cross section in first order. Moreover, only the ground state of $^6$He is particle stable; the double excitation process, so common in heavy ion

reactions, will not be detected. Finally, $^{6}$He will be the most (magnetically) rigid reaction product. This may make it possible to take data at $0^{o}$, a great advantage in enhancing sensitivity to L=0 transitions.

A number of considerations enter into the choice of energy. It must be high enough to ensure that higher order processes, which apparently affected earlier studies,[175] do not dominate the reaction mechanism. (The increasing importance of $V_{\sigma\tau}$ in this energy region should increase the dominance of first order processes). On the other hand, the resolution will be worse at higher energies. It appears, overall, that the incident energy range from 25 to 35 MeV/u, where intense $^{6}Li^{++}$ beams are available from the cyclotron, is the probable best choice.

When one wishes to extract quantitative information from a reaction of complex projectiles it seems better to calibrate the reaction empirically rather than to rely on apriori DWBA calculations. Such procedures are especially useful at small momentum transfer where the reaction depends mainly on the volume integral of $V_{\sigma\tau}$ and not its detailed shape. The initial measurements then will deal with the observation of transitions to states in light nuclei whose β-decay matrix elements are known from analog transitions and with a comparison of the measured cross sections, perhaps corrected for obvious distortion effects, with the β-decay matrix elements. One hopes to establish a calibration curve from which the β-decay matrix can be read, given the observed cross section; it is likely

that this curve will be a straight line. To extend the calibration to heavier nuclei we will also observe the giant Gamow-Teller transitions in isotopes of Zr, Sn, and Pb and compare the results to those from the better understood (p,n) reaction. These measurements will also provide a check on the nature of the enhancement observed at higher excitation for these targets in (p,n) reactions and believed to be the T-1 giant E1 resonance. If this description is correct, the enhancement should not occur in the ($^{6}$Li,$^{6}$He) spectrum since it presumably corresponds to S=0. We note in passing that the isobaric analog state, so prominent in Figs. 27 and 28, should also be absent; its intensity will monitor contributions from higher order processes.

Following these measurements a number of interesting experiments suggest themselves.

1) Study of transitions to resolved states in 2s-1d shell nuclei for comparison with large basis shell model calculations. (See Sec. III.B2.) A comparison of these results and M1 matrix elements may permit one to understand the relative importance of mesonic and configuration mixing effects in the renormalization of the relevant operator.[176]

2) Searches for the giant Gamow-Teller and electric dipole resonances in nuclei with A<90. In such cases the strength often occurs in resolvable states, and

the resolution afforded by ($^{6}$Li,$^{6}$He) will be important. In these nuclei, where the neutron excess is small, one should also see those resonances having isospin T as well as T-1. Estimates of the symmetry potential and of the location of M1 strength in the target nucleus will then be straightforward. Nuclei that would be studied here include $^{40,48}$Ca[177] and $^{58}$Ni.[178,179]

3) Study of the β-decay strength function at energies below the giant resonance. Such studies are relevant both for nuclear structure and for applications in astrophysics (see Sec. III.C2$_{\beta}$). The low background and good resolution of ($^{6}$Li,$^{6}$He) will be critical for these studies since one will be looking for small weak cross sections.

4) Search for critical opalescence phenomena (see Sec. III.C4$_{\rho}$).

h. Deep Hole States in One and Two Particle Transfer Reactions

The single particle strength function of a wide range of nuclei has been investigated in a number of different pickup reactions including (p,d), (d,t), and ($^3$He,$\alpha$) reactions.[180-187] Perhaps the most extensive work has been done on the neutron hole states ($g_{9/2}$ and p shells) in the tin isotopes and in $^{208}$Pb where hole state strength up to an excitation energy of 12.7 MeV has been reported.[188] One of the interesting features of the latter work was the observation of the $T_> = \frac{45}{2}$ components of some of these hole states.[189] (See Fig. 29.)

At present, a collaboration from MSU, Orsay, Melbourne, and Indiana is carrying out experiments to investigate deep hole states in Zr, Sn, and Pb using a polarized proton beam with an energy of about 90 MeV from the Indiana University Cyclotron. Preliminary results suggest that at this bombarding energy the analyzing power of the outgoing deuterons is an excellent guide to the $J^\pi$ of the final state. Figure 30 shows the analyzing power for some of the low lying states including two with $J^\pi$ values of $1/2^-$ and $3/2^-$. One can see that these analyzing powers are clearly out of phase. This work with polarized beams will be completed at IUCF

The K500 cyclotron, particularly when used with the K320 spcetrograph, will also provide an exciting opportunity for additional studies of the nuclear strength

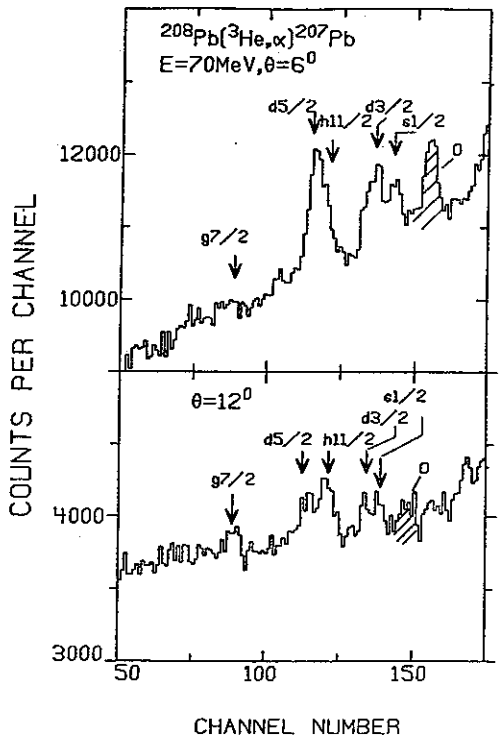


FIG.III.29. α-particle spectra from the reaction $^{208}$Pb-($^{3}$He,α)$^{207}$Pb at laboratory angles of 6° and 12°. The arrows indicate the position of the $T = \frac{45}{2}$ deep-hole configurations in $^{207}$Pb. The symbol O refers to a state arising from ($^{3}$He,α) reaction on $^{16}$O.

function. Two possible kinds of experiments which are planned for the new facility are given in the following paragraphs.

i) Single Particle Strength Function from Stripping Reactions--With the higher energy and the variety of beams available from the new accelerator it would be interesting

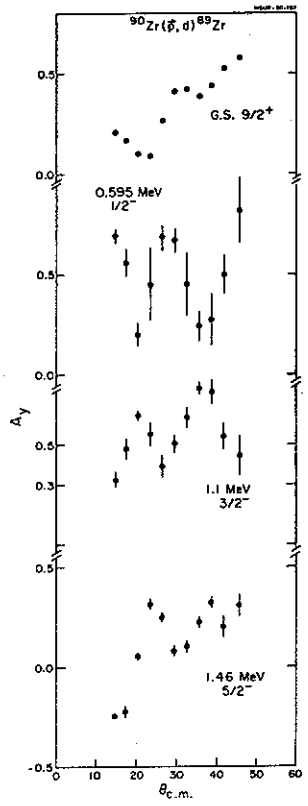


FIG.III.30. Analyzing Power (Ay) versus angle for low lying states in $^{89}Zr$ from the reaction $^{90}Zr(p,d)^{89}Zr$ at $E_p$ = 90 MeV.

to see whether there is any clustering of strength corresponding to particle states at high excitation energies. For example, (d,p), ($\alpha$,$^3$He), and ($^7$Li,$^6$Li) experiments could all be carried out with high energy projectiles. The different momentum matching conditions for these dif ferent reactions means that they would preferentially excite final states having different $J^\pi$. This technique has proven very useful in investigating hole states.

Another valuable experiment would be to compare the spectroscopic strengths and widths of particle states and hole states at comparable excitation energies; e.g., in the tin and lead isotopes. This comparison should test not only our understanding of the basic mixing process in which a simple state spreads among the background states, but should also give some indication of the level density of various kinds of states as a function of excitation energy. At present, very little information on higher lying particle states exists, largely because the experimental tools have not been readily available.

ii) Two Particle Strength Function--The first observation of the clustering of strength at high excitation in two particle transfer reactions was reported in a (p,t) experiment on the tin isotopes using the MSU K50 cyclotron.[190] One of the spectra is shown in Fig. 31. Similar structures have now been observed in a wide variety of nuclei. A review[191] of much of the work carried out at MSU was published recently and will, therefore, not be repeated. However, there still remain a number of open questions regarding this phenomenon, such as the basic structure of the state and the reason for the rather narrow strucutre observed; the structure is about twice as wide as in the one particle case.

One approach which might cast some more light on this phenomenon and which can be carried out with the K500 cyclotron is to study the same final nucleus by a

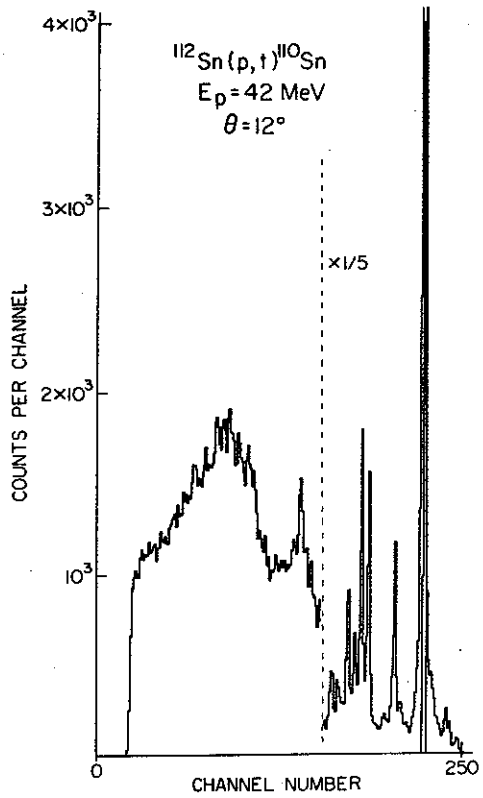


FIG.III.31. Triton spectrum from the $^{112}$Sn(p,t)$^{110}$Sn reaction at a laboratory angle of $\theta_{lab} = 16^o$ and a proton bombarding energy of $E_p$ = 42 MeV.

variety of two particle transfer reactions. At the least we will supplement the (p,t) work already done at 42 MeV by studying the Sn isotopes with the ($\alpha$,$^6$He) reaction. A clarification of the angular momentum transfer involved should result since this reaction will tend to favor higher L-transfer than did the (p,t) reaction.

Two proton transfer is another class of experiments for which no information is available in either the pickup

or stripping process. Experiments like ($^{6}$Li,$^{8}$B) and ($^{16}$O,$^{14}$C), where one can investigate a wide range of excitation energies with the new machine, should be possible. A comparison of the excitation energies of structures observed in two neutron and two proton pickup to the same final nucleus and on the same target would help to resolve the question of whether both particles picked up come from deep orbits.

## B4. AN EMPIRICAL INTERACTION FOR CHARGE EXCHANGE AND INELASTIC SCATTERING

The description of inelastic scattering and charge exchange reactions in a microscopic model requires a specification of the effective two-body interaction $V_{eff}$ between the projectile and the valence nucleons of the target. Both theoretical and empirical estimates of $V_{eff}$ are available in the 20-50 MeV range. The theoretical estimates, based in most cases on a shell model G matrix, are quite detailed[192] but suffer from uncertainties in the bare two-nucleon interaction and in the computationally difficult procedures used to estimate these uncertainties.

The empirical interactions, on the other hand, are obtained by choosing calibration reactions sensitive only to a single spin-isospin transfer component of $V_{eff}$ and then adjusting the strength of the selected component to match the cross section. Thus, the consistency of results obtained for a variety of cases serves as a built in measure of the uncertainty in the empirical procedure. and furthermore, the empirical interaction is automatically renromalized for any systematic deficiency of the reaction mechanism. Following an earlier review of empirical information on $V_{eff}$, much new data has become available which bears on the isospin transfer T=1 parts of $V_{eff}$. These now appear[193] to be known at least as precisely as those for T=0.

We write the central part of the effective interaction as:

$$V_{ip}^{cent} = V_{00} + V_{10}\bar{\sigma}_i\cdot\bar{\sigma}_p + V_{01}\,\bar{\tau}_i\cdot\bar{\tau}_p + V_{11}(\bar{\sigma}_i\cdot\bar{\sigma}_p)(\bar{\tau}_i\cdot\bar{\tau}_p)$$

$$= V_0 + V_\sigma\bar{\sigma}_i\cdot\bar{\sigma}_p + V_\tau\bar{\tau}_i\cdot\bar{\tau}_p + V_{\sigma\tau}(\bar{\sigma}_i\cdot\bar{\sigma}_p)(\bar{\tau}_i\cdot\bar{\tau}_p),$$

where $V_{ST}$ describes a direct amplitude with spin transfer S and isospin transfer T. Each $V_{ST}$ is taken to have a Yukawan radial shape with a range of 1.0 fm chosen to yield about the same mean square radius as the theoretical effective interactions.[192]

The results of the present survey for energies between 20 and 50 MeV are:

$V_0 = -27.9 \pm 3.5$ MeV,

$V_\sigma \lesssim 11.5$ MeV,

$V_\tau = 15.2 \pm 2.2$ MeV, and

$V_{\sigma\tau} = 11.7 \pm 1.7$ MeV.

The values for $V_0$ and and $V_\sigma$ are essentially those reported earlier,[193] except that in the case of $V_\sigma$ it has been found that the spin flip amplitude does not dominate the cross section for $^{16}O(p,p')^{16}O(2^-,T=1)$. Therefore, values of $V_\sigma$ based on the spin flip assumption for this reaction become upper limits.

The tabulated values for $V_\tau$ and $V_{\sigma\tau}$ are shown in detail in Figs. 32 and 33. In these figures the short horizontal lines at the right represent strengths corresponding to volume-integral estimates of various theoretical

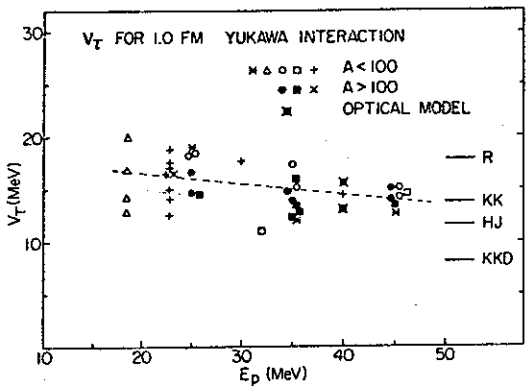


FIG.III.32. Values of $V_\tau$ for a real, 1.0 fm range, Yukawa interaction. The mean (± standard deviation) of the points is 15.2 ± 2.2 MeV. The dashed line is drawn through the points by eye and has a slope $dV_\tau/dE_p = -0.1$.

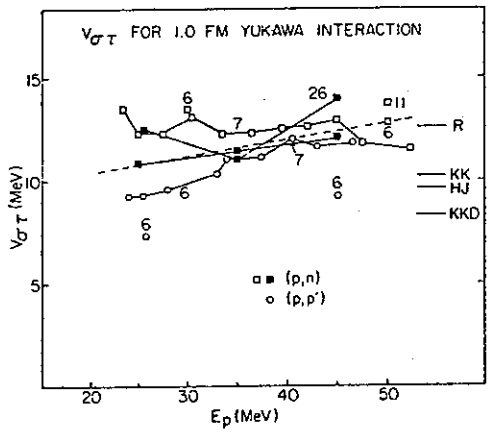


FIG.III.33. Values of $V_{\sigma\tau}$ for a real 1.0 fm range Yukawa interaction. The mean of the points is 11.7 ± 1.7 MeV. The dashed line is drawn through the points by eye and has a slope $dV_{\sigma\tau}/dE_p = 0.075$.

portentials: the Hamada-Johnston potential (HJ), the Reid soft-core potential (R), the Kallio-Kolltveit potential (KK), and the density dependent Kallio-Kolltveit potential averaged over the lead nucleus (KKD). The numbers near the points in Fig. 33 represent the masses of the targets. Results of a given experiment or analysis are denoted by a common symbol and/or connected by lines.

These results imply that the interaction between two like nucleons ($V^{pp}$ or $V^{nn}$) is substantially weaker than that between unlike nucleons ($V^{pn}$), i.e.,

$$\frac{V^{pn}}{V^{pp}} = \frac{V_0 - V_\tau}{V_0 + V_\tau} = 3.4 \pm 1.2.$$

In this energy range inelastic proton scattering is then sensitive mainly to the neutron configurations of the target, and comparisons with electron scattering, which is sensitive to proton configurations, should yield the isospin structure of nuclear core excitations.

Recent studies[194] have established that a reasonable estimate of the imaginary part of the interaction $V_\tau$ can be obtained from the forward scattering amplitude approximation. Conveniently, its inclusion affects the value of $V_\tau$ extracted by only about -15%, and this in a systematic fashion; therefore, it can be incorporated into the real part of $V_\tau$.

Other work has been aimed at determining whether the ratio of $V_{\sigma\tau}/V_\tau$ increases with energy, as suggested

by recent theoretical estimates. Studies of the $^{7}Li(p,n)^{7}Be$[195] and $^{26}Mg(p,n)^{26}Al$[196] have been analyzed in an almost model independent fashion involving the use of ratios of cross sections to yield this interaction ratio directly. These results are summarized in Fig. 34 where they are compared with the theoretical estimates[192] and with a measurement of Goodman, et al.[197] at 120 MeV. It is clear that $V_{\sigma\tau}/V_{\tau}$

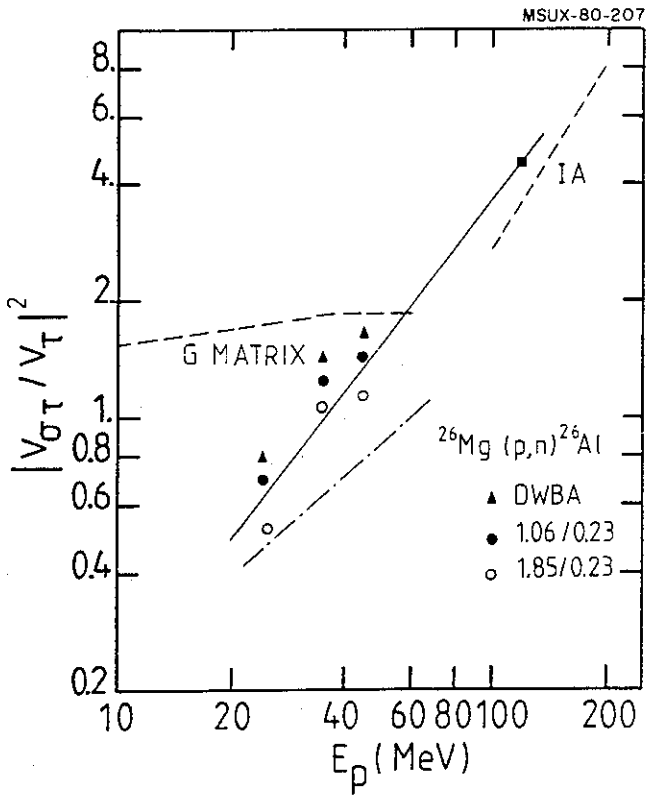


FIG.III.34. Values of $(V_{\sigma\tau}/V_{\tau})$ as a function of bombarding energy. The experimental results are indicated by the symbols ▲,●, and o from analyses of $^{26}Mg(p,n)$ data and by ■ from Ref. 197. The solid line in an approximation to the energy dependence of the $^{26}Mg(p,n)$ results; the dot-dash line is from the $^{7}Li(p,n)$ data[195] and the summary of Ref. 193; and the dashed lines summarize the theoretical predictions of Love, Ref. 192.

increases over this energy range and that $V_{\sigma\tau}$ dominates strongly at high energies. This result indicates that searches for spin flip strength will be easier and their results less ambiguous if carried out at high energy where the spin transfer amplitude dominates. This advantage is shown in an unmistakable fashion in the searches for Gamow-Teller strength discussed in Sec. III.B3.f. These results also strongly influence our plan to study spin transfer reactions with the ($^{6}$Li,$^{6}$He) reactions near 35 MeV/u where the spin transfer amplitude should already be quite large.

## C. EXOTIC PROCESSES

### C1. STUDIES OF NUCLEI FAR FROM STABILITY

a. Q-value Measurements with the Spectrographs

b. Program of the RPMS (Recoil Product Mass Separator)

c. Isotope Production Cross Section Survey with the RPMS

d. Lifetime Measurements with the RPMS

e. Laser Spectroscopy with the RPMS

f. The He Jets

### C2. ASTROPHYSICS

a. Creation of the Light Elements

b. β-Decay Strength Functions

### C3. WEAK INTERACTION RESEARCH

### C4. SEARCH FOR CRITICAL OPALESCENCE PHENOMENA

### C5. PION PRODUCTION EXPERIMENTS

a. The Total Cross Section

b. Inclusive Measurements

c. Exclusive Measurements

## C1. STUDIES OF NUCLEI FAR FROM STABILITY

Measuring the properties of new nuclei continues to be one of the basic and productive tasks of nuclear science. If our understanding of stable and near-stable nuclei is correct, then it should bear the test of extrapolation to regions of very different proton and neutron numbers. A large part of our effort with the K500 cyclotron is expected to go into this study and there are five different devices which can be used. Of central importance is the fact that the beams of Phase I and Phase II will range over a great choice of projectiles with energies high enough to optimize almost any production process. Exploiting these possibilities will involve many scientists and a variety of techniques In this section we will discuss several projects which are planned to be carried out by MSU staff

### a Q-value Measurements with the Spectrographs

Approximately 50 new nuclear masses were measured at MSU with the K50 cyclotorn and the Enge split-pole spectrograph [198] The techniques developed for these studies can be directly applied to the K500 program with the Enge and the K320 spectrographs. The $\alpha$ and $^{6}Li$ beams have properties perfectly suited to direct multinucleon transfer and rearrangement collisions. The first experiments will be of the type:

$^{48}Ca(\alpha\ ^{8}B)^{44}Cl$

$^{24}Mg(^{6}Li\ ^{8}He)^{22}Al$, and

$^{40}Ca(^{7}Li\ ^{8}He)^{39}Sc$

There are many other possibilities, and both proton rich and neutron-rich masses can be measured. Beams of heavier ions have also been used to make new nuclei and to measure their masses. Figure 35 shows one of the last results from the K50 cyclotron and one of the first successful uses of heavy ion transfer reactions to measure a heavy nuclear mass. These results make one optimistic about measuring masses with reactions of the type $^{48}Ca(^{18}O, ^{22}Mg)^{44}S$, reactions which go very far from β stability and which could test whether or not mass predictions are on the right track.

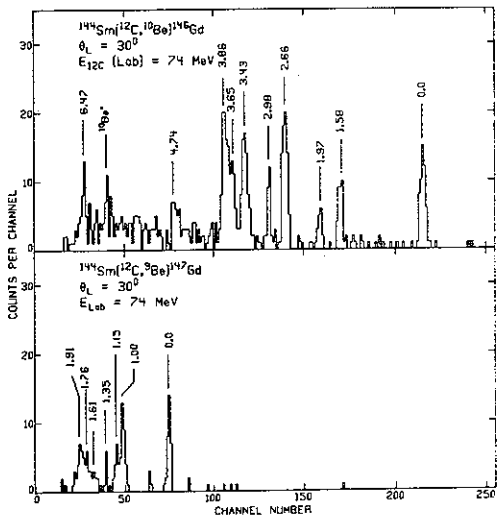


FIG.III.35. Spectra of states in Gd nuclei found in transfer reactions with heavy ions.

Q-value measurements are the only method by which masses of nuclei far from stability can be measured with a precision of 10 KeV or better. Special techniques can be used when mass measurements of ≈1 keV accuracy are required. As an example, see Ref. 199 for the redetermination of the mass of $^{9}C$. Precise measurements of reaction Q-values are important for astrophysics, for β-decay theory and isobaric multiplets, and for the calibration of α- and β-decay chain measurements

b Program of the RPMS (Reaction Product Mass Separator)

As described in Sec. II.C., the RPMS is a device intended mainly for studies of nuclei far from stability In essence, it prepares a beam of reaction products with a given $\frac{q}{M}$ and delivers it to the experimentalist to measure some property of interest with specialized equipment. This secondary beam can itself be used in high cross section scattering or reaction experiments; but mainly experiments will be performed to measure masses, lifetimes, decay schemes, energy levels, electromagnetic moments, and charge radii. Before these experiments can be carried out, however, a survey of production mechanisms will be made both theoretically and experimentally. The first series of experiments will therefore be a survey of isotope production cross sections.

c. Isotope Production Cross Section Survey with the RPMS

There are basically four mechanisms for the production of nuclei far from stability which are suited to the RPMS

These are the fusion deep inelastic, fragmentation and direct reactions. In addition, one has a choice of particle, target, and beam energy. It is valuable (and also of interest to studies of these reaction mechanisms, see Sec. III.A3 ) to gain an insight into the yields of isotopes as functions of their various characteristics.

In the case of fusion reactions, theoretical treatments exist which calculate the production cross section of various residues. The falloff in yield as one goes away from β-stable nuclei can be understood in terms of the energetics and penetrabilities; those always favor the decay of the compound or fused state back towards the line of stability. In any case, highly proton-rich medium weight nuclei like the light tin isotopes can be made in Phase I only with reactions of this type, and the question of the optimum beam energy and beam-target combinations must be studied

In the case of deep inelastic processes, the basic cross section is so large that one can be very optimistic about its use as a source of new nuclei Beams of $^{48}Ca$ or $^{50}Ti$ for example, at 10-20 MeV/u will produce prolific yields of a variety of nuclei, as has already been shown.[200] Much theoretical attention has been given to isotope production rates for this process, and this is a field of its own (as discussed in Sec. III.A3.).

Fragmentation processes, important at high energies, are probably not a strong consideration for isotope production with the K500 cyclotron because they are not expected to be large enough at energies of 80 MeV/u and

below. Nonetheless, we will begin experiments like those near 200 MeV/u in the MSU LBL project at the Bevalac[201], because the narrow, forward cone of the products of fragmentation are perfectly suited to the RPMS. Perhaps with beams of 20-40 MeV/u $^{26}$Mg ions, for example, fragmentation and deep inelastic scattering will combine to give optimum production cross sections for nuclei far from stability. Previous work has shown that the fall-off of yield as one leaves the line of β stability is strongly dependent on nuclear structure effects such as level density and ground state mass.[202]

Direct or rearrangement processes have been used previously for Q value measurements. The yield is very low because of the requirement that there be only two products and that each be in its ground state. However, in these experiments continuum yields have been observed which are much greater than the ground state yields.

For the survey experiments on isotope yields either gas counters or silicon detector telescopes will be used on the focal plane of the RPMS. Thus one can simultaneously optimize and calibrate the performance of the instrument. Observation of several new nuclides is also expected during this series of experiments. Observation of the particle stability of nuclides near the limits of particle stability can be very valuable in distinguishing between theories of nuclear masses.

d. Lifetime measurements with the RPMS

To illustrate one type of experiment which can be done with the RPMS, one can consider two neutron rich, T=5/2, light isotopes for which the only known properties are the masses, viz., $^{15}B$ and $^{17}C$. The masses were obtained from the Q-values of the transfer reactions $^{48}Ca(^{18}O,^{17}C)$ and $^{48}Ca(^{18}O,^{15}B)$ with $^{18}O$ beam energies of 102 MeV.[203,204] From the cross sections and spectra observed in these measurements it is possible to design an experiment to measure the lifetimes of these very neutron rich isotopes. This seems to be an ideal early measurement to do with the RPMS because it does not push the design limits of either the cyclotron or the RPMS. The measurements can be done with an $^{18}O^{3+}$ or $^{32}Ne^{4+}$ beam with an energy between 100 and 250 MeV. The low charge states should permit beam intensities well over $10^{11}$ particles per sec and source lifetimes of a day or more for these experiments Also, target thicknesses of up to several $mg/cm^2$ can be used.

The count rates and background estimates can be made from the spectra and yields observed in Refs. 198 and 199. An E - ΔE plot form the focal plane detector of a Q3D magnetic spectrograph is given in Fig. 35. In this case ions were separated by p/q only and were spread along a 1-m-long focal plane. The group shown represented a very small fraction of the total number of $^{17}O$ ions produced. With the RPMS, ions of a variable velocity range (typically 8%) pass through the Wien filter and are focussed

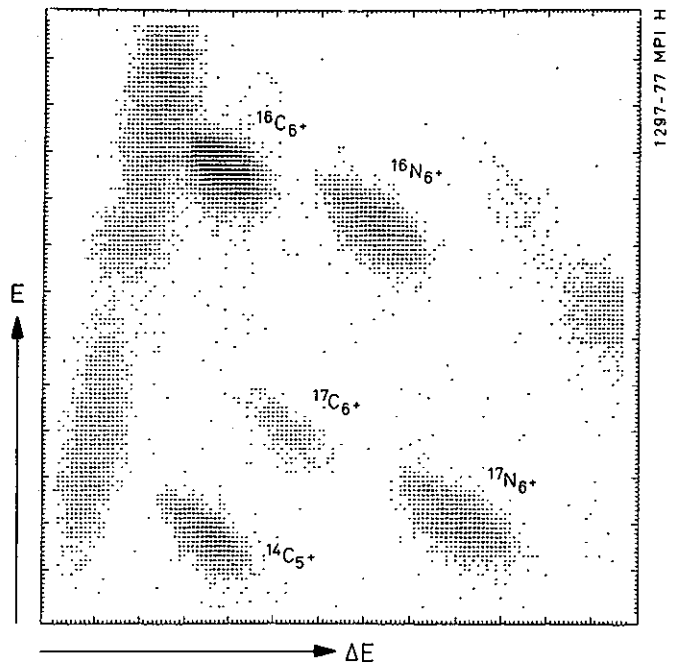


FIG. III.36. A section of an E - ΔE plot from the focal plane detector of the Heidelberg Q3D spectrograph (Ref. 192). The beam was $^{18}O$ at 102 MeV, and the target was $^{48}Ca$.

according to m/q on the final focal plane. Hence all $^{17}C$ ions within a 16% energy range are concentrated in a spot less than 2 cm in diameter. Other ions of the same m/q are focussed to the same spot, as indicated schematically on the left hand side of Fig. 37. $^{14}C^{5+}$ and $^{17}N^{6+}$ in this example. Very intense groups such as the $^{16}C^{6+}$ ions seen in Fig. 36 are separated by their different m/q values.

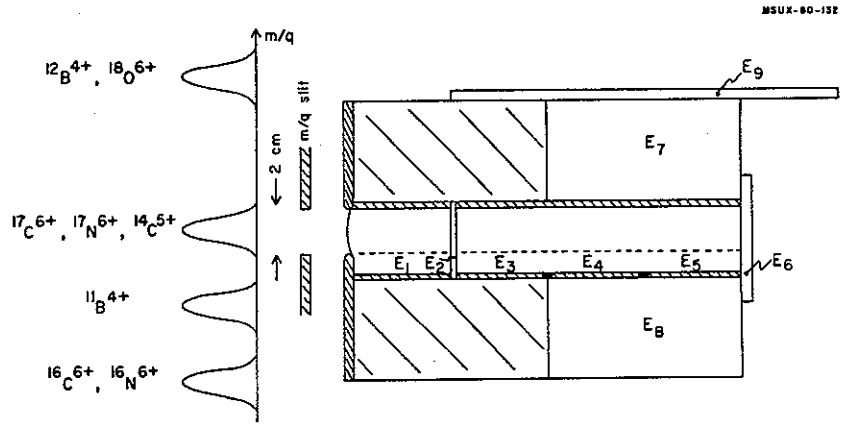


FIG. III.37. Schematic view of various ion groups dispersed according to m/q at the focal plane of the RPMS (shown on the left) and a possible focal plane detector system for particle identification and lifetime measurements.

The ambiguities in m/q can be removed by a combination of E – ΔE measurements such as indicated in Fig. 36. and measurements of range, lifetime, and decay energy. In this example $^{17}C$ has the largest range and the shortest lifetime (by about a factor of 10). A detector system of the type indicated schematically in Fig. 37 will be used for this measurement. It consists of two gridded gas ion chambers and five plastic scintillators. Signals from region $E_1$ - $E_5$ are used for E - ΔE heavy ion isotope identification. The gas pressures and the thickness of scintillator $E_2$ are chosen to stop $^{17}N^{6+}$ ions in $E_2$ and

$^{17}C^{6+}$ ions in the region of $E_4$ or $E_5$. The $^{14}C^{5+}$ ions would then stop in region $E_3$. Overlap between these regions due to the 16% energy range accepted is not a serious limitation. After stopping, the $^{17}C$ ions will β-decay with a half-life in the vicinity of 100 msec and an end point energy of up to 13 MeV; the β's will be detected in the large scintillators $E_7$ or $E_8$. The scintillators $E_9$ and $E_6$ serve as a cosmic ray veto and a long range particle veto, respectively.

With estimated $^{17}C$ event rates of ≈1/sec and a half-life <<1 sec, the time interval between the arrival and decay of each individual ion can be measured with continuous beam on target. Hence, the beam time required for the actual half-life measurement should be only a few hours.

The same, or similar apparatus, can also be used to measure the yields of other neutron rich light isotopes, such as $^{17}B$, $^{18}C$, $^{20}N$, $^{21,22}O$, etc. In some cases heavier projectiles, such as $^{22}Ne$ or $^{26}Mg$ may produce higher yields via the fragmentation or deep inelastic process. A compound nuclear reaction[205] at low energy $^{10}Be(^{11}B,2p)$, has been used to make $^{19}N$. The applicability of reactions of this type to neighboring nuclei requires further investigation. We do have in the laboratory two $^{10}Be$ targets of the same type used in the $^{19}N$ experiment.

The experiment described above is the first of a series of lifetime and decay property measurements of light nuclei far from the line of beta stability. The next step will be to move simultaneously to measure branching

ratios and beta decay end points. In the RPMS the neutron-rich, fully stripped nucleus will always have greater range and energy than the competing, less interesting species with the same m/q. This indicates that the improved understanding of production mechanisms will permit extension of the measurements to $T_z>3$ light nuclei.

The ability of the RPMS to produce beams of separated, energetic isotopes also allows precision measurements of half-lives of nuclei closer to the line of stability. Such measurements are of interest in the study of $0^+ \rightarrow 0^+$ Fermi β-decay coupling constants as a function of Z. Precision half-life measurements are made difficult in many cases by the presence of contaminant activities and by migration of gaseous source material during the counting interval. Both of these problems can be effecively eliminated by using the RPMS. With a suitable choice of heavy ion reaction on a light target it is possible to produce proton-rich nuclei in the fully stripped state with a unique value of m/q. For example, the $^{9}Be(^{12}C,^{18}Ne)^{3}N$ reaction in the RPMS can produce a useful $^{18}Ne^{10+}$ beam without interference from other activities; sufficient resolution is available to reject $^{14}O^{8+}$, the nearest competition. The $^{18}Ne$ will then be implanted in a stopping material for counting with Ge(Li) detectors.

e. Laser Spectroscopy with the RPMS

Many new nuclei have been identified as particle stable in the past few years, but little further work

has been done toward measuring even the most fundamental properties of the ground states. At the MSU cyclotron facility, with the unique combination of intense beams and the RPMS, it should be possible to measure properties of ground states and isomers of these isotopes as well as those of presently unobserved isotopes. Laser spectroscopy provides a model independent technique for measuring spins, magnetic moments, quadrupole moments, and isotope shifts of nuclei far from stability. With the recent introduction of commercially available, tuneable, dye lasers, various techniques are rapidly being developed. The combination of cyclotron, mass separator, and dye laser thus provides an irresistible combination for studying nuclei far from stability, and we are presently investigating the feasibility of such experiments.

The hyperfine splitting of atomic levels results from the effects of the nuclear size, charge distribution, and magnetism distribution on the electron wave function at the position of the nucleus. Nuclear spins, magnetic moments, and quadrupole moments may be obtained from the measured hyperfine splitting of an optical line. In this procedure the magnetic hyperfine field and the electric field gradient at the nucleus are calibrated from nuclear magnetic and quadrupole moments measured for one of the stable isotopes (by other techniques). In addition, changes in the nuclear rms radius with changing neutron number can be determined from isotope shifts (changes in the center of gravity of a hyperfine multiplet).

A variety of laser techniques has already been applied to the study of nuclei far from stability; these include radiation-detected optical pumping (RADOP), fluorescence of atoms in cells or in atomic beams, and optical pumping followed by magnetic state selection. Whereas the RADOP technique, followed by $\beta$, $\gamma$, or fission fragment detection, has the greatest demonstrated sensitivity, it is not universally applicable. Study of a wide variety of nuclei will require development of several different techniques. These are well described in recent reviews of laser applications to nuclear physics.[206-208]

Most previous laser work has been done with on-line isotope separators looking at products of high energy proton spallation reactions and at fission fragments produced in reactors. Typical isotope yields in these experiments were $10^4$ per second or greater, but one experiment has been successful with a yield of the order of 1 per second.[210] With the K500 cyclotron it will be possible to achieve isotope yields adequate for laser spectroscopy when transfer reactions are employed. The reaction 290 MeV $^{58}Ni + {}^{58}Ni$, for example, has produced several new proton rich isotopes of Z=52, 53, 54.[209] When beams from the coupled cyclotrons become available, fragmentation reactions will produce even larger yields of nuclei far from stability. It will be possible to use very thick targets, and the products will be emitted into a very small solid angle centered at $0^o$.[201] This situation may

be approximated during Phase I operation for fragmentation of relatively light nuclei at energies of the order of 20 to 50 MeV/u. Measurements of spins and moments of neutron rich light isotopes might thus be possible.

Transitions in ions tend to be in the ultraviolet, out of reach of dye lasers. Therefore, a major problem which must be overcome is that of neutralizing the ions which reach the focal plane while providing for sufficient overlap with a laser beam during the atomic excitation process. Doppler broadening must be reduced in the case of the lighter isotopes. Techniques for stopping the ions and transporting the atoms to another location are available but result in a loss of potential for studying very short-lived nuclei. An advantage in starting with energetic ions is that the time of arrival at the focal plane may be tagged by a detector. This can provide a means for greatly increasing the sensitivity of a fluorescence experiment, as pulses from the photomultiplier tube may then be counted only when an atom is present, thus eliminating background from stray light or dark current.

f. The He Jets

Two working He jet systems exist at MSU. These are a room temperature and a cryogenic (see Sec.III.C.) system. Each has advantages for certain types of experiments. The cryogenic system has a shorter transfer time, a much cleaner environment, but a poorer efficiency than the

room temperature device. In cases for which cleanliness is essential, the cryogenic system is the only choice. Such applications enable precise studies of β spectra, high resolution studies of delayed heavy particle emission, and fundamental weak interaction studies which utilize detailed spectral shapes of β-delayed particle lines. The He jets work for several cases which are not possible in the RPMS, for example, when very low energy is imparted to the product, as in production of transuranium elements or when high efficiency is needed for continuous production. The He jets continuously feed all charge states and all energies of the products which escape from the target. Some typical experiments are described below.

i) Room temperature He jet--The immediate plans for the K500 cyclotron with the room temperature He jet call for studying nuclei in three regions: 1) the region with $Z>50$ and $N<82$, where one can trace the onset of deformation with increasing N, 2) the region of mirror ($T=\frac{1}{2}$) nuclei along the $N=Z$ line, where we expect to discover useful information about the Fermi and Gamow-Teller components of β-decay, and 3) transuranic and transactinide nuclei.

The room temperature He jet system is also used to transport reaction products to SIEGFRIED, which can be used for mass identification of the products in nuclear spectroscopic studies.

ii) Cryogenic He jet--A series of experiments on heavy, alpha-particle emitting nuclei is planned using

the cryogenic helium jet system. The unique mass identification capability (time of flight of the recoil) removes the well known ambiguities that arise in studies of transfermium nuclei due to the near equality of their alpha decay energies with those of Po nuclei produced in reactions on target impurties. The cryogenic helium jet system has already been used in the study of $^{24}$Si, produced at the 1 b level in the $^{24}$Mg($^{3}$He,3n) reaction,[211] and it is expected to function with improved efficiency and mass resolution for heavy alpha emitters. A brief preliminary experiment on $^{12}$C + $^{197}$Au with the K50 cyclotron demonstrated the usefulness of the device for these studies, and much higher beam intensities will be available with the K500 machine. In particular, we hope to clarify the nuclidic assignments of some of the disputed transfermium nuclei and to explore the change in nuclear properties that occurs at N=158 and drastically reduces the lifetimes of more neutron-rich nuclei.

This program will involve setting up and equipping a suitable laboratory, establishing methods for handling the radioactive targets, and developing special techniques to maximize the beam currents that can safely be used on those targets.

## C2. ASTROPHYSICS

### a. Creation of the Light Elements

Since the pioneering and persuasive work of Burbidge Burbidge, Fowler, and Hoyle[212] it has been generally accepted that most of the elements were created in stars as byproducts of the fusion processes which supply stellar energy. However, with the exception of $^{4}He$, and possibly $^{3}He$, the nuclides with A<12 cannot originate in stellar centers because they are unstable against proton induced reactions at the temperatures and densities found there. Alternative sources of these elements have since been found.[213,214] Some elements are formed by reactions of galactic cosmic rays on interstellar targets and others by the primordial big-bang explosion. Models for both of these processes require nuclear reaction rate information as input. We have been engaged in a long term program of such measurements,[214] and their results, combined with those from other laboratories, have provided adequate cross sections for the critical p + C,N,O reactions, but essentially no information for the $\alpha+\alpha$ reactions leading to $^{6,7}Li$. For cosmic ray interactions, the contribution of a given reaction is proportional to the product of the cosmic ray flux and the interstellar density of the interacting particles. This product is an order of magnitude larger for $\alpha+\alpha$ than for other reactions. This reaction will then dominate the production of $^{6,7}Li$ if the cross sections for these channels are substantial.

A few years ago we, therefore, undertook a series of measurements at MSU and (in collaboration with Viola's group) at Maryland. The results[215-217] are summarized in Fig. 38. The cross sections for mass 7, which are large at low energy but decrease rapidly with energy indicate only small contributions to $^{7}$Li production at energies above the measured range. The cross section

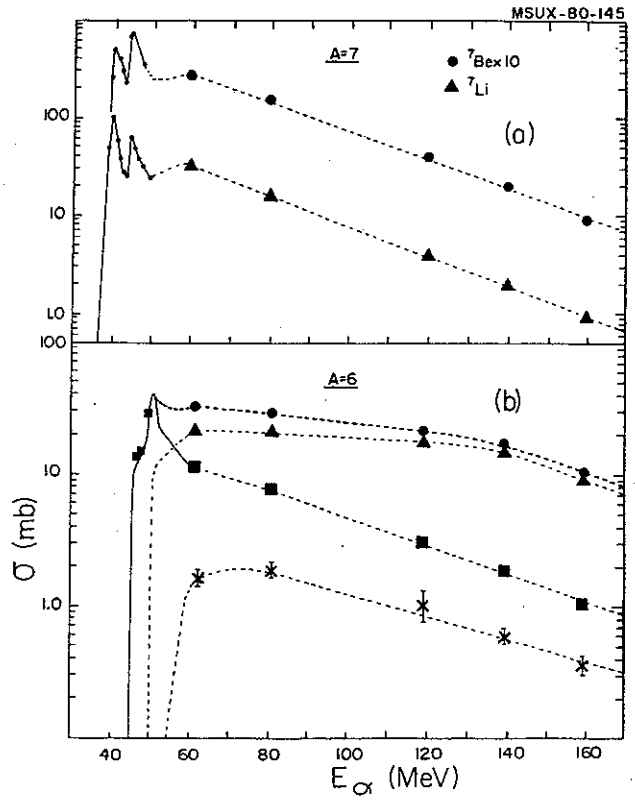


FIG.III.38. Excitation functions for A=6 and 7 production in the α+α reaction: (a) $^{7}$Be and $^{7}$Li (sum of ground state and first excited state); (b) $^{6}$Li ground state. Solid line based on detailed balance for $(\alpha,d)^{6}$Li from inverse reactions. Dashed line from this work: χ , $(\alpha,2p)^{6}$He reaction; ▲ , $(\alpha,pn)$ Li reaction; ■, $(\alpha,d)$ Li reaction; and ●, total $^{6}$Li cross section.

for mass 6, however, is still large at 160 MeV and appears to be decreasing rather slowly with energy. The $\alpha+\alpha$ reaction is indeed likely to be an important source of $^{6}Li$, and it becomes important to know its cross section at higher energies

We intend to measure the $\alpha+\alpha$ reaction cross sections at energies up to 320 MeV at MSU by using techniques similar to those of Ref. 217. Measurements[218] of the production of $^{7}Be$ carried out at 400, 600, and 1000 MeV indicate that the mass 7 cross section remains small at higher energies. But its value, about 0.02 mb, is still much larger than expected on the basis of a simple extrapolation of the data in Fig. 38. The authors[218] speculate that this marks the onset of a new reaction mechanism involving subthreshold production of $\pi$'s. Whether this is true or not, experiments up to 320 MeV will permit a study of this reaction in the transition region between 150 and 400 MeV

Straightforward calculations using the available cross section information indicate[213,214] that all of $^{6}Li$, $^{9}Be$, $^{10,11}B$, and 10-20% of $^{7}Li$ are made by cosmic ray processes. (Of course the $^{6}Li$ conclusion is tentative to the extent that measured cross sections differ from the theoretical estimates.) At least some, and probably all, of the remaining light elements are made naturally in a standard big bang explosion at a particular, and hence determinable, universal density. Previously, the abundance of $^{2}H$ had been used[219] to determine this density

with the result implying that the universe was open and would continue to expand forever. Such an important conclusion requires confirmation. We realized[220] that the abundance of $^{7}Li$ could be used to place an upper limit on the density and that this upper limit also required an open universe.

It happens that the predictions for $^{6}Li$ production in the big bang, while indicating it was an unimportant source of $^{6}Li$, were particularly uncertain since the relevant reaction rate had not been measured. A recent measurement[221] of the cross section for the $\alpha + d \rightarrow {}^{6}Li + \gamma$ reaction was carried out at MSU in connection with the search for parity violation in nuclei. It was learned that the assumed cross section was probably too large and, consequentially, that the production of $^{6}Li$ in the big bang is indeed negligible.

b. β-Decay Strength Functions

Many heavy nuclei are produced in a rapid neutron capture process (dynamic r process), the understanding of which depends on the strength functions $S_{\beta}$ for Gamow-Teller (GT) β-decay. Since little is known about $S_{\beta}$ simple structureless forms have been assumed in most calculations. However, simple shell model arguments[222] lead one to expect local enhancements in decay strength, and if such an enhancement should occur within the energy window accessible to β decay it would greatly affect the β-decay lifetime. Changes in the β-decay lifetime would

result in changes[223] in the production of elements in the dynamical r-process affecting both the r process path itself and post-event decay back towards the valley of stability. Furthermore, the onset of β-delayed fission processes near A=250 is expected to affect the production ratio of chronological pairs (e.g. $^{238}U/^{235}U$) and hence the measurements of lifetimes of the elements extracted from them.[224]

To understand these phenomena one needs accurate information about $S_\beta$, but, unfortunately, little is known to date. Some β-delayed neutron experiments bear on this subject (see, for example, Kratz et al.[225]), and Firestone[226] has observed structure in classical $\beta\gamma$ decay studies of $^{145}Gd$. We have shown (see Sec.III.B3.) that (p,n) reactions at $E_p \gtrsim 45$ MeV can yield at least qualitative information about $S_\beta$, and have located both the allowed GT giant resonance and the T-1 giant electric dipole resonance. These enhancements in the strength function are of great interest in themselves but do not lie in the region available to β decay in N>Z nuclei. Moreover, neutron backgrounds have made it difficult to search for smaller peaks lying at low excitation energy, and the thick targets ($\sim$100 mg/cm$^2$) required for neutron work preclude measurements on rare nuclei far from stability.

We intend to search for low lying GT strength with the ($^6Li$ $^6He$) reaction discussed elsewhere in this proposal, Sec.III.B3. For the present purpose, the main

advantages of this reaction are: 1) the higher resolution and, likely, smaller background compared to (p,n) (this will permit one to search for relatively small enhancements) and 2) the possibility of using thin targets of rare isotopes far from stability. Unfortunately, the nuclei along the r-process path are unstable and one must rely on studying a sufficiently wide range of nuclei to fix the parameters of theoretical models well enough to permit an extrapolation into the region of interest.

Initial studies will follow the calibration of the ($^{6}$Li,$^{6}$He) reaction discussed earlier and will be concentrated on the medium heavy and heavy nuclei likely to influence the r process[223] and specifically on nuclei in the lead region where electric dipole strength may be important.[224] Following this work, it may be profitable to study $S_{\beta}$ for nuclei farther from stability through observation of $\beta$-delayed neutron emission[224,225] by neutron rich nuclei made, for example, in the collision of neutron rich projectiles with heavy targets. Recent studies have shown that either deeply inelastic reactions of $^{48}$Ca at low energies (<10 MeV/u) or fragmentation reactions at higher energies (>100 MeV/u) are effective methods for the production of neutron rich nuclei. Projectiles such as $^{22}$Ne at 37 MeV/u, which will be available, will combine some advantages of both methods. The reaction product mass filter (see Sec.II.C.) combined with simple neutron detectors[225] will be very useful for these purposes.

## C3. WEAK INTERACTION RESEARCH

One of the predictions of the highly successful unified guage theory of weak and electromagnetic interactions postulated by Weinberg, Salam Ward, and Glashow[227] is the existence of a weak neutral current mediated by a heavy ($\sim$90 GeV) neutral vector boson. Abundant information about the weak neutral current has been obtained in leptonic and semi-leptonic interactions but not as yet in purely hadronic interactions. Only in nuclei is it feasible to observe the effects of the hadronic current. Experimental tests make use of the principle that a weak neutral current can give rise to a parity violating, $\Delta T=1$, nucleon-nucleon force, a force very much suppressed if only charged currents act.

Four experiments in nuclear physics bear directly on this problem: 1) the asymmetry of gamma radiation from polarized neutron capture by protons[228] 2) the circular polarization of gamma rays emitted by $^{18}F$(1.08 MeV)[229], 3) the cross section for gamma rays emitted in the capture of alpha particles by polarized $^{6}Li$[230], and 4) the alpha decay of the $0^{+}$,T=1 state of $^{6}Li$.[231] The first two experiments have been completed with null results (at a level slightly above that where effects are expected); the third is in preparation at Argonne and should have sufficient sensitivity; and the fourth is in the final data taking stages at Chalk River. This last experiment, which is being carried out by a Michigan

State-Chalk River-Argonne collaboration, should have sufficient sensitivity to see neutral current effects at the upper end of the anticipated range. With only the first few days of data taking completed the upper limit on the parity violating alpha width of the $0^+$,T=1 state of $^6$Li has been improved more than 2 orders of magnitude over the best previous measurement.[232]

The principle of the experiment differs substantially from that of previous efforts. An alpha particle beam of 6.237 MeV bombards a supersonic gas jet of deuterium in the target position of the QDDD spectrometer at Chalk River. If capture occurs to the ground state of $^6$Li there is sufficient center-of-mass momentum for the $^6$Li ion to enter the spectrometer and be detected in the focal plane. The efficiency is close to unity, and the full power of charged particle identification techniques can be used for background rejection.

Significant milestones in this experimental program have included (a) development of a windowless supersonic jet target of sufficient thickness, (b) calibration of the beam energy to 1 keV accuracy by magnetic rigidity matching with a 30 keV $Tl^+$ beam from a surface ionization source, (c) development of a focal plane detector with special pileup-rejection features to permit detection of a few $^6$Li events per hour in the presence of 3000 counts per second of degraded alpha particles, (d) measurement of the excitation energy of the $0^+$,T=1 state to a precision of 0.1 keV, (e) measurement of the ground state mass of $^6$Li to a precision of 0.6 keV (the result differs by 2

standard deviations from the value in the mass table), and (f) first observation of the non-resonant direct capture process $^{2}H(\alpha,\gamma)^{6}Li$ with a cross section of about 20 nb.

The sensitivity of the experiment is determined entirely by the statistical accuracy attainable, because systematic effects are believed to be negligible for practical running times. Data from a preliminary 2-day run with a target of half the design thickness are shown in Fig. 39. Within statistical uncertainities, there

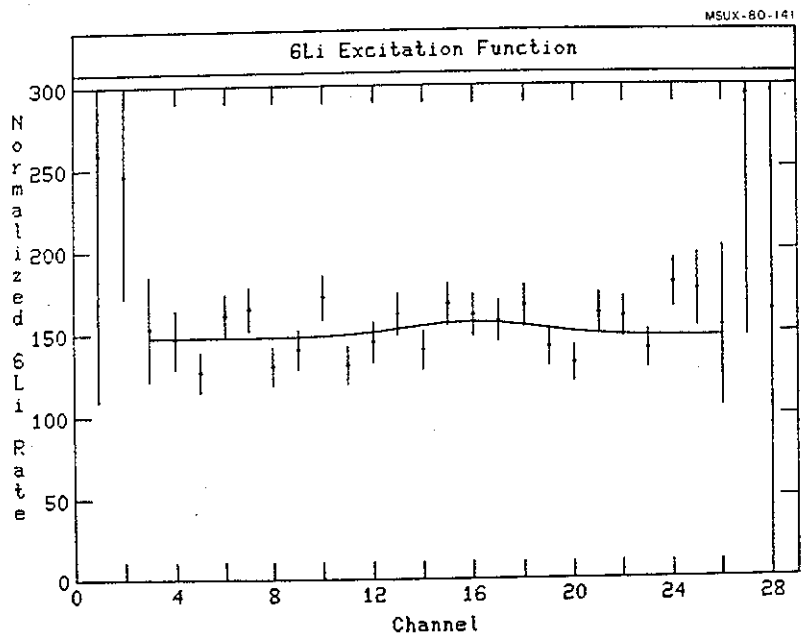


FIG.III.39. Plot of normalized $^{6}Li$ count rate in the $^{2}H(\alpha,\gamma)^{6}Li$ reaction as a function of beam energy. The energy range covered is approximately 8 keV, and the resonance is expected to appear in channel 13±5. The curve shown, the best fit to the data, corresponds to a width of $\Gamma_{\alpha}=(2\pm2)\times10^{-6}$ eV for the $0^{+}$,T=1 state of $^{6}Li$.

is no resonance: $\Gamma_\alpha = (2 \pm 2)\times10^{-6}$ eV. The previous upper limit (obtained by the Milan group)[232] was $\Gamma_\alpha \leq 8 \times 10^{-4}$ eV. A detailed theoretical treatment remains to be done, but a rough estimate using an effective one-body interaction indicates that the parity violating alpha width may be of the order of $\Gamma_\alpha = 3 \times 10^{-8}$ eV. (This width is proportional to the square of the parity impurity, and its value is currently uncertain by an order of magnitude.)

In its present form, the experiment is expected to reach the $5 \times 10^{-7}$ eV level within practical running times of 20 - 30 microampere days. If no resonance is seen by then, we may proceed to activate a new version of the experiment which can offer, in principle, a 20-fold increase in sensitivity

The new experiment will make use of the very high currents available from some low energy, single ended accelerators. A gaseous $^4$He target will be bombarded with 3.1-MeV deuterons at currents of $\sim$100 $\mu$A. Detection of the recoiling $^6$Li under these hostile conditions is the vital experimental element whose feasibility remains to be demonstrated - the technique proposed consists of allowing the $^6$Li to stop in a very thin tungsten or iridium foil at a high temperature. Lithium ions diffusing through the foil will desorb from the surface as $Li^+$ (by surface ionization). They may then be detected in a simple low resolution mass spectrometer. It is not at present known whether foils sufficiently free of natural Li and sufficiently durable can be prepared to make this technique

viable. Relatively few accelerators are capable of the required performance - the Argonne Dynamitron is potentially suitable but will require extensive ion source modification and some local shielding.

## C4. SEARCH FOR CRITICAL OPALESCENCE PHENOMENA

It was first pointed out by Migdal[233] that nuclear matter at sufficiently high density would be characterized by a pion condensed phase, the source of which is a long range ordering of nuclear spins and isospins under the influence of the tensor force [2] It now seems clear that such a condensation does not occur at normal nuclear densities $\rho_o$ but should appear instead near $2\rho_o$. Such densities presumably occur in neutron stars and perhaps in collisions of heavy ions, but given our present understanding of these phenomena, it is perhaps premature to use them to study the pion condensate. Fortunately another approach to the problem has been suggested.

Several authors[235-239] have pointed out that while nuclei are not condensed and hence do not exhibit long range order, there may be intermediate-range fluctuations in the pion field which correspond to "domains" of spin-isospin order and which can strongly affect scattering cross sections for momentum transfers $q_c \approx (2\text{-}3)m_\pi$ (Note: $m_\pi \approx 0.7\ fm^{-1} \approx 140$ MeV/c). This phenomenon is analogous to the critical opalescence that occurs near phase transitions in condensed atomic systems.

When these considerations are formulated for nuclear matter, it appears that states of unnatural parity: $0^-$, $1^+$, $2^-$,..., tend to become critical at roughly the same rate provided $J < J_{max} = q_c R$ where R is the nuclear radius.[235,240]

Specific calculations of these effects for finite nuclei have been made by Saperstein et al.,[235] Toki and Weise,[237] Fayans et al.[238], and Delorme et al.[239]. The calculation of Toki and Weise for the $1^+$,T=1 state at 15.1 MeV in $^{12}C$ is shown in Fig. 40. The effects of the precritical behavior are strong for $q \sim (1.5\text{-}3)m_\pi$ and of course, depend very much on the Migdal parameter g'. This parameter can be taken to be a measure of the proximity of nuclei to the pion-condensate instability.

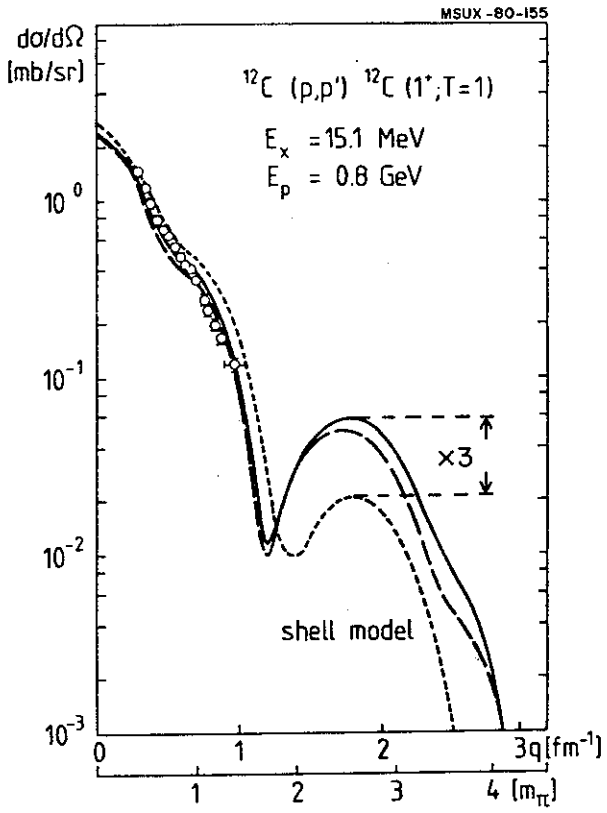


FIG.III.40. Glauber model calculation of 800 MeV inelastic proton scattering into the $^{12}C(1^+,T=1)$ state. Short dashed curve: Cohen-Kurath shell model; Long-dashed curve: pionic Q-space polarization added; solid curve: additional effect of $V_{2\pi}$. The spin-isospin dependent primary NN amplitude has been adjusted to reproduce the low q data.

The figure illuminates one of the major problems in searches via inelastic scattering; namely, that unnatural parity, T=1 states that can easily be resolved from their neighbors occur mainly in rather light nuclei where the enhancement effects are strongly affected by momentum averaging. Thus, the enhancemnt is by a factor of three rather than by the order of magnitude found in a similar calculation in $^{208}$Pb.[237,238] Experiments on heavy nuclei are possible, but much better resolution is needed to resolve the unnatural parity states from the neighbouring states.[238]

It appears that the giant Gamow-Teller ($1^+$) states seen in (p,n) reactions (see Sec. III.B3.) might provide an ideal laboratory for study of these phenomena. The states dominate the spectrum at small angles and they exhaust a substantial part of the sum rule strength. Hence, their structure should be relatively well known, and, most importantly, they exist in nuclei sufficiently heavy that one expects large enhancements. Nevertheless these states will be hard to observe at large angles with the (p,n) reaction because of background from other neutron producing processes.

We plan, therefore, to study the Gamow-Teller states in $^{94}$Zr and $^{124}$Sn with the ($^{6}$Li $^{6}$He) reaction at, e.g., 20 and 35 MeV/A. Backgrounds are expected to be smaller than with (p,n), and the relatively good resolution will permit rejection of interference from narrow natural parity states. The major difficulty with interpretation of these experiments rests in the details of the reaction mechanism,

but there is hope that the large enhancement expected will lead to an unambiguous result. Should the enhancement be sufficiently large that it can be seen in (p n) experiments, a comparison with (p,n) results would be useful.

One hopes that experiments such as those discussed here can provide information on the Migdal parameter and its momentum dependence. Preliminary evidence from $^{12}C$ $(e,e')^{12}C(15.1\ MeV,\ 1^+,T=1)$ indicates that $g' \simeq 0.5$[237] for large momentum transfers. This value is perhaps less reliable than will be obtained from the hadronic experiments since the M1 operator relevant to (e,e') does not couple directly to the pion-condensate structure.[236]

## C5 PION PRODUCTION EXPERIMENTS

Pions have several properties which make their observation as the product of nucleus-nucleus collisions extremely valuable for studies of the collision process and, consequently, of nuclear dynamics and nuclear structure. Because of the 140 MeV rest mass energy which must be created in the collision, direct production by nucleon-nucleon collisions at the energies of the K500 cyclotron is almost a negligible process. Direct production can occur only for nucleons above the Fermi energy in both projectile and target. If the production mechanism is viewed as a thermal process the high rest mass leads to an extreme sensitivity to the nuclear temperature following the collision. Thus the weakness of direct and thermal processes leads to a strong sensitivity to coherent processes, an idea which has been frequently discussed in the literature. (Below 80 MeV/u a situation very similar to the Mossbauer effect could occur in that the process could be strongly enhanced if the nucleons acted collectively.)

Another property of pions which gives them special interest is that they exist both positively charged and negatively charged. The importance of Coulomb effects in heavy ion collisions was first shown in an MSU-LBL experiment[241] in which large values of the ratio $\pi^-/\pi^+$ were observed for pion velocities closest the beam's velocity. This ratio is insensitive to many experimental and theoretical

uncertainties but is sensitive to the charge, shape, and size of the objects which exist after the collision.

One can distinguish three different types of pion production experiments which will be performed with the K500 cyclotron. These are measurements of: a) the total cross sections, b) the inclusive pion energy spectra and cross sections, and c) the exclusive (or two-body-final state) cross sections. Figure 41 illustrates the difference between the last two of these three quantities. The total

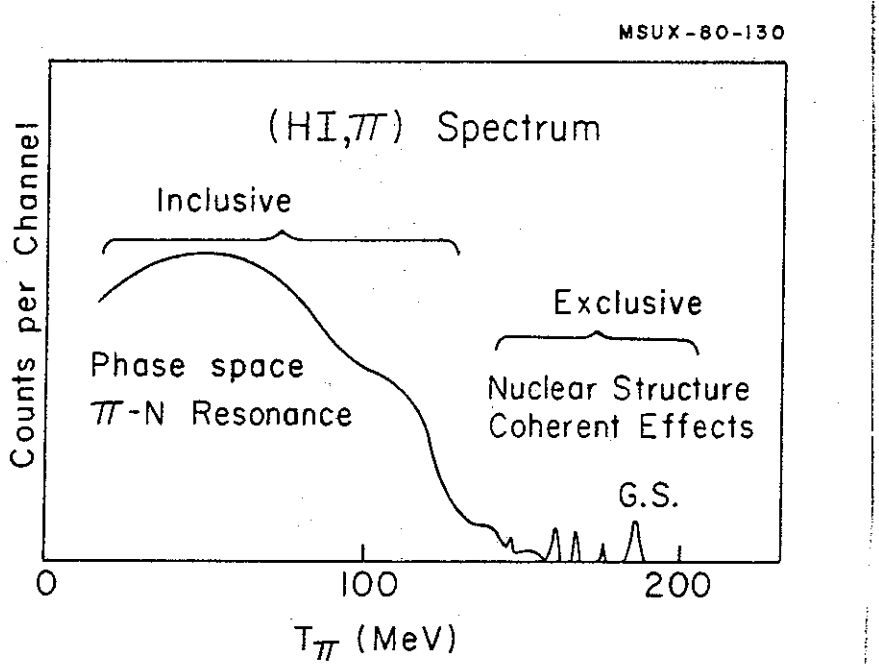


FIG.III.41. A schematic spectrum for pion production by heavy ions. The absolute value of the cross section is very low in both inclusive and exclusive regions. The energy scale is approximately correct for $^{16}O$ ions from the K500 cyclotron on a light target.

cross section is the sum over all pion energies and angles. The only data for composite particles for any of these three quantities in this energy range are the inclusive cross sections taken at the Bevalac[241] in the same experiment in which Coulomb effects were observed. The results show clearly that the inclusiye cross sections at 80 MeV/u are measurable.

a. The Total Cross Section

The total cross section for pion production, because it is an integration over all angles and energies, lends itself to a relatively simple measurement in certain cases. For example, the $\pi^+$-$\mu^+$-$e^+$ decay produces uniquely high energy electrons. The best way to do this experiment is to pulse the beam in the μsecond range and look between beam bursts for electrons with energy greater than ∿25 MeV in a plastic scintillator. With fast electronics the time between bursts can possibly be reduced to the point at which the natural cyclotron frequency is used. Although an absolute calibration of the equipment would involve considerable uncertainty, comparison between targets, beam types, and beam energies would be straightforward and accurate. This is an excellent way to search for phase transitions in nuclei since they may occur as changes in slope of the total cross section. A very important advantage of this type of experiment is its sensitivity to very low energy pions which, although difficult to measure otherwise, may be the most sensitive to phase transitions.

b. Inclusive Measurements

With the sole exception of proton induced reactions performed at Indiana[242] and Upsala[243], all pion production experiments have been inclusive. That is, there is no knowledge of the final state of the products of the reaction. Theories[244] exist which predict the properties of such inclusive pion spectra and yields from composite particle reactions. At MSU we have a unique opportunity to derive nuclear structure information from the application of these theories. If Fermi motion is important in the production, then a comparison of d, $^{3}$He, $\alpha$, and $^{6}$Li production of low energy pions at 80 MeV/u will provide a crucial test. The Coulomb effect at $0^{o}$ will be used to measure what fragments remain at the beam velocity.

Inclusive measurements will be performed with the Enge split pole spectrograph. If the low-radius end of the focal plane is used, the loss of pions due to decay in flight will not be a serious consideration (< 50%). The double focussing and broad range of the device make a measurement possible from E =10 to 50 MeV in two bites. Existing single-wire detectors and plastic scintillators will be used on the focal plane with a thin abosrber to stop all other particles. Multiwire proportional counters are being developed and will be used in case the background in a single wire detector proves to be too high. The techniques developed[245] for low cross section multinucleon transfer reactions are directly applicable to both inclusive and exclusive measurements of pion spectra.

As can be seen in Fig. 42 the inclusive yield of 34 MeV pions drops very rapidly with beam energy. It should be possible to trace this dependence to well below 80 MeV/u. This study will be limited to Ne and lighter projectiles (until phase II). Once again the energy dependence can be measured to look for phase transitions, but in this case one can also study the pion angular and energy dependence and look for revealing Coulomb effects at $0^{\circ}$.

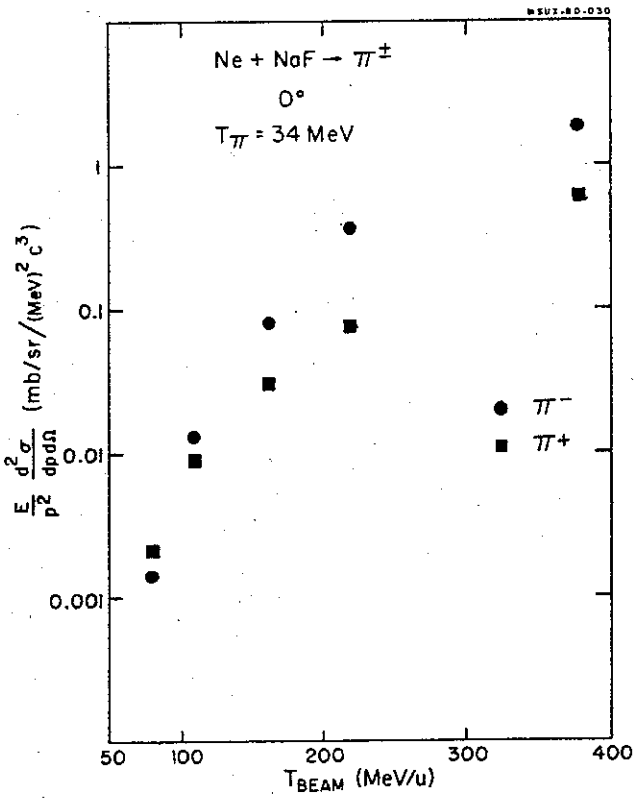


FIG.III.42. The beam energy dependence of 34 MeV pion production by the Ne + NaF reaction from Ref. 241.

c. Exclusive Measurements

Coherent processes could have a very strong effect on certain two body final state interactions or on certain special cases which are not quite exclusive. In a process of this type for which calculations have been made[246] pions are produced by the decay of isobars in the target and the projectile, $^{12}C$, is left in its S=1, T=1 vibrational state at 15.1 MeV. We consider this experiment to be very difficult but worth attempting nevertheless.

We will start with an exploratory look at other exclusive processes, for example:

$$^{6}Li + \alpha \rightarrow \pi^{\pm} + \begin{matrix} ^{10}Be \\ ^{10}C \end{matrix} \text{ and}$$

$$^{12}C + ^{6}Li \rightarrow \pi^{\pm} + \begin{matrix} ^{18}O \\ ^{18}Ne \end{matrix} .$$

The energy resolution will be more than adequate to resolve final states in processes of this type, and relatively thick targets can be used. Techniques employed at Indiana[242] for working very near the threshold for $(p,\pi)$ reactions can be adapted to certain cases of composite-particle induced reactions. These include detection of the heavy recoil, use of a miniature spectrometer which fits into a scattering chamber, and chemical techniques. However, the first experiments will consist of extending the inclusive spectra up into the exclusive region shown in Fig. 40 by progressively lowering the beam energy and raising the spectrograph field until the yield becomes prohibitively

small. During this process we will look for regions of enhanced production as indications of as yet unknown processes.

REFERENCES SECTION III:


1. R.P. DeVito, S.M. Austin, U.E.P. Berg and W. Sterrenburg, BAPS 24, 830 (1979), BAPS 24, 853 (1979).
2. W.T.H. van Oers, Huang Waw, N.E. Davison, A. Ingemarsson, B. Fagerstrom and G. Tibell, Phys. Rev. C 10, 307 (1974).
3. J.P. Jeukenne, A. Lejeune and C. Mahaux, Phys. Rev. C 15, 10 (1977).
4. J.W. Negele, Nucl. Phys. A165, 305 (1971).
5. J. Rapaport, T.S. Cheema, D.E. Bainum, R.W. Finlay and J.D. Carlson, Nucl. Phys. A296, 95 (1978).
6. R. Huffman, A. Galonsky, R. Markham and C. Williamson, Phys. Rev. C, submitted.
7. W.E. Frahn, Ann. Phys. 72 (1972) 524.
8. J.B. Ball, C.B. Fulmer, E.E. Gross, M.L. Halbert, D.C. Hensley, C.A. Ludemann, M.J. Saltmarsh, and G.R. Satchler, Nucl. Phys. A252, 208 (1975).
9. J.G. Cramer, R.M. DeVries, D.A. Goldberg, M.S. Zisman and C.F. Maguire, Phys. Rev. C 14, 2158 (1976).
10. G.R. Satchler, Nucl. Phys. A279, 493 (1977).
11. J.R. Birkelund, J.R. Huizenga, H. Freiesleben, K.L. Wolf, J.P. Unik and V.E. Viola, Jr., Phys. Rev. C 13, 133 (1976).
12. R. Vandenbosch, M.P. Webb, T.D. Thomas, S.W. Yates and A.M. Friedman, Phys. Rev. C 13, 1893 (1976).
13. F. Puhlhofer, private communication.
14. W.G. Love, T. Terasawa, and G.R. Satchler, Phys. Rev Lett. 39, 6 (1977), Nucl. Phys. A291, 183 (1977).

15. C.E. Thorn, M.J. LeVine, J.J. Kolata, C. Flaum, P.D. Bond, and J.C. Sens, Phys. Rev. Lett. 38, 384 (1977).

16. P. Doll, M. Bini, D.L. Hendrie, S.K. Kauffman, J. Mahoney, A. Menchaca-Rocha, D.K. Scott, T.J.M. Symons, K. van Bibber, Y.P. Viyogi, and H. Wieman, Phys. Lett. 76B, 556 (1978).

17. A.Z. Schwartzschild, E.H. Auerbach, R.C. Fuller, and S. Kahana, Proc. Symp. on Macroscopic Features of Heavy-Ion Collisions, Argonne, April 1976.

18. H. Oeschler, H.L. Harney, D.L. Hillis and K.S. Sim, Nucl. Phys. A325, 463 (1979).

19. R.M. DeVries and J.C. Peng, Phys. Rev. Lett. 43, 1373 (1979).

20. P. Braun-Munzinger, G.M. Berkowitz, T.M. Cormier, C.M. Jachcinski, J.W. Harris, J. Barrette, and M.J. LeVine, Phys. Rev. Lett. 38, 944 (1977).

21. J. Barrette, M.J. LeVine, P. Braun-Munzinger, G.M. Berkowitz, M. Gai, J.W. Harris, and C.M. Jachcinski, Phys. Rev. Lett. 40, 445 (1978).

22. C.K. Gelbke, T. Awes, U.E.P. Berg, J. Barrette, M.J. LeVine, and P. Braun-Munzinger, Phys. Rev. Lett. 41, 1778 (1978).

23. R.R. Betts, S.B. DiCenzo, and J.F. Petersen, Phys. Rev. Lett. 43, 253 (1979).

24. H. Doubre, J.C. Jacmart, E. Plagnol, N. Poffe, M. Riou and J.C. Roynette, Phys. Rev. C 15, 693 (1977).

25. G. Baur and C.K. Gelbke, Nucl. Phys. A204, 138 (1973).

26. K. Dietrich, Ann. Phys. 66, 480 (1971).

27. R.A. Broglia, C.H. Dasso, S. Landowne, B.S. Nilssson and A. Winther, Phys. Lett. 73B, 401 (1978).

28. C. Olmer, M.C. Mermaz, M. Buenerd, C.K. Gelbke, D.L. Hendrie, J. Mahoney, A. Menchaca-Rocha, D.K. Scott, M.H. Macfarlane, and Steven C. Pieper, Phys. Rev. Lett. 38, 476 (1977).

29. R.C. Pardo, S. Gales, R.M. Ronningen, and L.H. Harwood, Physics Lett., in press.

30. J.S. Vaagen and K. Kumar, J. Phys. G 5, 1211 (1979).

31. F. Pougheon, M. Bernas, M. RoyStephan, C. Detraz, D. Guillemaud, E. Kashy, M. Langevin, F. Naulin, and P. Roussel, to be published.

32. R. Jahn, D.P. Stahel, G.J. Wozniak, R.J. de Meijer, and Joseph Cerny, Phys. Rev. C 18, 9 (1978).

33. R.J. de Meijer, R. Kamermans, J. Van Driel, and H.P. Morsch, Phys. Rev. C 16, 2442 (1979).

34. N. Anyas-Weiss, J.C. Cornell, P.S. Fisher, P.N. Hudson, A. Menchaca-Rocha, D.J. Millener, A.D. Panagiotou, D.K. Scott, D. Shrottman, D.M. Brink, B. Bruk, P.J. Ellis, and T. Engeland, Phys. Reports 12C, 201 (1974).

35. B. Buck and A.A. Pilt, Nucl. Phys. A295, 1 (1978); L.H. Harwood and K.W. Kemper, Phys. Rev. C 20, 1383 (1979); B. Buck, C.B. Dover, and J.P. Vary, Phys. Rev. C 11, 1803 (1975).

36. K. Nagatani, F. Shimada, D. Tanner, R. Tribble, and T. Yamaya, Phys. Rev. Lett. 43, 1480 (1979).

37. R.L. Phillips, K.A. Erb, D.A. Bromley, and J. Weneser, Phys. Rev. Lett. 42, 566 (1979).

38. E. Kashy, W. Benenson, I.D. Proctor, P. Hauge, and G. Bertsch, Phys. Rev. C 1, 2251 (1973).

39. G. Delic and D. Kurath, Phys. Rev. C 14, 619 (1976).

40. V.V. Volkov, Phys. Reports 44, 93 (1978).

41. W.U. Schroder, J.R. Birkelund, J.R. Huizenga, K.L. Wolf and V.E. Viola, Jr., Phys. Reports 45, 301 (1978).

42. M. Lefort and C. Ngo, Rivista del Nuovo Cimento Vol. 2, N. 12, 1 (1979).

43. For recent developments, see, e.g., Proceedings of the "Symposium on Heavy Ion Physics from 10 to 200 MeV/amu", held at Brookhaven National Laboratory, July 1979, BNL-51115.

44. A.S. Goldhaber and H.H. Heckman, Ann. Rev. Nucl. Sci. 28, 161 (1978).

45. See, e.g., Proceedings of the "4th High Energy Heavy Ion Summer Study", held at the Lawrence Berkeley Laboratory, July 1978, LBL 7766 (1978).

46. C.K. Gelbke, C. Olmer, M. Buenerd, D.L. Hendrie, J. Mahoney, M.C. Mermaz and D.K. Scott, Phys. Reports 42, 311 (1978).

47. K. Van Bibber, D.L. Hendrie, D.K. Scott, H.H. Wieman, L.S. Schroeder, J.V. Geaga, S.A. Chessin, R. Treuhaft, Y.J. Grossiord, J.O. Rasmussen and C.Y. Wong, Phys. Rev. Lett. 43, 840 (1979).

48. D.E. Greiner, P.J. Lindstrom, H.H. Heckman, B. Cork, and F.S. Bieser, Phys. Rev. Lett. 35, 152 (1975).

49. P. Braun-Munzinger, C.K. Gelbke, J. Barrette, B. Zeidman, M.J. LeVine, A. Gamp, H.L. Harney and Th. Walcher, Phys. Rev. Lett. 36, 849 (1976).

50. Y. Eyal, A. Gavron, J. Tserruya, Z. Fraenkel, Y. Eisen, S. Wald, R. Bass, C.R. Gould, G. Kreyling, R. Renfordt, K. Stelzer, R. Zitzman, A. Gobbi, U. Lynen, H. Stelzer, J. Rode and R. Bock, Phys. Rev. Lett. 41, 625 (1978).

51. D. Hilscher, J.R. Birkelund, A.D. Hoover, W.U. Schroder, W.W. Wilcke, J.R. Huizenga, A.C. Mignerey, K.L. Wolf, H.F. Breuer, and V.E. Viola, Jr., Phys. Rev. C 20, 576 (1979).

52. C.K. Gelbke, M. Bini, C. Olmer, D.L. Hendrie, J.L. Laville, J. Mahoney, M.C. Mermaz, D.K. Scott, and H.H. Wieman, Phys. Lett. 71B, 83 (1977).

53. A. Olmi, U. Lynen, J.B. Natowitz, M. Dakowski, P. Doll, A. Gobbi, H. Sann, H. Stelzer, R. Bock and D. Pelte, Phys. Rev. Lett. 44, 383 (1980).

54. P. Dyer, T.C. Awes, C.K. Gelbke, B.B. Back, A Mignerey K.L. Wolf, H. Breuer, V.E. Viola, Jr., Phys. Rev. Lett. 42, 560 (1979).

55. B.B. Back, K.L. Wolf, A.C. Mignerey, T.C. Awes, C.K. Gelbke, H. Breuer, V.E. Viola, Jr., and P. Dyer, to be published.

56. D.K. Scott, M. Bini, P. Doll, C.K. Gelbke, D.L. Hendrie, J.L. Laville, J. Mahoney, A. Mechaca-Rocha, M.C. Mermaz, C. Olmer, T.J.M. Symons, Y.P. Viyogi, K. Van Bibber, H. Wieman and P.J. Siemens, Lawrence Berkeley Laboratory Report, LBL-7729 (1978).

57. D.H.E. Gross and J. Wilszynski, Phys. Lett. 67B, 1 (1977).

58. J.P. Bondorf and W. Norenberg, PHys. Lett. 44B, 487 (1973).

59. P.A. Gottschalk and M. Westrom, Phys. Rev. Lett 39, 1250 (1977).

60. J.P. Bondorf, J.N. De, A.O.T. Karvinen, G. Fai, and B. Jakobsson, Phys. Lett. 84B, 162 (1979).

61. L. Westerberg, D.G. Sarantites, D.C. Hensley, R.A. Dayras, M.L. Halbert, and J.H. Barker, Phys. Rev. C 18, 796 (1978).

62. J.B. Natowitz, M.N. Namboodiri, P. Kasiraj, R. Eggers, L. Adler, P. Gonthier, C. Cerruti, and T. Alleman, Phys. Rev. Lett. 40, 751 (1978).

63. A. Olmi, H. Sann, D. Pelte, Y. Eyal, A. Gobbi, W. Kohl, U. Lynen, G. Rudolf, H. Stelzer and R. Bock, Phys. Rev. Lett. 41, 688 (1978).

64. P. Glassel, R.S. Simon, R.M. Diamond, R.C. Jared, I.Y. Lee, L.G. Moretto, J.O. Newton, R. Schmidt, and F.S. Stephens, Phys. Rev. Lett. 38, 331 (1977).

65. K.A. Geoffroy, D.G. Sarantites, M.L. Halbert, D.C. Hensley, R.A. Dayras, and J.H. Barker, Phys. Rev. Lett. 43, 1303 (1979).

66. A.G. Artukh, V.V. Avdeichikov, G.F. Gridnev, V.L. Mikheev, V.V. Volkov, J. Wilczynski, Nucl. Phys. A176, 284 (1971).

67. P. Auger, T.H. Chiang, J. Galin, B. Gatty, D. Guerreau, E. Nolte, J. Pouthas, X. Tarrago, and J. Girard, Z. Physik A289, 255 (1979).

68. G.D. Westfall, T.J.M. Symons, D.E. Greiner, H.H. Heckman, P.J. Lindstrom, J. Mahoney, A.C. Shotter, D.K. Scott, H.J. Crawford, C. McParland, T.C. Awes, C.K. Gelbke and J.M. Kidd, Phys. Rev. Lett. 43, 1859 (1979).

69. J. Barrette, P. Braun-Munzinger, C.K. Gelbke, H.L. Harney, H.E. Wegner, B. Zeidman, K.D. Hildenbrand and U. Lynen, Nucl. Phys. A299, 147 (1978).

70. Y.P. Viyogi, T.J.M. Symons, P. Doll, D.E. Greiner, H.H. Heckman, D.L. Hendrie, P.J. Lindstrom, J. Mahoney, D.K. Scott, K. Van Bibber, G.D. Westfall, H. Wieman, H.J. Crawford, C. McParland and C.K. Gelbke, Phys. Rev. Lett. 42, 33 (1979).

71. D.J. Morrissey, L.F. Oliveira, J.O. Rasmussen, G.T. Seaborg, Y. Yariv and Z. Fraenkel, Phys. Rev. Lett. 43, 1139 (1979).

72. J.P. Bondorf, G. Fai and O.B. Nielsen, Phys. Rev. Lett. 41, 391 (1978); Nucl. Phys. A312, 149 (1978).

73. D.J. Morrissey, W.R. Marsh, R.J. Otto, W. Loveland and G.T. Seaborg, Phys. Rev. C 18, 1267 (1978).

74. M. Berlanger, A. Gobbi, F. Hanappe, U. Lynen, C. Ngo, A. Olmi, H. Sann, H. Stelzer, H. Ridel, and M.F. Rivet, Z. Physik A291, 133 (1979).

75. U. Brosa, Z. Physik A292, 385 (1979).

76. F. Puhlhofer, W.F.W. Schneider, F. Busch, J. Barrette, P. Braun-Munzinger, C.K. Gelbke and H.E. Wegner, Phys. Rev. C 16, 1010 (1977) and references given there.

77. T.J.M. Symons, P. Doll, M. Bini, D.L. Hendrie, J. Mahoney, G. Mantzouranis, D.K. Scott, K. Van Bibber, Y.P. Viyogi, H.H. Wieman, and C.K. Gelbke, Lawrence Berkeley Laboratory Report LBL-8379 (1978).

78. T.C. Awes, C.K. Gelbke, B.B. Back, A.C. Mignerey, K.L. Wolf, P. Dyer, H. Breuer, and V.E. Viola, Jr., Phys. Lett. 87B, 43 (1979).

79. W. Scheid, H. Muller and W. Greiner, Phys. Rev. Lett. 32, 741 (1974).

80. A.A. Amsden, G.F. Bertsch, F.H. Harlow, and J.R. Nix, Phys. Rev. Lett. 35, 905 (1975).

81. W.G. Meyer, H.H. Gutbrod, Ch. Lukner, and A. Sandoval, to be published.

82. G. Bertsch and A.A. Amsden, Phys. Rev. C 18, 1293 (1978).

83. C.Y. Wong, Phys. Lett. 88B, 39 (1979).

84. O. Herlund, private communication.

85. S.E. Koonin, Phys. Lett. 70B, 43 (1977).

86. C.H. King, J.E. Finck, G.M. Crawley, J.A. Nolen, Jr., and R.M. Ronningen, Phys. Rev. C 20, 2084 (1979).

87. R.S. Mackintosh, Nucl. Phys. A266, 379 (1976).

88. R.C. Melin, R.M. Ronningen, J.A. Nolen, Jr., G.M Crawley, C.H. King, J.E. Finck, and C.E. Bemis. Jr., Int. Conf. on Band Structure and Nuclear Dynamics Tulane University, New Orleans, Vol. 1, p. 69 (1980).

89. P.T. Deason, C.H. King, T.L. Khoo, R.M Ronningen, F.M. Bernthal and J.A. Nolen, Jr., to be published.

90. P.T. Deason, C.H. King, T.L. Khoo, J.A. Nolen, Jr., and F.M. Bernthal, Phys. Rev. C 20, 927 (1979)

91. A. Arima and F. Iachello, Ann Phys. (N.Y.) 99, 253 (1976), Ann. Phys. (N.Y.) 111, 201 (1978), Ann. Phys. (N.Y.) 123, 468 (1979).

92. F.T. Baker, Phys. Rev. Lett. 43, 195 (1979).

93. R. Huffman, A. Galonsky, R. Markham, and C. Williamson, Phys. Rev. C, in press.

94. C. Williamson, A. Galonsky, R. Huffman, and R. Markham, Phys. Rev. C, in press.

95. M. Austern and J.S. Blair, Ann. Phys. (N.Y.) 33, 15 (1965).

96. E. Grosse, Symposium on High-Spin State Phenomenon in Nuclei, Argonne Nat. Lab., Mar. 1979, ANL/Phy-79-4, p. 223.

97. R.B. Piercey, H. Emling, P. Fuchs, E. Grosse, J.H Hamilton, H. Ower, A.V. Ramayya, D. Schwalm, N. Trautmann, and H.J. Wollersheim, Int. Conf. on Band Structure and Nuclear Dynamics, Tulane University, New Orleans, Vol. 1, p. 57 (1980).

98. N.R. Johnson, D. Cline, S.W. Yates, F.S. Stephens, L.L. Riedinger, and R.M. Ronningen, Phys. Rev. Lett. 40, 151 (1978); S.W. Yates, I.Y. Lee, N.R. Johnson, E. Eichler, L.L. Riedinger, M.W. Guidry, A.C. Kahler, D. Cline, S.R. Simon, P.A. Butler, P. Colombani F.S. Stephens, R.M. Diamond, R.M Ronningen, R.D Hichwa, J H. Hamilton and E.L. Robinson, Phys. Rev. C, in press.

99. I.Y. Lee, D. Cline, P.A. Butler, R.M. Diamond, J.O Newton, R.S. Simon, and F.S. Stephens, Phys. Rev. Lett. 39, 684 (1977).

100. K. Stelzer, F. Rauch, Th.W. Elze, Ch.E. Gould, J. Idzko, G.E. Mitchell, H.P. Nottrodt, R. Zoller, H.J. Wollersheim, and H. Emling, Phys. Lett. 70B, 297 (1977).

101. I.Y. Lee, N.R. Johnson, F.K. McGowan, M W Guidry, R.L. Robinson, and L.L. Riedinger, ORNL Progress Report, ORNL-5498, p. 33 (1978).

102. R.E. Neese, M.W. Guidry, R. Donangelo, and J.O. Rasmussen, Phys. Lett. 85B, 201 (1979).

103. M.H. Macfarlane, Proc. Symp. on Heavy Ion Physics from 10 to 200 MeV/amu, BNL, July 16-20 (1979), BNL-51115, p. 673.

104. W.G. Love, T. Terasawa, and G.R. Satchler, Phys. Rev. Lett. 39, 6 (1979); Nucl. Phys. A291, 183 (1977).

105. S.F. Faber, L.E. Young, and F.M. Bernthal, MSUCL-275, to be published.

106. R. Kalish, J.L. Eberhardt, and K. Dybdal, Proc. Madison Conf. 1977.

107. M. Hass, N. Benczer-Koller, J.M. Brennan, H.T. King, and P. Goode, Phys. Rev. C 17, 997 (1978).

108. O. Hausser, B. Haas, D. Ward, and H.R. Andrews, Nucl. Phys. A314, 161 (1979).

109. D. Ward, O. Hausser, H.R. Andrews, P. Taras, P. Skensved, N. Rud, and C. Broude, Nucl. Phys. A330, 225 (1979).

110. M. Sano, T. Takemasa, and M. Wakai, J. Phys. Soc. Japan suppl. 34, 365 (1975).

111. O. Hausser, T.K. Alexander, H.R. Andrews, H.-E. Mahnke, J.F. Sharpey-Schafer, M.L. Swanson, P. Taras, and D. Ward, Proc. New Orleans Conf. 1980.

112. R.A. Warner, F.M. Bernthal, J.S. Boyno, and T.L. Khoo, Phys. Rev. Lett. 31, 835 (1974).

113. T.L. Khoo, F.M. Bernthal, C.L. Dors, M. Piiparinen, S. Saha, P.J. Daly, and J. Meyer-ter-Vehn, Phys. Lett 60B, 341 (1976).

114. T.L. Khoo, F.M. Bernthal, R.G.H. Robertson, and R.A. Warner, Phys. Rev. Lett. 37, 823 (1976); T.L. Khoo and G. Lovhoiden, Phys. Lett. 67B, 389 (1977).

115. M. Piiparinen, J.C. Cunnane, P.J. Daly, C.L. Dors, F.M. Bernthal, and T.L. Khoo, Phys. Rev. Lett. 34, 1110 (1975).

116. H. Beuscher, W.F. Davidson, R.M Lieder, A. Neskakis and C. Mayer-Boricke, Phys. Rev. Lett 32, 843 (1974).

117. H. Helppi, S.K. Saha, P.J. Daly, S.R. Faber, T.L. Khoo, and F.M. Bernthal, Phys. Lett. 67B, 279 (1977).

118. P.M. Walker et al., Phys. Lett. 86B, 9 (1979).

119. R. Araeinejad, R.B. Firestone, B.H. Bentley, and WM. C. McHarris, MSU Annual Report 1978-1979 pp. 45,46.

120. T.L. Khoo, R.K. Smither, B. Haas, O. Hausser, H.R. Andrews, D. Horn, and D. Ward, Phys. Rev. Lett. 41, 1027 (1978).

121. B. Haas, H.R. Andrews, O. Hausser, D. Horn, J.F Sharpey-Shafer, P. Taras, W. Trautmann, D. Ward, T.L. Khoo, and R.K. Smither, Phys. Lett. 84B, 178 (1979).

122. O. Hausser, H.-E. Mahnke, J.F. Sharpey-Schafer, M.L. Swanson, P. Taras, D. Ward, H.R. Andrews, and T.K. Alexandr, Phys. Rev. Lett. 44, 132 (1980)

123. H.J. Korner, D.L. Hillis, C.P. Roulet, P. Auger, C. Ellegaard, D.B. Fossan, D. Habs, M. Neiman, F.S. Stephens, and R.M. Diamond, Phys. Rev. Lett., 43, 490 (1979).

124. O. Andersen, J.D. Garrett, G.B. Hagemann, B. Herskind, D.L. Hillis, and L.L. Riedinger, Phys. Rev. Lett., 43, 687 (1979).

125. M.A. Deleplanque, F.S. Stephens, O. Andersen, C. Ellegaard, J.D. Garrett, B. Herskind, D. Fossan, M. Neiman, C. Roulet, D.L. Hillis, A. Kluger, R. Diamond, and R.S. Simon, to be published.

126. J.D. Garrett and B. Herskind, "Study Weekend on Nuclei Far from STability" Daresbury, Sept. 22, (1979).

127. H. Backe, L. Richter, R. Willwater, E. Kankeleit, E. Kuphal, Y. Nakayama, and B. Martin, Z. fur Physik A285, 159 (1978).

128. W. Chung, Ph.D. Thesis, Michigan State University 1976.

129. B.H. Wildenthal, pps. 383-462, Elementary Modes of Nuclear Excitations, eds. A. Bohr and R.A. Broglia (North-Holland) 1977.

130. B.H. Wildenthal and W. Chung. pps 723-753, Mesons in Nuclei, eds. D.H. Wilkinson and M. Rho. (North Holland) 1979.

131. B.A. Brown, W. Chung and B.H. Wildenthal. Phys Rev. C (in press).

132. B.A. Brown, W. Chung and B.H. Wildenthal, Phys Rev. Lett. 40, 1631 (1978).

133. B.A. Brown, W. Chung and B.H. Wildenthal, Phys Rev. C (in press).

134. B.H. Wildenthal and W. Chung, The (p n) Reaction and the Nucleon - Nucleon Force, ed. C.D. Goodman (Plenum) 1980.

135. W. Chung, J. Van Hienen, B.H. Wildenthal and C.L. Bennett, Physics Letters 79B, 391 (1978).

136. H.T. Fortune, L. Bland, R. Middleton, W. Chung, and B.H. Wildenthal, Physics Letters 87B, 29 (1979).

137. B.H. Wildenthal and W. Chung, (unpublished)

138. B.H. Wildenthal and W. Chung, (unpublished).

139. B.H. Wildenthal, Phys. Rev. Lett. 22. 1118 (1969).

140. A. Moalem, W. Benenson, and G.M. Crawley, Phys. Rev. Letters 31, 482 (1973).

141. F.E. Bertrand, Ann. Rev. Nucl. Sci. 26, 457 (1976).

142. F.E. Bertrand, Varenna Summer School on Nuclear Structures and Heavy Ion Collisions, Varenna, Italy, July 2-20, 1979.

143. D.H. Youngblood, Proceedings of the Giant Multipole Topical Conference, Oak Ridge, October 15-17, 1979, to be published.

144. C.K. Gelbke, Giant Multiple Resonances: Topical Conference, Oak Ridge 1979, to be published.

145. P. Ring and J. Speth, Nucl. Phys. A235, 315 (1974) J. Speth, E. Werner and W. Wild, Phys. Reports 33C, 127 (1977).

146. M. Sasao and Y. Torizuka, Phys. Rev. C15, 217 (1977).

147. D.H. Youngblood, C.M. Rozza, J.M. Moss, D.R. Brown, and J.R. Bronson, Phys. Rev. Letters 39, 1188 (1977).

148. M. Buenerd, C. Bonhonme, D. Lebrun, P. Martin, J. Chauvin, G. Duhamel, G. Perrin, and P. de Ssintignon, Phys. Lett. 84B, 305 (1979).

149. A.M. Sandorfi, Proceedings of the "Symposium on Heavy-Ion Physics from 10 to 200 MeV/amu", July 1979 Brookhaven National Lab., BNL Report No. 26598, to be published.

150. H.T. Knopfle, Int. Conf. Nucl. Phys. with E. Mag. Interactions, Mainz, June 1979.

151. J. Wambach, V.A. Madsen, G.A. Rinker, and J. Speth, Phys. Rev. Letters 39, 1443 (1977).

152. N. Marti - private communication.

153. A. Moalem, W. Benenson, G.M. Crawley, and T.L. Khoo Phys. Lett. 61B, 167 (1976).

154. G.J. Wagner, Giant Multipole Resonances Topical Conference, Oak Ridge, 1979, to be published.

155. J. van der Plicht, M.N. Harahek, A. van der Woude, P. David, and J. Debrus Phys. Rev. Lett. 42, 1121 (1979).

156. A.C. Shotter, C.K. Gelbke, T.C. Awes, B.B. Back, J. Mahoney, T.J.M. Symons, and D.K. Scott, Phys. Rev. Lett. 43, 569 (1979).

157. R. Pardo, R.G. Markham, W. Benenson, A.I. Galonsky, and E. Kashy, Phys. Lett. 71B, 301 (1977).

158. P. Doll, D.L. Hendrie, J. Mahoney, A. Menchaca-Rocha, D.K. Scott, T.J.M. Symons, K. van Bibber, Y.P. Viyogi, and H. Wieman, Phys. Rev. Letters 42, 366 (1979).

159. R.A. Broglia G. Pollarolo, Phys. Rev. Letters 41B, 25 (1978) and preprint (1979).

160. A.M. Sandorfi, private communication.

161. R.A. Broglia, C.H. Dasso, and A. Winther, Phys. Lett. 61B, 113 (1976).

162. N. Frascaria, G. Stephan, P. Colombani, Y.P. Garron, M. Rion, and L. Tassan-Gof, Phys. Rev. Lett. 39, 918 (1977).

163. D. Hilscher, J.R. Birkeland, A.D. Hoover, W.U. Schroder, W.W. Wilcke, J.R. Huizenga, A.C. Mignerey, K.L. Wolf, H.F. Breuer, and V.E. Viola, Jr., Phys. Rev. C 20, 556 (1979).

164. J.D. Anderson and C. Wong Phys. Rev. Lett. 7, 250 (1961).

165. R.R. Doering, A. Galonsky, D.M. Patterson, and G.F. Bertsch, Phys. Rev. Lett. 35, 1691 (1975).

166. W.A. Sterrenburg, S.M. Austin, R.P. Devito, and A.I. Galonsky, BAPS 24, 649 (1979).

167. A. Galonsky, W. Sterrenburg, S. Austin, and R. Devito, BAPS, Washington Mtg., 1980.

168. A. Galonsky, S. Austin, T. Nees, W. Sterrenburg, D. Bainum, J. Rapaport, C. Foster, C. Goodman, D. Horen, C. Goulding, and M. Greenfield, BAPS, Washington Mtg., 1980.

169. W. Knupfer, R. Frey, A. Friebel, W. Mettner, D. Meuer, A. Richter, E. Spamer, and O. Titze, Phys. Lett. 77B, 367 (1978).

170. E. Cecil, G.T. Garvey, and W.J. Braithwaite, Nucl. Phys. A232, 22 (1974).

171. R. Leonardi, Phys. Rev. Lett. 28, 836 (1977) and Phys. Rev. C 14, 385 (1976).

172. R.O. Akyuz and S. Fallieros, Phys. Rev. Lett. 27, 1016 (1971).

173. A. Galonsky, J.P. Didelez, A. Djaloeis, and W. Oelert, Phys. Lett. 74B, 176 (1978).

174. D. Ovazza, A. Willis, M. Morlet, N. Marty, P. Martin, P. de Saintignon, and M. Buenard, Phys. Rev. C 18, 2438 (1978).

175. W.R.W. Wharton and P.T. Debevec, Phys. Rev. C 11, 1963 (1975).

176. B.A. Brown, W. Chung, and B.H. Wildenthal, Phys. Rev. Lett. 40, 1631 (1978).

177. C. Gaarde, J.S. Larsen, M.N. Harakeh, S.Y. van der Werf, M. Igarishi, and A. Muller-Arnke, Nucl. Phys. A334, 248 (1980).

178. E.R. Flynn and J.D. Garrett, Phys. Rev. Lett. 29, 1748 (1972).

179. R.A. Lindgren, W.L. Bendel, E.C. Jones, Jr., L.W. Fagg, X.K. Maruyama, J.W. Lightbody, Jr., and S.P. Fivozinsky, Phys. Rev. C 14, 1789 (1976).

180. M. Sakai, M. Sekiguchi, F. Soga, Y. Hirao, K. Yagi, and Y. Adki, Phys. Lett. 51B, 51 (1974).

181. E. Gerlic, J. Kallne, H. Langevin-Joliot, J. Van de Wiele, and G. Duhamel, Phys. Lett. 57B, 338 (1975).

182. S.Y. Van der Werf, B.R. Kooistra, W.H.A. Wesselink F. Iachello, L.W. Puts, and R.H. Siemssen, Phys. Rev. Lett. 33, 712 (1976).

183. S. Gales, E. Hourani, S. Fortier, H. Laurent, J.M. Maison, and J.P. Schapira, Nucl. Phys. A288, 221 (1977) and Nucl. Phys. A288, 201 (1977).

184. G. Berrier-Ronsin, G. Duhamel, E. Gerlic, J. Kalifa, M. Langevin-Joliot, G. Rotbard, M. Vergnes, J. Vernotte, and K.K. Seth, Phys. Lett. 67B, 16 (1977).

185. M. Sekiguchi, Y. Shida, F. Soga, Y. Hirao, and M. Sakai, Nucl. Phys. A278, 231 (1977).

186. S.Y. Van der Werf, Nucl. Phys. A289, 141 (1977).

187. J. Van De Wiele, E. Gerlic, H. Langevin-Joiot, and G. Duhamel, Nucl. Phys. A297, 61 (1978).

188. S. Gales, G.M. Crawley, D. Weber, and B. Zwieglinski Phys. Rev. C 18, 2475 (1979).

189. S. Gales, G.M. Crawley, D. Weber, and B. Zwieglinski, Phys. Rev. Letters, 41, 292 (1978).

190. G.M. Crawley, W. Benenson, D. Weber, and B. Zwieglinski Phys. Rev. Letters, 39 1451 (1977).

191. G.M. Crawley, Inst. Phys. Conference Series No. 49, Structure of Medium Heavy Nuclei 1979 p. 127–150 (1980).

192. W.G. Love, Proceedings: Conference on the (p,n) Reaction and the Two Nucleon Force, Telluride, 1979.

193. S.M. Austin, Proceedings: Conference on the (p,n) Reaction and the Two Nucleon Force, Telluride, 1979.

194. S.D. Schery, S.M. Austin, A. Galonsky, L.E. Young and U.E.P. Berg, Phys. Lett. 79B, 30 (1978).

195. S.M. Austin, L.E. Young, R.R. Doering, R. DeVito, R.K. Bhowmick, and S.D. Schery, submitted for publication.

196. W Sterrenburg, S.M. Austin, U.E.P. Berg and R. DeVito, Phys. Lett., to be published.

197. C.D. Goodman, Proceedings of the Vancouver Conf., 1979. Contributed papers, p. 65 and private communication.

198. W. Benenson, E. Kashy, D. Mueller, and H. Nann, Proceedings Third International Conference on Nuclei far from Stability, Cargese, 1976. CERN 76-13.

199. E. Kashy, W. Benenson, J.A. Nolen, Jr., H. Robertson, and A. Ledebuhr, Sixth International Confernce on Atomic Masses, E. Lansing, MI, 1979. Plenum Press.

200. P. Auger, T.H. Chiang, J. Galin, B. Gatty, D. Guerreau, E. Nolte, J. Pouthas, X. Tarrago and J. Girard, A289, 255 (1979).

201. G.D. Westfall, T.J. Symons, D.E. Greiner, H.H. Heckman, P.J. Lindstrom, J. Mahoney, A.C. Shotter, D.K. Scott, H.J. Crawford, C. McParland, T.C. Awes, C.K. Gelbke and J.M. Kidd, phys Rev. Lett. 43, 1859 (1979)

202. Y.P. Viyogi, T.J.M. Symons, P. Doll, D.E. Greiner H.H. Heckman, D.L. Hendrie, P.J. Lindstrom, J. Mahoney D.K. Scott, K. Van Bibber, G D Westfall H. Wieman, H.J. Crawford, C. McFarland, and C.K. Gelbke, Phys Rev. Lett. 42, 33 (1979)

203. J.A. Nolen, T S. Bhatia, H. Hafner, P. Doll, C.A. Wiedner and G.J. Wagner Physics Letters 71B, 314 (1977).

204 T.S. Bhatia, H. Hafner, J.A. Nolen, W. Saathoff R. Schumacher, R.E. Tribble, G.J. Wagner, and C.A. Wiedner, Physics Letters 76B 562 (1978).

205. G. Guillaume, P. Finte, F. Jandt, I. Ordonez, A Gallmann, D.E. Alburger, K.W. Jones, and D.R. Goosman, Nucl. Phys. A233, 357 (1974).

206. D.W. Murnick and M.S. Feld, Ann. Rev. Nucl. Part. Sci. 29, 411 (1979).

207. H.J. Kluge, in Progress in Atomic Spectroscopy ed. W. Hanle, H. Kleinpopen, Plenum, 1979.

208. P. Jacquinot and R. Klapisch, Rep. Prog. Phys., 1979.

209. R. Kirchner, O. Klepper, G Nyman, W. Reisdorf, E Roeckl, D. Schardt, N. Kaffrell, P. Peuser, and K. Schneeweiss, Phys. Lett. 70B, 150 (1977).

210. C.E. Bemis, Jr., J.R. Beene, J.P. Young, and S.D. Kramer, Phys. Rev. Lett. 43, 1854 (1979) and C.E. Bemis. Jr. J.R. Beene, J.P. Young, and S.D. Kramer, Phys. Rev. Lett. 44, 500 (1980)

211. A.G. Ledebuhr, L.H. Harwood, R.G.H. Robertson and T.J. Bowles, Phys. Rev. C, to be published. See also R.G.H. Robertson, T.J. Bowles, and S J. Freedman Nucl. Instr. and Meth. 147, 361 (1977).

212. E.M. Burbidge, G.R. Burbidge, W A. Fowler and F. Hoyle, Rev. Mod. Phys. 29, 547 (1957) and, for more recent references, V. Trimble, Rev. Mod. Phys. 47, 877 (1975).

213. H. Reeves, Ann, Rev. Astron. Astrophys. 12, 437 (1974) and H. Reeves and J.P. Meyer, Ap. J. 226, 613 (1978).

214. S.M. Austin, Proceedings of the International Symposium on Nuclear Physics at Cyclotron Energies (1977), in press.

215. C.H. King, H.H. Rossner, S.M. Austin, W.S Chien, G.J. Mathews, V.E. Viola, and R.G. Clark, Phys. Rev. Lett. 35, 988 (1975).

216. C.H. King, S.M. Austin, H.H. Rossner, and W.S. Chien. Phys. Rev. C 16, 1712 (1977).

217. B.G. Glagola, G.J. Mathews, H.F. Breuer, V.E. Viola, P.G. Roos, A. Nadasen, and S.M. Austin, Phys. REv. Lett. 41, 1698 (1978).

218. F. Yiou, G.M. Raisbeck and H. Quechon, Proceedings of the 15th Int'l. Cosmic Ray Conf., Plovdiv, 13-26 Aug. 1977.

219. J.R. Gott, James E. Gunn, David N. Schramm, and Beatrice M. Tinsley, Ap. J. 194, 543 (1974)

220. S.M. Austin and C.H. King, Nature 269, 782 (1977)

221. See next section, III.C3, and MSU Ann. Rpt. 1977-78, p. 63.

222. B.F. Petrow, et al., Z. Phys. A292, 73 (1979).

223. H.V. Klapdor and C.-O. Wene, Ap. J. 230, L113 (1979).

224. H.V. Klapdor, Proceedings of Conf. on Nuclear Spectroscopy and Structure of the Nucleus, Rega 27-30 March 1979. MPI report H-1979-V13, Heidelberg.

225. K.L. Kratz, et al., Nucl. Phys. A317, 335 (1979).

226. R. Firestone, R.C. Pardo, and Wm. C. McHarris, Phys. Lett. 89B, 36 (1979) and private communication.

227. S. Weinberg, Phys. Rev. Lett 19, 1264 (1967) and Phys. Rev. Lett. 27, 1688 (1971); A Salam in Elementary Particle Theory: Relativistic Groups and Analyticity (Nobel Symposium No. 8), edited by N. Szartholm (Almqzist and Wiksell, Stockholm, 1968), p. 367.

228. J.F. Cavaighac, B. Vignon, and R. Wilson, Phys. Lett. 67B, 148 (1977).

229. M.M. Laury. J.M. Davidson R.E. Marrs, C.A. Barnes F.M. Morinigo, B. Chang, E.G. Adelberger, and H.E. Swanson, Phys. Rev. Lett. 40, 840 (1978)

230 S.J. Freedman. C.A. Gagliardi, G T. Garvey, R. McKeown T.J. Bowles, B. Laurikkainen, and R.G H. Robertson, private communication.

231. R.G.H. Robertson, P.L. Dyer, R.C Melin, R.A. Warner, T.J. Bowles, A.B. McDonald, G C. Ball, W.G. Davies and E.D. Earle; MSU Ann. Rpt 1977-78. p. 62.

232. E. Bellotti, E. Fiorini, P Negri, A Pullia, L. Zanotti, and I. Filosofo, Nuovo Cim. 29A, 106 (1975)

233. A.B. Migdal, Zh. Eksp. Teor. Fiz. 61, 2210 (1971) and JETP 34 1184 (1972).

234. T. Takatsuka, K. Tamiya, T. Tatsumi, and R. Tamagaki, Prog. Th. Phys. (Japan) 59, 1933 (1978).

235. E.E. Saperstein, et al., Pis ma Zh. Eksp. Teor. Fiz. 25, 548 (1977) and E.E. Saperstein JETP Lett. 25, 513 (1977).

236. M. Ericson and J. Delorme, Phys. Lett. 76B, 241 (1978).

237. H. Toki and W. Weise, Phys. Rev. Lett 42, 1034 (1979).

238. S.A. Fayans, E.E. Saperstein and S.V. Tolokonnikov, preprint IAE - 3254, 1980.

239. J. Delorme, et al., LYCEN 17953 and addendum (1979), to be published

240. H. Toki and W. Weise, Z. Physik A292, 389 (1979). private communication.

241. W. Benenson, G. Bertsch, G.M. Crawley, E. Kashy J.A. Nolen, H. Bowman, J.G. Ingersoll, J.O. Rasmussen, J. Sullivan, M. Sasao, and M. Koike, Phys. Rev. Lett. 43, 683 (1979) and 44, 54 (1980).

242. See I.U.C.F. Technical and Scientific Report 1978.

243. B. Hoisted, T. Johansson, and O. Jonsson, Phys. Lett. 73B, 123 (1978) and references therein.

244. G. Bertsch, Phys. Rev. C 15, 713 (1977) and Nature 283, 280 (1980); J. Kapusta, Phys. Rev. C 16, 1494 (1977).

245. W. Benenson, E. Kashy, D. Mueller, and H. Nann, Proceedings of the 3rd Intern. Conf. on Nuclei Far From Stability, Cern 76-13 (1976), p. 235.

246. G.E. Brown and P.A. Deutchman, Proceedings of Workshop on High Resolution Heavy Ion Physics at 20-100 MeV/A, Saclay May 1978, p. 212.

## IV. PUBLICATIONS

This section consists of a list of published papers, a list of contributions to conference proceedings, and a list of abstracts of talks at meetings for the three year period 1977, 1978 and 1979. An asterik(*) marks papers describing work done in collaboration with workers from other laboratories or in collaboration with MSU workers supported by other programs (the separately supported nuclear theory program, etc.).

### ARTICLES PUBLISHED

Observation of Hole States at High Excitation in (p,t) Reactions, G.M. Crawley, W. Benenson, D. Weber, and B. Zwieglinski, Phys. Rev. Lett. 39(77)1451.

* Anomalous Optical-Model Potential for Sub-Coulomb Protons for 89<A<130, C.H. Johnson, A. Galonsky, and R.L. Kernell, Phys. Rev. Lett. 39(77)1604.

* Island of High-Spin Isomers Near N=82, J. Pedersen, B.B. Back, F.M. Bernthal, S. Bjørnholm, J. Borggreen, O. Christensen, F. Folkmann, B. Herskind, T.L. Khoo, M. Neiman, F. Pühlhofer, and G. Sletten, Phys. Rev. Lett. 39(77)990.

Empirical Renormalization of the On-Body Gamow-Teller β-Decay Matrix Elements in the 1s-0d Shell, B.A. Brown, W. Chung, and B.H. Wildenthal, Phys. Rev. Lett. 40(78)1631.

Observation of the $T_> = \frac{45}{2}$ Components of Deep Hole States in $^{207}$Pb via the ($^3$He,α) Reaction at 70 MeV, S. Gales, G.M. Crawley, D. Weber and B. Zwieglinski, Phys. Rev. Lett. 41(78)292.

* Direct Determination of $[(sd)^3]_{5/2\ 1/2}(1p^{-2})_{01}$ Component in $^{17}$O(g.s.), H.T. Fortune, J.N. Bishop, L.R. Medsker, and B.H. Wildenthal, Phys. Rev. Lett. 41(78)527.

* Production of A=6 and 7 Isotopes in the α+α Reaction, B.G. Glagola, G.J. Mathews, H.F. Breuer, V.E. Viola, Jr., P.G. Roos, A. Nadasen and Sam M. Austin, Phys. Rev. Lett. 41(78) 1698.

* Comparison of Heavy-Ion-Induced α Transfer and Backward-Angle Elastic Scattering, C.K. Gelbke, T. Awes, U.E.P. Berg, J. Barrette, M.J. LeVine and P. Braun-Munzinger, Phys. Rev. Lett. 41(78)1778.

* Fragmentations of $^{40}Ar$ at 213 MeV/Nucleon, Y.P. Viyogi, T.J.M. Symons, P. Doll, D.E. Greiner, H.H. Heckman, D.L. Hendrie, P.J. Lindstrom, J. Mahoney, D.K. Scott, K. Van Bibber, G.D. Westfall, H. Wieman, H.J. Crawford, C. McParland and C.K. Gelbke, Phys. Rev. Lett. 42(79)33.

* Incomplete Momentum Transfer in Peripheral Heavy-Ion Collisions at 20 MeV/Nucleon, P. Dyer, T.C. Awes, C.K. Gelbke, B.B. Back, A. Mignerey, K.L. Wolf, H. Breuer, V.E. Viola, Jr. and W.G. Meyer, Phys. Rev. Lett. 42(79)560.

* Observation of Isoscalar Giant-Resonance Structure in the Fission of $^{238}U$ Following Inelastic Scattering of $^{6}Li$, A.C. Shotter, C.K. Gelbke, T.C. Awes, B.B. Back, J. Mahoney, T.J.M. Symons, and D.K. Scott, Phys. Rev. Lett. 43(79)569.

* Production of Neutron-Rich Nuclides by Fragmentation of 212 MeV/amu $^{48}Ca$, G.D. Westfall, T.J.M. Symons, D.E. Greiner, H.H. Heckman, P.J. Lindstrom, J. Mahoney, A.C. Shotter, D.K. Scott, H.J. Crawford, C. McParland, T.C. Awes, C.K. Gelbke and J.M. Kidd, Phys. Rev. Lett. 43(79)1859.

* Pion Production with Heavy Ions from 125 to 400 MeV/Nucleon, W. Benenson, G. Bertsch, G.M. Crawley, E. Kashy, J.A. Nolen, Jr., H. Bowman, J.G. Ingersoll, J.O. Rasmussen, J. Sullivan, M. Koike, M. Sasao, J. Peter and T.E. Ward, Phys. Rev. Lett. 43(79)683.

* Structural Changes in the Yrast States of $^{178}Hf$, T.L. Khoo and G. Løvhøiden, Phys. Lett. 67B(77)271.

* High-Spin Neutron Hole Excitations in Light Odd-A Pb Nuclei, H. Helppi, S.K. Saha, P.J. Daly, S.R. Faber, T.L. Khoo and F.M. Bernthal, Phys. Lett. 67B(77)279.

$\alpha + \alpha$ Phase Shifts and the $p+^{7}Li$ and $n+^{7}Be$ Channels, C.H. King, Sam M. Austin, W.S. Chien, and H.H. Rossner, Phys. Lett. 67B(77)389.

* Spectroscopy of $^{16}C$, H.T. Fortune, R. Middleton, M.E. Cobern, G.E. Moore, S. Mordechal, R.V. Kollarits, H. Nann, W. Chung and B.H. Wildenthal, Phys. Letts. 70B(77)408.

Excitation of Giant Resonances in $^{90}Zr$ by Inelastic $^{6}Li$ Scattering, R. Pardo, R.G. Markham, W. Benenson, A.I. Galonsky and E. Kashy, Phys. Letts. 71B(77)301.

* Connection Between Backbending Behaviour and a High Spin Isomer in $^{179}W$, F.M. Bernthal, B.B. Back, O. Bakander, J. Borggreen, J. Pedersen, G. Sletten, H. Beuscher, D. Haenni, and R. Lieder, Phys. Lett. 74B(78)211.

* Observation of the T=4 and T=5 Components of the Giant Gamow-Teller Resonance in the ($^{3}$He,t) Reaction at 130 MeV, Aaron Galonsky, J.P. Didelez, A. Djaloeis and W. Oelert, Phys. Lett. 74B(78)176.

* The Mass of $^{15}$B Via a Three-Proton Stripping Reaction, T.S. Bhatia, H. Hafner, J.A. Nolen, Jr., W. Saathoff, R. Schuhmacher, R.E. Tribble, G.F. Wagner and C.A. Wiedner.

Cross Sections for the Quasielastic $^{112,116,124}$Sn(p,n) and $^{58}$Ni(p,n) Reactions: A Test of the Forward Scattering Amplitude Approximation, S.D. Schery, S.M. Austin, A. Galonsky, L.E. Young and U.E.P. Berg, Phys. Lett. 79B(78)30.

* Shell-Model Predictions of Alpha-Spectroscopic Factors Between Ground States of $16 \leq A \leq 40$ Nuclei, W. Chung, J. van Hienen, B.H. Wildenthal and C.L. Bennett, Phys. Lett. 79B (78)381.

* Electroexcitation and the Determination of the K-Band Structure in $^{24}$Mg, H. Zarek, S. Yen, B.O. Pich, T.E. Drake, C.F. Williamson, S. Kowalski, C.P. Sargent, W. Chung, B.H. Wildenthal, M. Harvey and H.C. Lee, Phys. Lett. 40B(78)26.

Monopole Excitations in $^{4}$He, $^{12}$C and $^{24}$Mg in a Collective Model Description, H.P. Morsch and P. Decowski, Phys. Lett. 42B(79)1.

* Light-Particle Spectra Observed in Central and Peripheral Collisions of $^{16}$O+$^{238}$U at 20 MeV/nucleon, T.C. Awes, C.K. Gelbke, B.B. Back, A.C. Mignerey, K.L. Wolf, P. Dyer, H. Breuer, V.E. Viola, Jr., Phys. Lett. 87B(79)43.

Observation of Particle Alignment in the Octupole Band of $^{172}$Yb, P.M. Walker, S.R. Faber, W.H. Bentley, R.M. Ronningen, and R.B. Firestone, Phys. Lett. 87B(79)339.

Negative-Parity Yrast Band in $^{170}$Yb:Rotation-Aligned Neutrons with Deformation-Coupled Bandhead?, P.M. Walker, S.R. Faber, W.H. Bentley, R.M. Ronningen, R.B. Firestone, and F.M. Bernthal, Phys. Letts. 86B(79)9.

Experimental Resolution of the $^{145}$Gd $\varepsilon/\beta$-Decay Anomalies, R.B. Firestone, R.C. Pardo, and Wm. C. McHarris, Phys. Lett. 89B(79)36.

* Systematics of Ground-State (t,p) Cross Sections in the 2s-1d Shell, H.T. Fortune, L. Bland, R. Middleton, W. Chung, and B.H. Wildenthal, Phys. Lett. 87B(79)29.

* High-Spin Levels in $^{191}$Pt and $^{193}$Pt and the Triaxial Rotor Model, S.K. Saha, M. Piiparinen, J.C. Cunnane, P.J. Daly, C.L. Dors, T.L. Khoo and F.M. Bernthal, Phys. Rev. C 15(77),94.

Odd-Parity Rotational Band Structure in $^{48}$V, L.E. Samuelson, W.H. Bentley, W.H. Kelly, R.A. Warner, F.M. Bernthal and Wm. C. McHarris, Phys. Rev. C 15 (77)821.

Measurement of the Internal Pair Emission Branch of the 7.654-MeV State of $^{12}$C, and the Rate of the Stellar Triple- Reaction, R.G. H. Robertson, R.A. Warner, and Sam M. Austin, Phys. Rev. C 15(77)1072.

Coulomb Displacement Energies of the A=4n+3, T=1/2 Mirror Nuclei in the $1f_{7/2}$ Shell, D. Mueller, E. Kashy and W. Benenson, Phys. Rev. C 15(77)1282.

High-Spin State of $(fp)^2$ Character in $^{34,35,36}$Cl and $^{37,39}$Ar, H. Nann, W.S. Chien, A. Saha and B. H. Wildenthal, Phys. Rev. C 15(77)1959.

* Calculation of Recoil-Order Matrix Elements for the Beta Decays of $^{20}$F and $^{20}$Na, Frank P. Calaprice, W. Chung and B. H. Wildenthal, Phys. Rev. C 15(77),2178.

* $^{40}$Ar(p,d)$^{39}$Ar Reaction at $E_p$=35 MeV, J.F. Tonn, R.E. Segel, J.A. Nolen, W.S. Chien and P.T. Debevec, Phys. Rev. C 16(77)1357.

Levels of $^{16}$F, H. Nann, W. Benenson, E. Kashy, H.P. Morsch, and D. Mueller, Phys. Rev. C 16(77)1684.

$^{7}$Li and $^{7}$Be Production in the $\alpha+\alpha$ Reaction, C.H. King, Sam M. Austin, H.H. Rossner, and W.S. Chien, Phys. Rev. C 16(77)1712.

* High-Spin Level Structure of the Five Neutron Hole Nucleus $^{203}$Pb, S.K. Saha, H. Helppi, P.J. Daly, S.R. Faber, T.L. Khoo, and F.M. Bernthal, Phys. Rev. C 16(77)2159.

ARTICLES PUBLISHED (Continued)

Mass of $^{6}$He, R.G. H. Robertson, E. Kashy, W. Benenson and A. Ledebuhr, Phys. Rev. C 17(78)4.

Decay of $^{143}$Gd$^{m+g}$ by Positron Emission and Electron Capture, R. B. Firestone, R. A. Warner, Wm. C. McHarris and W.H. Kelly, Phys. Rev. C 17(78)718.

* Mass of $^{21}$O from the $^{18}$O($^{18}$O,$^{15}$O)$^{21}$O Reaction, F. Naulin, C. Detraz, M. Bernas, E. Kashy, M. Langevin, F. Pougheon and P. Roussel, Phys. Rev. C 17(78)830.

Inelastic Scattering of 40 MeV Protons from $^{24}$Mg. I. Natural Parity Transitions, B. Zwieglinski, G.M. Crawley, H. Nann and J. A. Nolen Jr., Phys. Rev. C 17(78)872.

(p,t) and (p,$^{3}$He) Reaction on $^{39}$K, H. Nann and B.H. Wildenthal, Phys. Rev. C 17(78)916.

* Mass of Lowest T=2 State of $^{12}$C, R.G. H. Robertson, T.L. Khoo, G.M. Crawley, A.B. McDonald, E.G. Adelberger and S.J. Freedman, Phys. Rev. C 17(78)1535.

T=3/2 Levels in $^{15}$F and $^{15}$O, W. Benenson, E. Kashy, A.G. Ledebuhr, R.C. Pardo, R.G.H. Robertson, and L. W. Robinson, Phys. Rev. C 17(78)1939.

* $^{31}$P($^{3}$He,d)$^{32}$S Reaction at 25 MeV, J. Kalifa, J. Vernotte, Y. Deschamps, F. Pougheon, G. Rotbard, M. Vergnes and B.H. Wildenthal, Phys. Rev. C 17(78)1961.

Search for Parity Mixing in the $^{93}$Tc 17/2$^{-}$ Isomer: Measurements of Internal Conversion Coefficients, B.A. Brown, R. A. Warner, L.E. Young and F.M. Bernthal, Phys. Rev. C 17(78)2040.

* $^{21}$Ne($^{3}$He,p)$^{23}$Na Reaction, H.T. Fortune, J.R. Powers, R. Middleton, H. Nann and B.H. Wildenthal, Phys. Rev. C 18(78)1.

Inelastic Scattering of 40 MeV Protons from $^{24}$Mg. II. Microscopic Calculations for Positive Parity States, B. Zwieglinski, G.M. Crawley, W. Chung, H. Nann, and J.A. Nolen, Jr., Phys. Rev. C 18(78)1228.

Mass Measurement of Proton-Rich, Medium-Weight Nuclei by the ($^{3}$He,$^{6}$He) Reaction, R.C. Pardo, E. Kashy, W. Benenson, and L.W. Robinson, Phys. Rev. C 18(78)1249.

* Configuration of $^{19}$Ne(4.033, $3/2^+$), H.T. Fortune, H. Nann, and B.H. Wildenthal, Phys. Rev. C 18(78)1563.

* Energy Levels in $^{57}$Ni from a Study of the $^{59}$Ni(p,t)$^{57}$Ni Reaction, H. Nann, S. Saha and S. Raman, Phys. Rev. C 18(78)1619.

$^{52}$Cr(p,α)$^{49}$V Reaction, P.A. Smith, J.A. Nolen, Jr., R.G. Markham and M.A.M. Shahabuddin, Phys. Rev. C 18(78)2065.

High-Spin States in $^{146}$Sm, C.H. King, B.A. Brown and T.L. Khoo, Phys. Rev. C 18(78)2127.

Inner Hole States in $^{207}$Pb via the $^{208}$Pb($^3$He,α)$^{207}$Pb Reaction at 70 MeV, S. Gales, G.M. Crawley, D. Weber and B. Zwieglinski, Phys. Rev. C 18(78)2475.

$^{208}$Pb(p,α)$^{205}$Tl Reaction, P.A. Smith, G.M. Crawley, R.G. Markham and D. Weber, Phys. Rev. C 18 (78)2486.

* Interpretation of the Anomalous Electron-Capture to Positron Decay Ratio in $^{22}$Na, R.B. Firesone, Wm. C. McHarris and Barry R. Holstein, Phys. Rev. C 18(78)2719.

* α-Transfer Spectroscopic Factors in $^{23}$Na, W. Chung, H.T. Fortune and B.H. Wildenthal, Phys. Rev. C 19(79)530.

g-Factor of the $19/2^-$ Isomer in $^{115}$Sb, S.R. Faber, L.E. Young and F.M. Bernthal, Phys. Rev. C 19(79)720.

* α-Particle Spectroscopy in Ni and Zn, C.L. Bennett, H.W. Fulbright, J.F.A. van Hienen, W. Chung and B.H. Wildenthal, Phys. Rev. C 19 (79) 1099.

* Parity of $^{19}$F(5.10) and $^{19}$Ne(5.09, H.T. Fortune, J.N. Bishop, H. Nann and B.H. Wildenthal, Phys. Rev. C 19(79)1147.

(p,t) and (p,$^3$He) Reactions on $^{33}$S, H. Nann and B.H. Wildenthal, Phys. Rev. C 19(79)2146.

* Mechanism of the $^{26}$Mg($^{18}$O,$^{16}$O)$^{28}$Mg Reaction at $E_{^{18}O}$=50 MeV and the Energy Levels of $^{28}$Mg, M. Bernas, M. Roy-Stephan F. Pougheon, M. Langevin, G. Rotbard, P. Roussel, J.P. LeFevre, M.C. Lemaire, K.S. Low and B.H. Wildenthal, Phys. Rev. C 19(1979)2246.

Ratios of Cross Sections for Elastic Scattering of 30.3 MeV Protons from $^{40,44,48}$Ca--A New Method, Sam M. Austin, E. Kashy, C.H. King, R.G. Markham, I. Redmount, and R.M. Ronningen, Phys. Rev. C 19(79)1186.

ARTICLES PUBLISHED (Continued)

* Multinucleon Transfer Reactions Induced by $^{18}O$ on $^{28}Si$, M.C. Mermas, A. Greiner, B.T. Kim, M.A.G. Fernandes, N. Lisbona, E. Muller, W. Chung and B.H. Wildenthal, Phys. Rev. C 20(79)2130.

* $^{17}O(^{3}He,p)^{19}F$ and the Structure of $^{19}F$, J.N. Bishop, L.R. Medsker, H.T. Fortune and B.H. Wildenthal, Phys. Rev. C 20(79)1221.

* $^{20}O$ from $^{18}O(t,p)$, S. LaFrance, H.T. Fortune, S. Mordechai, M.E. Cobern, G.E. Moore, R. Middleton, W. Chung and B.H. Wildenthal, Phys. Rev. C 20(79)1673.

* (p,n) Reaction for $89<A<130$ and an Anomalous Optical Model Potential for Sub-Coulomb Protons, C.H. Johnson, A. Galonsky, and R.L. Kernell, Phys. Rev. C 20(79)2052.

Multipole Moments of $^{154}Sm$, $^{176}Yb$, $^{232}Th$, and $^{238}U$ from Proton Inelastic Scattering, C.H. King, J.E. Finck, G.M. Crawley, J.A. Nolen, Jr., and R.M. Ronningen, Phys. Rev. C 20(79)2084.

* $^{14}C(p,n)^{14}N$ and the Isovector Tensor Component of the Effective Two-Nucleon Interaction, R.R. Doering, T.N. Taddeucci, Aaron Galonsky, and D.M. Patterson, Phys. Rev. C 20(79)1627.

$^{194,196,198}Pt(p,t)$ Reactions at 35 MeV, P.T. Deason, C.H. King, T.L. Khoo, F.M. Bernthal and J.A. Nolen, Jr., Phys. Rev. C 20(79)927.

The Decay of $^{201}Pb$, R.E. Doebler, Wm. C. McHarris, and W.H. Kelly, Phys. Rev. C 20(79)1112.

Rotational and Intrinsic Structure of $^{182}W$ from the $(\alpha,2n\gamma)$ Reaction and Decay of $^{182m}Re$, B.D. Jeltema, F.M. Bernthal, T.L. Khoo and C.L. Dors, Nucl. Phys. A280(77)21.

The $^{40}Ca(\alpha,d)^{42}Sc$ Reaction, H. Nann, W.S. Chien, A. Saha and B.H. Wildenthal, Nucl. Phys. A292(77)195.

Four-Particle One-Hole States in $^{43}Ca$ Strongly Populated by the $^{41}K(\alpha,d)$ Reaction, H. Nann, W.S. Chien and A. Saha, Nucl. Phys. A292(77)205.

Fine Structure in the Giant Resonance Region and the Collective Dipole Spin-Flip Excitation in $^{208}Pb$, H.P. Morsch, P. Decowski and W. Benenson, Nucl. Phys. A297 (78)317.

* Study of the $^{17}O(\alpha,d)^{19}F$ Reaction, H.T. Fortune, L.R. Medsker, H. Nann and B.H. Wildenthal, Nucl. Phys. A301 (78)441.

Levels of $^{52}$Fe Studied with the (p,t) Reaction, P. Decowski, W. Benenson, B.A. Brown and H. Nann, Nucl. Phys. A302(78)186.

* Search for Parity Mixing in the $^{93}$Tc $\frac{17}{2}$ Isomer: Measurements of Partial γ-Decay Widths, B.A. Brown, O. Hausser, T. Faestermann, D. Ward, H.R. Andrews and D. Horn, Nucl. Phys. A306(78)242.

* Role of the RMS Radius in DWBA Calculations of the (p,d) Reaction, A. Moalem, J.F.A. Van Hienen and E. Kashy, Nucl. Phys. A307(78)277.

* A Study of the $^{54}$Fe(p,d)$^{53}$Fe Reaction at 40 MeV, T. Suehiro, J.E. Finck and J.A. Nolen, Jr., Nucl. Phys. A313(79)141.

Study of $^{60}$Zn and $^{61}$Zn, D.J. Weber, G.M. Crawley, W. Benenson, E. Kashy and H. Nann, Nucl. Phys. A313(79)385.

* High-Spin Rotational Levels in $^{178}$W Populated in the $^{177}$Hf(α,3nγ) Reaction, C.L. Dors, F.M. Bernthal, T.L. Khoo, C.H. King, J. Borggreen and G. Sletten, Nucl. Phys. A314(79)61.

* Study of the $^{10}$Be(d,p)$^{11}$Be Reaction at 25 MeV, B. Zwieglinski, W. Benenson, R.G.H. Robertson and W.R. Coker, Nucl. Phys. A315 (79)124.

* Charge-Dependent Two-Body Interactions Deduced from Displacement Energies in the $1f_{7/2}$ Shell, B.A. Brown and R. Sherr, Nucl. Phys. A322(79)61.

* Elastic Scattering of 130 MeV $^{3}$He, A. Djaloeis, J.-P. Didelez, A. Galonsky and W. Oelert, Nucl. Phys. A306(78)221.

* Giant-Resonance Excitation by 130 MeV $^{3}$He, A. Djaloeis, J.-P. Didelez, A. Galonsky, and W. Oelert, Nucl. Phys. A325(79)93.

A He-Jet Chopper for Measuring Half-Lives of Short-Lived Nuclei, M.D. Edmiston, R.A. Warner, Wm. C. McHarris, and W.H. Kelly, Nucl. Inst. and Meth. 141(77)315.

Preparation of Isotopic Sulfur Targets, Mark. A. Hedemann, Nucl. Inst. and Meth. 141(77)377.

* Cyclotron Heavy Ion Beam Intensity Enhancement by Using an Easily Ionized Support Gas in the Ion Source, E.D. Hudson, G.A. Palmer, C.L. Haley and M.L. Mallory, Nucl. Inst. and Meth. 141(77)381.

The Neutron Time-of-Flight Facility at Michigan State University, Ranjan K. Bhowmik, Robert R. Doering, Lawrence E. Young, Sam M. Austin, Aaron Galonsky and Steve D. Schery, Nucl. Inst. and Meth. 143(77)63.

ARTICLES PUBLISHED (Continued)

* Cryogenic Helium Jet and Recoil Time-of-Flight Apparatus, R.G.H. Robertson, T.J. Bowles and S.J. Freedman, Nucl. Inst. and Meth. 147(77)361.

Activation and Angular Distribution Measurements of $^{7}Li(p,n)^{7}Be(0.0+0.429$ MeV) for $E_p$=25-45 MeV: A Technique for Absolute Neutron Yield Determination, S.D. Schery, L.E. Young, R.R. Doering, Sam M. Austin and R.K. Bhowmik, Nucl. Inst. and Meth. 147(77)399.

A Simple Ion Source for Target Preparation via Ion Beam Sputtering, J. A. Nolen Jr., M.S. Curtin and T.E. Dyson, Nucl. Inst. and Meth. 150(78)581.

Fast Resolution Optimization in a Magnetic Spectrograph, E. Kashy, P.S. Miller and J.A. Nolen, Jr., Nucl. Inst. and Meth. 156(78)591.

An Easily Prepared Scintillator for Viewing Accelerator Beam Spots, J.A. Nolen, Jr., Nucl. Inst. and Meth. 156(78) 595.

Tapped Delay Line Focal Plane Detectors, R.G. Markham, Nucl. Inst. and Meth. 162(79)327.

* Formation of Glutamine from ($^{13}N$) Ammonia, ($^{13}N$) Denitrogen, and ($^{14}C$)Glutamate by Heterocysts Isolated from Anabaena Cylindrica, Joseph Thomas, J.C. Meeks, C. Peter Wolk, Paul W. Shaffer, Sam M. Austin, and W.-S. Chien, Journal of Bacteriology, 129(77)1545.

A Constraint on the Universal Baryon Density from the Abundance of $^{7}Li$, Sam M. Austin and C.H. King, Nature 269(77)782.

* The Pathways of Assimilation of $^{13}NH_4^+$ by the Cyanobacterium, Anabaena Cylindrica, John C. Meeks, C.Peter Wolk, Joseph Thomas, Wolfgang Lockau, Paul W. Shaffer, Sam M. Austin, Wan-Shen Chien, and Aaron Galonsky, The Journal of Biological Chemistry 252(77)7894.

Isobaric Quartets in Nuclei, Walter Benenson and Edwin Kashy, Rev. Mod. Phys. 51(79)527.

Proton Decay of the Isobaric Analogs of the Ground States of $^{207}Pb$ and $^{208}Pb$, Ranjan Bhowmik, R.R. Doering, Aaron Galonsky, and P.S. Miller, Zeitschrift fur Physik A280 (77)267.

* Fluctuations in Inelastic Proton Scattering from $^{58}Ni$ in the Energy Range 17.1 to 20.6 MeV, A.D. Frawley, G.M. Crawley, and C.L. Hollas, Zeitschrift fur Physik A 286 (78)307.

* Pathways of Assimilation of ($^{13}$N)$N_2$ and $^{13}NH_4^+$ by Cyanobacteria with and without Heterocysts, John C. Meeks, C. Peter Wolk, Wolfgang Lockau, Norbert Schilling, Paul W. Shaffer and Wan-Shen Chien, Journal of Bacteriology 134 (78)125.

* Initial Organic Products of Fixation of ($^{13}$N) Dinitrogen by Root Nodules of Soybean (Glycine max), John C. Meeks, C. Peter Wolk, Norbert Schilling, Paul W. Shaffer, Yael Avissar and Wan-Shen Chien, Plant Physiol. 61(78)980.

Analysis of Nuclear Spectroscopic Data with the Shell Model, B.H. Wildenthal, Nukleonika 23(78)9.

* Initial Organic Products of Assimilation of ($^{13}$N) Ammonium and ($^{13}$N) Nitrate by Tobacco Cells Cultured on Different Sources of Nitrogen, Thomas A. Skokut, C.Peter Wolk, Joseph Thomas, John C. Meeks, Paul W. Shaffer and W.S. Chien, Plant Physiol. 62(78)299.

* Observation of Giant Gamow-Teller Strength in (p,n) Reactions, R.R. Doering, A. Galonsky, D.M. Patterson, and G.F. Bertsch, Reprinted in Selected Papers in Physics, vol. 199, Giant Resonances, ed. Y. Torizuka and H. Ui, Physical Society of Japan, March 25, 1978.

CONFERENCE PROCEEDINGS

* Heavy Ion Source Support Gas Mixing Experiments, E.D. Hudson and M.L. Mallory, IEEE Transactions on Nucl. Sci. 24(77)1590.

A Quick Change Axial Cold Cathode Ion Source, M.L. Mallory, P.S. Miller and W.S. Chien, IEEE Transactions on Nucl. Sci. 24(77)1593.

Realistic Shell Model Calculations, B.H. Wildenthal, Proceedings of the 49th Summer School of Corsica, on Elementary Modes of Excitation in Nuclei,

The Observation of Hole States in (p,t) Reactions at High Excitation, G.M. Crawley, W. Benenson, D. Weber and B. Zwieglinski, Proc. Int. Conf. Nuclear Structure, Tokyo, 1977. (J. Phys. Soc. Japan 44(78)218.

Extraction of Deformation Parameters from Inelastic Proton Scattering, C.H. King, G.M. Crawley, J.A. Nolen, Jr. and J. Finck, Proc. Int. Conf. Nuclear Structure, Tokyo, 1977. (J. Phys. Soc. Japan 44(78)564.

R(4) Group Theoretical Description of Deformed Nuclear States, Wm. C. McHarris, Proceedings of the International Conference on Nuclear Structure, Tokyo, September 5-10, 1977.

Sub-KeV Mass Measurements and Super-Allowed Beta Decay, P.H. Barker and J.A. Nolen, Proceedings of the International Conference on Nuclear Structure Tokyo, September 5-10, 1977.

Gamow-Teller Beta Decay in sd-Shell Nuclei, B.A. Brown W. Chung and B.H. Wildenthal, Proceedings of the International Conference on Nuclear Structure Tokyo, September 5-10, 1977.

* (p,t) Reactions on $^{41}K$, $^{42}Ca$ and $^{43}Ca$ and Core Excited States, Kamal K. Seth, A. Saha, H. Nann and B.H. Wildenthal, Proceedings of the International Conference on Nuclear Structure Tokyo, September 5-10, 1977.

* (p,t) Reactions on $^{44}Ca$ and $^{45}Sc$ and Core-Excited States, A. Saha, Kamal K. Seth and H. Nann, Proceedings of the International Conference on Nuclear Structure Tokyo, September 5-10, 1977.

Shell Model Description of the $^{50}Ti(p,t)$ and $^{51}V(p,t)$ Reactions, B.A. Brown, A. Saha and H. Nann, Proceedings of the International Conference on Nuclear Structure, Tokyo, September 5-10, 1977.

* (p,t) Reactions on $^{50}$Ti and $^{51}$V and Core-Excited States, A. Saha, Kamal K. Seth and H. Nann, Proceedings of the International Conference on Nuclear Structure Tokyo, September 5-10, 1977.

* (p,t) Reactions on $^{88}$Sr and $^{87}$Sr and Core-Excited States, Kamal K. Seth, A. Saha and H. Nann, Proceedings of the International Conference on Nuclear Structure Tokyo, September 5-10, 1977.

Excitation of Giant Resonances in $^{90}$Zr by Inelastic $^{6}$Li Scattering, W. Benenson, A.I. Galonsky, E. Kashy, R.G. Markham and R. Pardo, Proceedings of the International Conference on Nuclear Structure Tokyo, September 5-10, 1977.

Observation of the Giant Gamow-Teller Resonance in the ($^{3}$He,t) Reaction at 130 MeV, Aaron Galonsky, Proceedings of the International Conference on Nuclear Structure Tokyo, September 5-10, 1977.

* High Resolution Study of the 'Deep' Hole States in $^{115}$Sn, Kamal K. Seth, A. Saha, J.A. Nolen and R. Melin, Proceedings of the International Conference on Nuclear Structure Tokyo, September 5-10, 1977.

Study of High-Spin States in $^{146}$Sm and $^{148}$Sm, B.A. Brown, T.L. Khoo and C.H. King, Proceedings of the International Conference on Nuclear Structure Tokyo, September 5-10, 1977.

* High-Spin Level Structure in Odd-Mass Pb Nuclei, P.J. Daly, H. Helppi, S.K. Saha, S.R. Faber, T.L. Khoo and F. M. Bernthal, Proceedings of the International Conference on Nuclear Structure Tokyo, September 5-10, 1977.

The Nuclear Coupling Constant for Analogs of Gamow-Teller Transitions in Charge Exchange Reactions--A Measurement at 25,35, and 45 MeV Using the $^{7}$Li(p,n)$^{7}$Be Reaction, L.E. Young, S.M. Austin, R.R. Doering, R.K. Bhowmik, S.D. Schery and R. DeVito, Proceedings of the International Conference on Nuclear Structure Tokyo, September 5-10, 1977.

* The $^{54}Fe(p,d)^{53}Fe$ Reaction at 40 MeV and the DWBA Analysis T. Suehiro, J.E. Finck and J.A. Nolen, Jr., Proceedings of the International Conference on Nuclear Structure Tokyo, September 5-10, 1977.

Experimental and Theoretical Studies of $^{22}Na$ Decay, R.B. Firestone, R.A. Warner and Wm. C. McHarris, Proceedings of the International Conference on Nuclear Structure Tokyo, September 5-10, 1977.

* Upper Limit on Parity Mixing in the $^{93}Tc$ $17/2^-$ Isomer, B.A. Brown, O. Hausser, T. Faestermann, D. Ward, H.R. Andrews and D. Horn, Proceedings of the International Conference on Nuclear Structure Tokyo, September 5-10, 1977.

Spectroscopic Amplitudes for Multi-Nucleon Transfer in the $1f_{7/2}$ Shell, B.A. Brown, Proceedings of the Symposium on Shell-Model Calculations for Light and Medium Weight Nuclei, Tokyo, September 1977.

The Creation of the Rare Light Elements--Implications for Cosmology, Sam M. Austin, International Symposium on Nuclear Physics at Cyclotron Energies Calcutta, India, September 14-16, 1977.

Inelastic Proton Scattering from Lanthanide and Actinide Nuclei, G.M. Crawley, C.H. King, J.A. Nolen, Jr. and J. Finck, International Symposium on Nuclear Physics at Cyclotron Energies Calcutta, India, September 14-16, 1977.

* Excitation of Giant Resonances by 130 MeV $^3He$, A Djaloeis, J.P. Didelez, A. Galonsky, and W. Oelert, Proc. International Conference on Nuclear Physics Tokyo, September 5-10, 1977, p. 857.

* Elastic Scattering of 130 MeV $^3He$, A. Djaloeis, J.P. Didelez, A. Galonsky, and W. Oelert, Proc. International Conference on Nuclear Physics, Tokyo, Sept. 5-10, 1977, p. 867.

* Island of High Spin Isomers Near N=82, J. Pedersen, B.B. Back, F.M. Bernthal, S. Bjørnholm, J. Borggreen, O. Christensen, F. Folkmann, B. Herskind, T.L. Khoo, M. Neiman, F. Pühlhofer, and G. Sletten, International Symposium on High-Spin States and Nuclear Structure, Dresden, German Democratic Republic, September 1977.

Collective and Intrinsic Aspects of Yrast Structure, F.M. Bernthal, Selected Topics in Nuclear Structure: Proceedings of the XV$^{th}$ Winter School, Zakopane, edited by Z. Stachura and J. Styczen (Cracow, Poland, 1977), p. 259.

CONFERENCE PROCEEDINGS (Continued)

* Cross Sections Relevant to Gamma Ray Astronomy, P. Dyer, D. Bodansky and D.R. Maxson, Proceedings of Symposium on Gamma Ray Spectroscopy in Astrophysics April, 1978.

* Use of $^{13}N$ in Studies of Fixation of Dinitrogen and Assimilation of Ammonium by Cyanobacteria, J.C. Meeks, C.P. Wolk, J. Thomas, S.M. Austin and A. Galonsky, International Atomic Energy Commission Meeting in Use of Isotopes in Study of $N_2$ Fixation, Vienna, Austria, 1978.

Shell-Model Interpretation of Inelastic Electron Scattering to Strong $2^+$ and $4^+$ States in the sd-Shell, W. Chung and B.H. Wildenthal, International Conference on Nuclear Physics with Electromagnetic Interactions, Mainz, Germany, June 1979.

Intermediate Energy Heavy Ions--from the Low Energy Perspective, C. Konrad Gelbke, Fourth High Energy Heavy Ion Summer Study, Berkeley, CA, July 1978.

* Pion Production Near Threshold in Heavy Ion Collisions, G.M. Crawley, W. Benenson, G. Bertsch, E. Kashy, J.A. Nolen, Jr., J.O. Rasmussen, H. Bowman, M. Sasao, J. Ioannou, M.C. Lemaire, J. Sullivan, D. Oliveira, M. Koike and J. Chiba, Proceedings of the International Conference on Nuclear Interactions, Canberra, Australia, August 1978.

The Michigan State University Superconducting Cyclotron Program, H.G. Blosser, Eighth International Conference on Cyclotrons and Their Applications, IEEE Trans. on Nuc. Sci. NS-26 #2,2040(1979).

Design Characteristics of the K=800 Superconducting Cyclotron at MSU, F. Resmini, G. Bellomo, E. Fabrici, H.G. Blosser and D. Johnson, Eighth International Conference on Cyclotrons and their Applications, IEEE Trans. on Nuc. Sci. NS-26 #2,2078(79).

Injection Studies for the K=800 Superconducting Cyclotron at MSU, G. Bellomo, E. Fabrici and F. Resmini, Eighth International Conference on Cyclotrons and their Applications, IEEE Trans. on Nuc. Sci. NS-26 #2,2090(1979).

A Method for Minimizing Trim Coil Power Requirements in Superconducting Cyclotrons, G. Bellomo and F. Resmini, Eighth International Conference on Cyclotrons and their Applications, IEEE Trans. on Nuc. Sci. NS-26 #2,2095(1979).

Beam Extraction System for the K=500 Superconducting Cyclotron, M.M. Gordon and E.M. Fabrici, Eighth International Conference on Cyclotrons and Their Applications, IEEE Trans. on Nuc. Sci. NS-26 #2,2101(1979).

Design of the Central Regions for the MSU 500 MeV Superconducting Cyclotron, E. Liukkonen, J. Bishop, S. Motzny and T. Antaya, Eighth International Conference on Cyclotrons and their Applications, IEEE Trans. on Nuc. Sci. NS-26 #2,2107(79).

Magnetic Field Measurements in the MSU 500 MeV Superconducting Cyclotron, P. Miller, H. Blosser, D. Gossman, B. Jeltema, D. Johnson, and P. Marchand, Eight International Conference on Cyclotrons and their Applications, IEEE Trans. on Nuc. Sci. NS-26 #2,2111(1979).

Operating Experience with the Michigan State University Superconducting Cyclotron Cryogenic System, M. L. Mallory, Eighth International Conference on Cyclotrons and their Applications, IEEE Trans. on Nuc. Sci. NS-26 #2,2138(1979).

Beam Emittance Measurements with a Dispersion-Matched Magnetic Spectrograph, P.S. Miller, E. Kashy and J.A. Nolen, Jr., Eighth International Conference on Cyclotrons and their Applications, IEEE Trans. on Nuc. Sci. NS-26 #2,2334(1979).

* Charge Exchange Losses During Cyclotron Acceleration: Experiment and Theory, R.A. Gough and M.L. Mallory, Eighth International Conference on Cyclotrons and their Applications, IEEE Trans. on Nuc. Sci. NS-26 #2,2384(1979).

Progress Report on the 500 MeV Superconducting Cyclotron, H. Blosser and F. Resmini, Proceedings of the 1979 Particle Accelerator Conference, IEEE Trans. on Nuc. Sci. NS-26 #3,3653(79).

Lifetime Improvements of Heavy Ion Source Cathodes, P.S. Miller, H. Laumer, M.L. Mallory and J.A. Nolen, Proceedings of the 1979 Particle Accelerator Conference, IEEE Trans. on Nuc. Sci. NS-26 #3,3716(1979).

* Cross Sections Relevant to Gamma Ray Astronomy, P. Dyer, D. Bodansky and D.R. Maxson, Proceedings of a Symposium held at the Goddard Space Flight Center, Greenbelt, MD, April 1978.

The MSU Superconducting Cyclotron Project, Au, Bellomo, Blosser, Burleigh, Fabrici, Gordon, Jeltema, D. Johnson, W. Johnson, Laumer, Lawton, Mallory, Miller, Resmini, Riedel, Stork, Proceedings of the Symposium on Heavy Ion Physics from 10 to 200 MeV/AMU, BNL-51115 (1979)307.

Heavy Ion Reactions at Intermediate Energy: Observations, Extrapolations, Speculations, C.K. Gelbke, Proceedings of the Symposium on Heavy Ion Physics from 10 to 200 MeV/AMU, BNL-51115 (1979)1.

Sub-threshold Pion Production with Heavy Ions, W. Benenson, Proceedings of the Symposium on Heavy Ion Physics from 10 to 200 MeV/AMU, BNL-51115 (1979)545.

A K=800 High Resolution Heavy Ion Spectrograph, J.A. Nolen, Proceedings of the Symposium on Heavy Ion Physics from 10 to 200 MeV/AMU, BNL-51115 (1979)635.

A Reaction Mass Spectrograph for Intermediate Energies, L. Harwood, Proceedings of the Symposium on Heavy Ion Physics from 10 to 200 MeV/AMU, BNL-51115 (1979)655.

Giant Resonance Excitations by Heavy Ions: Present Status and Future Possibilities, C.K. Gelbke, Proceedings of the Giant Multipole Resonance Topical Conference, Oak Ridge, October 1979.

Heavy Ion Reactions at E/A$\geq$10 MeV/nucleon, C.K. Gelbke, Proceedings of the Symposium on Deep-Inelastic and Fusion Reactions with Heavy Ions, Hahn-Meitner Institut fur Kernforschung, Berlin, October, 1979.

Continuum Spectra and Light Particle Emission at Incident Energies above 10 MeV/u, C.K. Gelbke, Proceedings of the International Symposium on Continuum Spectra of Heavy Ion Reactions, San Antonio, December 1979.

Giant Gamow-Teller Strength Observed in Charge-Exchange Reactions, R.R. Doering, BAPS 22(1977)86.

Inelastic Proton Scattering from $^{24}$Mg, B. Zwieglinski, G.M. Crawley, J.A. Nolen, Jr., and H. Nann, BAPS 22(1977)28.

The Excitation of M1 Strength in the $^{58}$Ni(p,n) $^{58}$Cu Reaction at 45 MeV Proton Energy, L.E. Young, Sam M. Austin, R.R. Doering and Aaron Galonsky, BAPS 22(1977)28.

Energy Levels of $^{60}$Zn, $^{61}$Zn, G.M. Crawley, W. Benenson, E. Kashy, H. Nann, and D.Weber, BAPS 22(1977)40.

R(4) Group Theory and Deformed Nuclei, Wm.C. McHarris, BAPS 22(1977)530.

Giant Resonance in $^{90}$Zr with $^{6}$Li Scattering, R.C. Pardo, R.G. Markham, W. Benenson, L.W. Robinson, and A. Galonsky, BAPS 22(1977)542.

* Particle Decays of the Lowest T=2 State in $^{36}$Ar, S.J. Freedman, M.A. Oothoude, R.G.H. Robertson, F.J. Zutavern, E.G. Adelberger, and A.B. McDonald, BAPS 22(1977)527.

* High-Spin Levels in $^{200}$Hg Revisited, S.K. Saha, H. Helppi, M. Piiparinen, P.J. Daly, T.L. Khoo, C.L. Dors, F.M. Bernthal, BAPS 22(1977)546.

* High-Spin Level Spectra of $^{197}$Hg and $^{199}$Hg, H. Helppi, S.K. Saha, P.J. Daly, S.R. Faber, T.L. Khoo, F.M. Bernthal, BAPS 22(1977)546.

* Mass of Lowest T=2 State of $^{12}$C, R.G.H. Robertson, T.L. Khoo, G.M. Crawley, A.B. McDonald, E.G. Adelberger and S.J. Freedman, BAPS 22(1977)551.

Gamow-Teller Beta Decay of sd-shell Nuclei, B.A. Brown and B.H. Wildenthal, BAPS 22(1977)576.

Status Report on 500 MeV Superconducting Cyclotron Magnet, H.G. Blosser, BAPS 22(1977)578.

Heavy Ion Beam Acceleration on the Michigan State University Cyclotron, M.L. Mallory, P.S. Miller, and W.S. Chien, BAPS 22(1977)578.

* Anamalous A-Dependence (23 A 130) for the Absorptive Potential for Protons below the Coulomb Berrier, C.H. Johnson, and A. Galonsky, BAPS 22(1977)544.

* High-Spin Isomers in $^{212}$Rn, D. Horn, A.B. McDonald, O. Hausser, T.K. Alexander, T. Faester-Mann, J.R. Beene, and J.C. Herrlander, BAPS 22(1977)643.

Performance of 500 MeV Superconducting Cyclotron Magnet, H.G. Blosser, BAPS 22(1977)991.

* The Spin-Flip Effective Interactions for the $1^+$ States in $^{12}C$ from the $^{12}C(p,p')$ $^{12}C$ reaction at 122 MeV, J.R. Comfort, P. Debevec, G. Moake, S.M. Austin, R.W. Findlay, and W.G. Love, BAPS 22(1977)997.

Recent Developments in the Analysis of the (p,n) Quasielastic Reaction in Terms of Matter Distribution Models, S.D. Schery and A. Galonsky, BAPS 22(1977)1013.

Heavy Ion Cyclotron Vacuum Calculations, M.S. Mallory, BAPS 22(1977)1015.

* Neutron Production from 710-MeV Alphas in Thick Targets, R. Cecil, B. Anderson, A. Baldwin, R. Madey, A. Galonsky, P. Miller, L. Young and F. Waterman, BAPS 22(1977)1006.

* Backbending Behavior and Decay of a High-Spin Isomer in $^{179}W$, F.M. Bernthal, B.B. Back, O. Bakander, J. Borggreen, J. Pedersen, G. Sleeten, H. Beuscher, D. Haenni, R. Leider, and C. Mayer-Böricke, BAPS 23 (1978)91.

* Coulomb Displacement Energies in the $1f_{7/2}$ Shell, B.A. Brown and R. Sherr, BAPS 23(1978)90.

The Origin of the Rare Light Elements and Whether the Universe will Expand Forever, Sam M. Austin, BAPS 23(1978)609.

* High-Spin Level Structure of $^{188}Pt$, C.L. Dors, H. Helppi, S.K. Saha, M. Piiparinen, P.J. Daly, F.M. Bernthal, and T.L. Khoo, BAPS 23(1978)628.

A Method for Finding Small Leaks in Large Cryogenic Vessels, M.L. Mallory and H.G. Blosser, BAPS, 23(1978)541.

The $^{10}Be(d,p)$ $^{11}Be$ reaction at $E_x$=25.0 MeV, B. Zwieglinski, W. Benenson, and R.G.H. Robertson, BAPS 23(1978)501.

* Extensive $\nu i_{13/2}$ Level Families in $^{187}Pt$ and $^{189}Pt$, S.K. Saha, C.L. Dors, M. Piiparinen, M. Helppi, P.J. Daly, T.L. Khoo, and F.M. Bernthal, BAPS 23(1978)628.

Status Report on 500 MeV Superconducting Cyclotron, H.G. Blosser, BAPS 23(1978)541.

Recoil Mass Identification Via Time-of-Flight, M. Distasio, R.B. Firestone, and Wm. C. McHarris, BAPS 23(1978)542.

The Observation of Inner-Hole States in ($^{3}$He,α) Reaction at 70 MeV on $^{90}$Zr, $^{144}$Sm and $^{208}$Pb Nuclei, G.M. Crawley, S. Gales, D. Weber, and B. Zwieglinski, BAPS 23(1978)539.

The Giant M1 resonance in $^{22}$Ne, $^{26}$Mg, $^{30}$Si, and $^{34}$S, U.E.P. Berg, BAPS 23(1978)507.

$^{145}$Gd EC/$\beta^{+}$ Decay Branching Ratios Revisited, R.B. Firestone, R.C. Pardo, and Wm. C. McHarris, BAPS 23(1978)626.

The $^{208}$Pb(p,α) and $^{206}$Pb(p,α) Reactions at 35 MeV, D. Weber, G.M. Crawley, and R.G. Markham, BAPS 23(1978)613.

Mass Measurements with the ($^{3}$He, $^{6}$He) Reaction on Nuclei with A>70, R. Pardo, E. Kashy, W. Benenson, and L.W. Robinson, BAPS 23(1978)574.

A Study of the $^{194,196,198}$Pt (p,p') Reactions and the $0^{+}$ (5) Limit of the Interacting Boson MOdel, P.T. Deason, C.H. King, T.L. Khoo, F.M. Bernthal, and J.A. Nolen, Jr., BAPS 23(1978) 613.

Measurement of the Magnetic Moment of the $19/2^{-}$ Isomer in $^{115}$Sb, S.R. Faber, L.E. Young and F.M. Bernthal, BAPS 23(1978)555.

* Study of Reaction Mechanisms with $^{40}$Ar Beam at 213 MeV/Nucleon, Y.P. Viyogi, T.J.M. Symons, F. Bieser, H.C. Crawford, P. Doll, D.E. Greiner, C.K. Gelbke, H.H. Heckman, D.L. Hendrie, P.J. Lindstrom, J. Mahoney, C. McParland, D.K. Scott, K. Van Bibber, G.D. Westfall and H. Wieman, BAPS 23(1978)959.

Highly Excited States in $^{24,25,26}$Al from the (p,n) Reaction, U.E.P. Berg, L.E. Young, A.I. Galonsky, Sam M. Austin, Y. Iwasaki, and R. DeVito, BAPS 23(1978)520.

* Cross Sections for A=6 and A=7 Isotopes in the α+α Reaction, V.E. Voila, Jr., B.G. Glagola, G.J. Mathews, P.G. Roos, A. Nadasen, and Sam M. Austin, BAPS 23(1978)633.

Fast Resolution Optimization in a Magnetic Spectrograph, E. Kashy, P.S. Miller, and J.A. Nolen, Jr., BAPS 23(1978)542.

Observation of the Radiative Capture Process $^{2}$H(α,γ)$^{6}$Li, R.G.H. Robertson, R.A. Warner, P. Dyer, and R.C. Melin, BAPS 23(1978)518.

The Measurement of the Magnetic Moment of the $19/2^{-}$ Isomer in $^{115}$Sb, S.R. Faber, L.E. Young, and F.M. Bernthal, BAPS 23(1978)555.

* Elastic Scattering of $^{16}O + ^{28}Si$ and $^{12}C + ^{32}Si$ and the $^{28}Si(^{16}O,^{12}C)^{32}S$ Transfer Reaction, T.C. Awes, U.E.P. Berg, C.K. Gelbke, J. Barrette, M.J. LeVine and P. Braun-Munzinger, BAPS 23(1978)940.

* Momentum Transfer in Peripheral Reactions of 20 MeV/A $^{16}O$ with $^{238}U$, B.B. Back, A. Mignerey, K.L. Wolf, T.C. Awes, P. Dyer, C.K. Gelbke, H. Breuer, V.E. Viola and W.G. Meyer, BAPS 23(1978)958.

Heavy Ion Source Operation in the MSU Superconducting Cyclotron Magnet, M.L. Mallory, BAPS 23(1978)936.

Cross Section Ratios for Elastic Scattering of 30.3 MeV Protons from $^{40,44,48}Ca$, S.M. Austin, C.H. King, E. Kashy, R. Markham, I. Redmount and R. Ronningen, BAPS 23(1978)926.

* Pion Production Near Threshold in Heavy Ion Collisions, W. Benenson, G. Bertsch, G.M. Crawley, E. Kashy, J.A. Nolen, Jr., J.O. Rasmussen, H. Bowman, M. Sasao, J. Oliveira, M. Loike and J. Chiba, BAPS 23(1978)959.

Elastic and Inelastic Scattering of $^{6}Li$, A. Galonsky, R. Huffman, R. Markham and C. Williamson, BAPS 23(1978)941.

* Design Considerations of a Recoil Mass Separator for MSU, J.A. Nolen, Jr., L. Harwood, E. Kashy and H.A. Enge, BAPS 24(1979)44.

Densely Measured $(p,t_o)$ Angular Distributions and a Zero-Range DWBA Analysis, Y. Iwasaki, E. Kashy and R.G. Markham, BAPS 24(1979)33.

The Masses of $^{10}C$ and $^{14}O$ and Superallowed Beta Decay, J.A. Nolen, Jr., P.H. Barker and M.S. Curtin, BAPS 24(1979)63.

In-Beam $\gamma$-Ray Spectroscopy of Excited States in $^{143}Eu$, R. Aryaeinejad, R.B. Firestone, W. Bentley and Wm. C. McHarris, BAPS 24(1979)52.

Mass of $^{6}Li$ in its ground and $0^+$, T=1 States, R.G.H. Robertson and J.A. Nolen, Jr. BAPS 24(1979)612.

Broad Cross Section Enhancements in (p,n) Reactions, W.A. Sterrenburg, S.M. Austin, U.E.P. Berg, R.DeVito and A.I. Galonsky, BAPS 24(1979)649.

Status Report on 500 MeV Superconducting Cyclotron, H.G. Blosser, BAPS 24(1979)669.

The Masses of $^{146}$Gd, $^{147}$Gd, and $^{108}$Sn, R.C. Pardo, S. Gales, R.M. Ronningen and L.H. Harwood, BAPS 24(1979)667.

Isomeric Negative-parity Yrast Band in $^{170}$Yb, P.M. Walker, S.R. Faber, W.H. Bentley, R.M. Ronningen, R.B. Firestone and F.M. Bernthal, BAPS 24(1979)668.

An Estimate of the Tensor Force and $V_{\sigma\tau}$ from the $^{7}$Li(p,n)$^{7}$Be Reaction, S.M. Austin, R. Devito, L. Young, and R.Doering,BAPS 24 (1979)610.

Proton Scattering at 35 MeV to Ground Band States in $^{152,154}$Sm, $^{176}$Yb, $^{186}$W, $^{232}$Th and $^{238}$U, R.M. Ronningen, G.M. Crawley, J.E. Finck, C.H. King, R.C. Melin, J.A. Nolen, Jr., P.T. Deason and F.M. Bernthal, BAPS 24(1979)668.

Analysis of the $^{194,196,198}$Pt(p,t) and (p,p') Reactions in Terms of the O(6) Limit of the Interacting Boson Approximation Model, P.T. Deason, R.M. Ronningen, C.H. King, J.A. Nolen, Jr., T.L. Khoo and F.M. Bernthal, BAPS 24(1979)685.

In-beam $\gamma$-Ray Spectroscopy in the Odd Mass N=80 REgion, R. Aryaeinejad, R.B. Firestone, W. Bentley and Wm. C. McHarris, BAPS 24(1979)650.

The $^{48}$Ca(d,n) $^{49}$Sc Reaction at $E_d$=20 MeV, Y. Iwasaki, A. Galonsky and D.J. Weber, BAPS 24(1979)594.

Search for Light Tin Isotopes, D.C. Coyle, R.B. Firestone and Wm.C. McHarris, BAPS 24(1979)649.

Mass of $^{89}$Mo, R.Pardo, L.W. Robinson, E. Kashy, W. Benenson and R.M. Ronningen, BAPS 24)1979)648.

Experimental Resolution of the $^{145}$Bd $\varepsilon/\beta^{+}$ Decay Branching Ratio Anomalies, R.B. Firestone, R.C. Pardo and Wm. C. McHarris, BAPS 24(1979)666.

Isobaric Mass Quartets for A=21, 29, and 37, L.W. Robinson, W. Benenson, E. Kashy and R. Pardo, BAPS 24(1979)612.

* High-Spin Isomers in $^{200,201,202}$Pb, C.L. Dors, J. Wilson, S.K. Saha, H. Helppi, P.J. Daly, S.R. Faber and F.M. Bernthal, BAPS 24(1979)685.

* The $^{14}$C(p,n) $^{14}$N(g.s.) and $^{14}$N(p,n) $^{14}$O(g.s.) Reactions and the Tensor Force, T.N. Taddeucci, R.R. Doering, L.C. Dennis, A. Galonsky and S.M. Austin, BAPS 24(1979)594.

* Cross-Section Measurements for $^{6}He$, $^{6,7}Li$ and $^{7}Be$ in the $\alpha+\alpha$ Reaction at 61.5-159 MeV, B.G. Glagola, H.F. Breuer, G.J. Mathews, A. Nadasen, P.G. Roos, V.E. Viola and S.M. Austin, BAPS 24(1979)593.

* Central and Peripheral Reactions of 20 MeV/A $^{16}O$ with $^{238}U$, B.B. Back, A. Mignerey, K.L. Wolf, C.K. Gelbke, T.C. Awes, P. Dyer, H. Breuer, V.E. Viola, Jr., and W.G. Meyer, BAPS 24 (1979)628.

* A Study of the Fission Decay of $^{238}U$ Following Inelastic Scattering of $^{6}Li$ Ions, A.C. Shotter, C.K. Gelbke, T.C. Awes, T.J.M. Symons, D.K. Scott, J. Mahoney and K. Van Bibber, BAPS 24(1979)647.

* Bombarding Energy Systematics of Linear Momentum Transfer in Interactions of $^{16}O$ with $^{238}U$, V.E. Viola, H. Breuer, B.B. Back, K.L. Wolf, A. Mignerey, C.K. Gelbke, T.C. Awes, and P. Dyer, BAPS 24(1979)826.

* Fission Decay of the Giant Quadrupole Resonance in $^{238}U$, B.B. Back, A.C. Shotter, C.K. Gelbke, T.C. Awes, A. Bice, D.K. Scott, and T.J.M. Symons, BAPS 24(1979)826.

## V. BUDGET

As stated in the Introduction, the funding requested in this proposal is based on the program level presented in our 1978 facility proposal, this being the proposal presented to NUSAC for fiscal year 1980. Table 3 on page 212-iv of the 1978 proposal gave estimated operating costs (in 1978 dollars) for the years 1981, 82, and 83, as follows:

| | 1981 | 1982 | 1983 |
|---|---|---|---|
| Phase I Engineering and Development | $ 100K | $ 100K | $ 100K |
| Accelerator Maintenance and Operation | 500K | 500K | 700K |
| MSU Nuclear Physics Program | 1000K | 1000K | 1000K |
| Total(78 dollars) | $1,600K | $1,600K | $1,800K |

The issue of what to assume for an inflation correction to these numbers is of course a matter of great uncertainity. The Producer Price Index (formaly the Wholesale Price Index) has increased by 24.07% for the 20 month period June 1978 to February 1980, which gives a monthly rate of 1.084%/month ( $(1.01084)^{20} = 1.2406$). Unfortunately the rate for the last two months of this period has been much higher than the 20 month average namely 2.064%/month. The question is then what to assume in making an extrapolation foward to the years 81, 82, and 83?

An important procedural issue relevant to this concerns details of NSF handling of a proposal of this size. In particular such a proposal requires action by the National Science Board and the total amount approved by the Board becomes an upper limit on the granting authority of the NSF Program Office. If actual inflation is more severe than that estimated, a new proposal and new Board approval are generally required. On the other hand, if inflation is lower than that estimated, the Program Office easily adapts to this by making grants smaller than the authorized amount (which they may of course also choose to do for a variety of other reasons as well). In view of the fact that the amounts stated here are upper bounds on funding but not lower bounds, it seems appropriate to estimate inflation at a relatively high level. From February 1980 forward we therefore use 1.5%/month, a figure sizeably higher than the previous 20 month average but also sizeably lower than the rate for the last two months. For the period June 1978 to February 1980 we use the actual 24.07% which wholesale prices have experienced. With these factors the total amounts from the 1978 table become:

| | 1978 $ | Year of Expenditure $ |
|---|---|---|
| 1981 | 1,600K | 2,520K |
| 1982 | 1,600K | 3,010K |
| 1983 | 1,800K | 4,050K |
| Total | $5,000K | $9,580K |

The total amount requested in this proposal is then $9,580,000. A detailed breakdown of the first year request is given in Table V.1. The distribution of funds into various categories is based on past Laboratory experience in trying to optimize these allocations to produce maximum scientific output. Detailed budgets for the years 1982 and 1983 will be furnished at the time the final budgets for those years are under consideration and will show distributions of funds similar to that in Table V.1.

Table V.1. Proposed Budget:Operating Support for a National Facility for Research with Heavy Ions using a 500 MeV Superconducting Cyclotron.
November 1, 1980 through October 31, 1981

| | NSF Man Months | NSF Budget |
|---|---|---|
| A. Salaries | | |
| 14 Co-Principal Investigators | 28.8 | $102,900 |
| 5 Faculty Associates | 39 | 71,100 |
| 12 Research Associates | 144 | 180,000 |
| 24 Non-faculty Professionals | 218 | 336,500 |
| 24 Graduate Students | | 158,400 |
| 42 Pre-Baccalaureate Students | | 88,200 |
| 4 Secretarial/Clerical | | 41,600 |
| 16 Technical, Shop & Other | | 200,700 |
| TOTAL SALARIES AND WAGES | | $1,179,400 |
| B. Fringe Benefits - 16% of non-student | | 149,200 |
| C. Permanent Equipment: Replacement Components, Test Instruments, Data Taking Modules | | 85,000 |
| D. Expendable Equipment & Supplies | | 189,900 |
| E. Domestic Travel | | 47,000 |
| F. Consultants | | 24,000 |
| G. Publication Costs | | 30,000 |
| H. Computer Costs | | 110,000 |
| I. Cyclotron Electricity | | 35,000 |
| TOTAL DIRECT COSTS | | $1,849,500 |
| INDIRECT COST 38% | | 670,500 |
| TOTAL BUDGET | | $2,520,000 |